

Fluorescent Probes for Plasma Membrane Proteins Based on Nile Red

THÈSE N° 7016 (2016)

PRÉSENTÉE LE 9 SEPTEMBRE 2016

À LA FACULTÉ DES SCIENCES DE BASE

LABORATOIRE D'INGÉNIERIE DES PROTÉINES

PROGRAMME DOCTORAL EN CHIMIE ET GÉNIE CHIMIQUE

ÉCOLE POLYTECHNIQUE FÉDÉRALE DE LAUSANNE

POUR L'OBTENTION DU GRADE DE DOCTEUR ÈS SCIENCES

PAR

Efthymia PRIFTI

acceptée sur proposition du jury:

Prof. V. Hatzimanikatis, président du jury

Prof. K. Johnsson, directeur de thèse

Dr P. Heppenstall, rapporteur

Prof. J. Gruenberg, rapporteur

Prof. C. Heinis, rapporteur



ÉCOLE POLYTECHNIQUE
FÉDÉRALE DE LAUSANNE

Suisse
2016

*As you set out for Ithaka
hope the voyage is a long one,
full of adventure, full of discovery.
Laistrygonians and Cyclops,
angry Poseidon – don't be afraid of them:
You'll never find things like that on your way
as long as you keep your thoughts raised high,
as long as a rare excitement stirs your spirit and your body.
Laistrygonians and Cyclops, wild Poseidon –
you won't encounter them
unless you bring them along inside your soul,
unless your soul sets them up in front of you.*

*Hope the voyage is a long one.
May there be many a summer morning when,
with what pleasure, what joy,
you come into harbors seen for the first time;
May you stop at Phoenician trading stations
to buy fine things, mother of pearl and coral, amber and ebony,
sensual perfume of every kind –
as many sensual perfumes as you can;
And may you visit many Egyptian cities
to gather stories of knowledge from their scholars.*

*Keep Ithaka always in your mind.
Arriving there is what you are destined for.
But do not hurry the journey at all.
Better if it lasts for years,
so you are old by the time you reach the island,
wealthy with all you have gained on the way,
not expecting Ithaka to make you rich.*

*Ithaka gave you the marvellous journey.
Without her you would not have set out.
She has nothing left to give you now.*

*And if you find her poor, Ithaka won't have fooled you.
Wise as you will have become, so full of experience,
you will have understood by then what these Ithakas mean.*

"Ithaka", Constantine P. Cavafy

Acknowledgements

First of all, I would like to thank my supervisor, Prof. Kai Johnsson for offering me the opportunity to do my PhD in his lab. I am grateful for the motivation and freedom he has given me. I have really appreciated his open minded comments, the fruitful scientific discussions, his kind character and humour.

Furthermore, I would like to thank the members of my jury committee, Prof. Christian Heinis, Dr Paul Heppenstall and Prof. Jean Gruenberg for taking the time to review my thesis and Prof. Vassily Hatzimanikatis for agreeing to chair the committee.

I owe special thanks to Dr Miwa Umebayashi and Prof. Howard Riezman, from the University of Geneva for our efficient collaboration and all the insightful discussions which have been of great importance for this project.

I also thank Dr Paul Heppenstall for welcoming me in his lab at EMBL, Monterotondo and Dr Mayya Sundukova for introducing me to the wonderful world of electrophysiology. Their help has been invaluable for the results presented in this thesis.

A special thanks to Anne-Lene Odegaard for always being so nice and helpful in administration matters for the doctoral school and in all the events we organized together.

I would like to thank all members of the Johnsson group for the great friendly atmosphere inside and outside of the lab, the ice cream breaks in the sun and for offering help whenever needed.

I thank all the following people for making my PhD a wonderful experience:

Luc Reymond, for introducing me further to the organic synthesis especially in the beginning of my PhD and kindly helping out whenever a reaction was not working.

Ruud Hovius, for thoroughly reviewing my thesis and always being keen on discussing about science and teaching. I will always remember the fun stories from the TP and the students!

Lin Xue and Alberto Schena, for always being willing to offer help in organic chemistry, their kind character and the fun discussions we had next to the HPLC.

Grazvydas Lukinavicius, for kindly sharing his wisdom on cell biology and fluorescence, for all the interesting scientific discussions that helped me a lot and for proofreading my thesis.

Helen Farrants, for being a great friend, for all the personal and professional advice, all the cinnamon buns she baked for us and for taking the time to proofread my thesis.

Rudolf Griss and Julien Hiblot, for being of great help in molecular biology, especially for projects that are not described in this thesis and for all the fun times at Sat or in town.

Olivier Sallin, for his help in the beginning of my PhD, for introducing me to the world of fluorophores and microscopy and for all the cool music concerts we went to.

Nicole Vassali, for being a great Master student and for all the good laughs we had when we stayed late in the dark microscope room.

Iuliia Karpenko, for all the interesting scientific discussions that helped a lot this project.

Anastasiya Masharina, for her kindness and willingness to help me in the beginning of my PhD, for introducing me in molecular biology techniques in the lab and all the nice times at Sat.

Nicolas Goeldel, for being a great neighbour during these four years always motivating me, all the nice birthday cards that made me smile and for all the fun moments we had inside and outside the lab.

Silvia Scarabelli, for making the lab atmosphere happier with her singing, for exploring Italy together, all the nice moments and discussions in coffee breaks and for being a great friend.

Jean-Eudes Ranvier, for his support, all the nice moments we had exploring new cities and for always being there to motivate me.

Last but not least, I thank my family for their continuous support and for always believing in me.

Abstract

Fluorescent probes are very important in basic research and in medicine, because of their sensitivity, versatility and quantitative capabilities. They allow the imaging of tissues or cellular compartments and the monitoring of biological events *in vivo*.

An ideal probe is specific and turns fluorescent only upon binding to its target. In recent years, efforts have been made for the development of such fluorogenic probes. These probes allow specific labeling without the requirement of extensive washing steps for removal of the excess of the dye before imaging. They allow the real-time monitoring of molecular events and they can be used in cases where a washing step is not possible, like in *in vivo* imaging.

With the work described in this thesis, we demonstrate the design of a fluorogenic probe based on the molecule Nile Red and SNAP-tag. It takes advantage of Nile Red, a solvatochromic dye highly fluorescent in an apolar environment, like the plasma membrane and almost non-fluorescent in an aqueous environment. We present our idea to tune the affinity of Nile Red for the plasma membrane by chemically derivatizing it, so that it would insert into the membrane only upon binding to its target receptor. Then, Nile Red - being in an apolar environment - would fluoresce, whereas the excess of the dye - being in a polar aqueous environment - would remain in its dark state. Moreover, we chose to direct our Nile Red derivatives to SNAP-tag, a self-labeling tag, in order to demonstrate the generality of our approach.

We describe the design of a large repertoire of Nile Red derivatives with different linkers and charges and we apply the probe for the visualisation of a pharmacologically interesting receptor, the SNAP-tagged human insulin receptor.

We then present the idea of using our Nile Red derivatives as potential voltage sensors targeted to SNAP-tag. We show the voltage sensitivity of NR12S, a molecule based on Nile Red, and describe our hypotheses on the lack of voltage sensitivity of our Nile Red derivatives and on the position of the latter after the reaction with SNAP-tag.

With this work, we introduce a turn-on probe for SNAP-tagged plasma membrane receptors that would become a valuable tool in bioimaging. Moreover, we suggest Nile Red as a new fluorophore for the generation of voltage sensors.

KEYWORDS

Fluorescence, Nile Red, fluorogenic probe, plasma membrane, SNAP-tag, human insulin receptor, voltage sensing, bioimaging

Résumé

Les sondes fluorescentes sont importantes en recherche fondamentale et en médecine de par leur sensibilité, leur polyvalence et la possibilité de les quantifier. Elles permettent la visualisation des tissus, des compartiments cellulaires ainsi que le suivi de phénomènes biologiques *in vivo*.

Une sonde idéale est spécifique et se révèle uniquement lors de sa fixation sur sa cible. Ces dernières années, de nombreux efforts se sont portés sur le développement de ce type de sondes dites fluorogéniques. Ces sondes permettent un étiquetage spécifique ne requérant pas d'étape de lavage, habituellement nécessaire afin d'éliminer l'excès de sonde non fixée avant visualisation. Elles permettent le suivi en temps réel d'évènement à l'échelle moléculaire et peuvent être utilisées dans les cas où un lavage n'est pas possible, par exemple *in vivo*.

Le travail présenté dans cette thèse décrit le design d'une sonde fluorogénique basée sur la molécule Nile Red et sur SNAP-tag. Ce travail est basé sur les propriétés solvatochromiques intrinsèques de Nile Red: hautement fluorescent dans les environnements apolaires, tel que la membrane plasmique, et quasi non fluorescent dans les environnements polaires. Modifiant Nile Red chimiquement, nous proposons de modifier son affinité pour la membrane plasmique de façon à ce que son intégration à la membrane soit dépendante de l'interaction avec son récepteur. Ainsi, uniquement les formes fixées de Nile Red, intégrées à la membrane apolaire, seront fluorescentes alors que l'excès restant, en solution, restera bloqué sous forme non fluorescente. De plus, nous avons choisi de développer nos dérivés de Nile Red de façon à former un adduit covalent avec SNAP-tag, une protéine capable d'auto-étiquetage, afin de démontrer le caractère généralisable de notre approche.

Nous décrivons un large répertoire de dérivés de Nile Red présentant différentes charges. Ces sondes sont utilisées afin de visualiser un récepteur d'intérêt pharmacologique: le récepteur à insuline (génétiquement liés à SNAP-tag).

Puis, nous proposons d'utiliser ces dérivés de Nile Red afin de suivre le potentiel de membrane. Nous montrons la sensibilité au potentiel de membrane de NR12S, une molécule basée sur Nile Red, et décrivons nos hypothèses quant à la non sensibilité de nos dérivés avant et après réaction avec SNAP-tag.

Avec ce travail, nous introduisons une sonde fluorogénique pour les récepteurs membranaires qui pourraient trouver leur application dans l'imagerie biologique. De plus, nous suggérons que Nile Red puisse être utilisé pour le développement d'un capteur de potentiel de membrane.

MOTS-CLÉS

Fluorescence, Nile Red, sonde fluorogénique, membrane plasmique, SNAP-tag, récepteur à insuline humain, senseur de potentiel de membrane, imagerie biologique.

Abbreviations

AcOH	Acetic acid
AGT	O^6 -alkylguanine-DNA alkyltransferase
ATP	Adenosine triphosphate
BC	O^2 -benzylcytosine
BG	O^6 -benzylguanine
BSA	Bovine serum albumin
CHO cells	Chinese hamster ovary cells
CLIP	CLIP-tag
Cya	Cysteic acid
DBU	1,8-Diazabicycloundec-7-ene
DCM	Dichloromethane
DIEA	Diisopropylethylamine
DMEM	Dulbecco's modified Eagle's medium
DMF	Dimethylformamide
DMPG	1,2-Dimyristoyl- <i>sn</i> -glycero-3-phosphatidylglycerol
DMSO	Dimethylsulfoxide
DPA	Dipicrylamine
DPPC	1,2-Dipalmytoyl- <i>sn</i> -glycero-3-phosphatidyl-choline
EB	Extracellular buffer
ER	Endoplasmic reticulum
ESI	Electrospray ionization
FBS	Fetal bovine serum
GFP	Green fluorescent protein
GPCR	G-protein coupled receptor
HCA	Human carbonic anhydrase
HBSS	Hank's buffered salt solution
HBTU	2-(1H-benzotriazol-1-yl)-1,1,3,3-tetramethyluronium hexafluorophosphate
HEK 293T	Human embryonic kidney cell line 293 transfected with the SV40 virus

HEPES	4-(2-Hydroxyethyl)-1-piperazineethanesulfonic acid
HMRS	High resolution mass spectrometry
HIR	Human insulin receptor
HOBt	Hydroxybenzotriazol
HOMO	Highest occupied molecular orbital
HPLC	High pressure liquid chromatography
LUMO	Lowest occupied molecular orbital
LysMe₃	Trimethyl-lysine
MeOD	Deuterated methanol
NA	Numerical aperture
NMR	Nuclear magnetic resonance
NPM	Normal physiological medium
NR	Nile red
NTA-lipid	1,2-Dioleoyl- <i>sn</i> -glycero-3-[(N-(5-amino-1-carboxypentyl)iminodiacetic acid)succinyl)]
Opti-MEM	Improved minimal essential medium
PBS	Phosphate buffered saline
PEG	Polyethylen glycol
POI	Protein of interest
ppm	Parts per million
PyBOP	Benzotriazol-1-yl-oxytripyrrolidinophosphonium hexafluorophosphate
QY	Quantum yield
R_{min}	Minimum Radius of a smooth sphere that could contain the given mass of a protein
ROI	Region of interest
RT	Room temperature
SDS	Sodium dodecyl sulfate
SDS-page	Sodium dodecyl sulfate polyacrylamide gel electrophoresis
S/N	Signal to noise ratio
SNAP	SNAP-tag
STED	Stimulated emission depletion
TFA	Trifluoroacetic acid
TICT	Twisted intramolecular charge transfer
TLC	Thin layer chromatography
TMP	Trimethoprim
TSTU	<i>O</i> -(<i>N</i> -Succinimidyl)-1,1,3,3-tetramethyl-uronium tetrafluoroborate

Contents

Acknowledgements.....	v
Abstract.....	vii
Résumé.....	ix
Abbreviations.....	xi
Contents.....	xiii
Chapter 1 Introduction.....	1
1.1 Fluorescence Microscopy.....	1
1.2 Principles of Fluorescence.....	2
1.3 Fluorescence Labeling Strategies for Imaging.....	3
1.3.1 Genetically Encoded Fluorescent Proteins.....	4
1.3.2 Chemical Tag-Probe Labeling Techniques.....	5
1.4 Fluorogenic Protein Labeling.....	6
1.5 Idea of the Project.....	9
1.6 Probe Design.....	10
1.6.1 SNAP-tag and CLIP-tag Labeling.....	11
1.6.2 Nile Red (NR).....	11
Chapter 2 Aim of the Project.....	17
Chapter 3 A Fluorogenic Probe Based on NR.....	19
3.1 Introduction.....	19
3.1.1 Aim.....	19
3.1.2 Design of the probe.....	20
3.1.3 Human Insulin Receptor (HIR).....	21
3.2 Results.....	21
3.2.1 Design of NR Derivatives 1-4.....	21
3.2.2 <i>In Vitro</i> Characterization of NR Derivatives 1-4.....	22
3.2.3 Imaging of Live HEK 293T Cells with NR Derivatives 1-4.....	24
3.2.4 Visualisation of the SNAP-tagged HIR.....	28

3.3	Conclusions.....	29
Chapter 4	A Voltage Sensor Based on NR.....	31
4.1	Introduction.....	31
4.1.1	Plasma Membrane	31
4.1.2	Membrane Potential	33
4.1.3	Action Potential	34
4.1.4	Patch Clamp Technique	34
4.1.5	Voltage Indicators.....	35
4.1.6	NR as a Potential Voltage Sensitive Dye	38
4.2	Results	38
4.2.1	Design of NR Derivatives with Additional Charges	38
4.2.2	<i>In Vitro</i> Characterization of NR Derivatives 2 and 4-9.	39
4.2.3	<i>In Cellulo</i> Characterization of NR Derivatives 2 and 4-9	40
4.2.4	Compound NR12S as a Control for the Voltage Sensitivity of NR	49
4.3	Conclusions.....	65
Chapter 5	Position of the NR Derivatives	67
5.1	Introduction.....	67
5.2	Results	67
5.2.1	Spectral Measurements	67
5.2.2	FLIM Measurements.....	72
5.3	Conclusions.....	77
Chapter 6	General Conclusions and Outlook.....	79
Chapter 7	Materials and Methods	83
7.1	Chemistry	83
7.2	Biology.....	97
	Appendix.....	103
	References.....	107
	List of Figures	115
	List of Tables	123
	List of Equations.....	125
	Curriculum Vitae	127

Chapter 1 Introduction¹

1.1 Fluorescence Microscopy

The development of the first microscopes by Robert Hooke and Anton Van Leeuwenhoek in the 1600s was a major step for understanding that our world is full of microorganisms invisible to the naked eye. They were the first ones to discover that the organisms they were observing under the microscope were alive and moving.¹ From that point on, a lot of progress was made and better tools were created for studying the structures of living cells and unraveling the complexity of molecular pathways taking place inside them. The goal of these improvements was to separate the object of interest from the background as much as possible. Thus, fluorescence microscopy was developed. In 1904, the German physicist August Kohler was the first to notice that certain tissues fluoresce when illuminated with UV light (autofluorescence) and shortly after, in 1941, Albert Hewett Coons used for the first time anthracene-isocyanate and later fluorescein to directly label pneumococcal anti-serum.²

Fluorescence microscopy is a non-invasive method that allows the visualisation of cellular compartments or biological processes in live cells in a black background. Normally, cellular compartments are colourless and therefore impossible to visualise under a microscope unless they are stained.³ In fluorescence microscopy the components of interest are stained with fluorophores, which absorb excitation light at a certain wavelength and emit at a longer wavelength. Using special emission filters, the localisation of the fluorophores and of the stained components is revealed. The large spectral range of available fluorophores allows the simultaneous imaging of different cell compartments and events. In addition, the use of fluorescent gene products, like GFP, has allowed the visualisation of specific cellular proteins via genetic-tagging.³ Moreover, fluorescence microscopy is sensitive down to a single molecule level, has a time resolution from nanoseconds to days and allows visualising biomolecules of nanometer dimensions.

The development of laser-scanning confocal microscope, 2 photon and STED microscopy in the recent years have advanced greatly fluorescence imaging. These new techniques gave us the possibility to visualise cell structures in 3D dimensions, penetrate living tissues and image biological processes inside living cells down to nanometer scale.³ The importance of optical microscopy has been highlighted with the award of the Nobel Prize in Chemistry to Stefan Hell, William Moerner and Eric Betzig for the development of super-resolved fluorescence microscopy

¹ Parts of this chapter have already been published. Adapted with permission from Prifti *et al.*⁹¹ Copyright (2014) American Chemical Society.

in 2014.⁴ The discovery of fluorescent proteins and the development of innovative chemical labeling strategies have been necessary for this recognition.

The use of fluorescent probes for the visualisation of membrane receptors has been very important in basic research and medicine.⁵ They have been used extensively for the detection of protein location, the assessment and activation of tissue anatomy and molecular function, the study of molecular events in living cells and microorganisms and for medical diagnostics. But before delving into the extensive use of fluorescent probes, what do we mean when we use the terms fluorescence and fluorophores?

1.2 Principles of Fluorescence

Fluorophores are chemical compounds that have some degree of conjugated double bonds, and usually aromatic structures that easily distribute outer orbital electrons over a wide area.³ They have a very interesting property: after absorbing light of a certain wavelength (photons), they then rapidly emit light, which typically has a longer wavelength (Stokes' shift). This property is called fluorescence.³ The processes that take place during absorption and emission of photons are described with the Jablonski diagram (Figure 1A).⁶

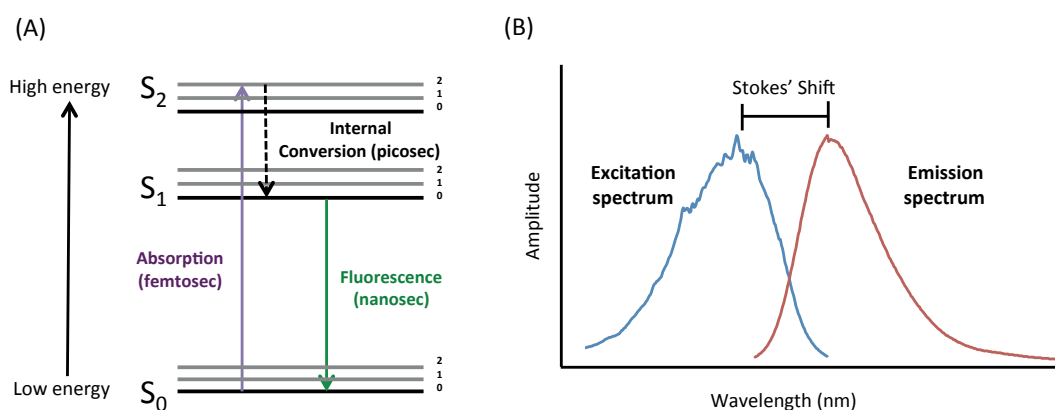


Figure 1: (A) Jablonski diagram. Adapted from Lakowicz *et al.*⁶ (B) A schematic representation of excitation and emission spectra.

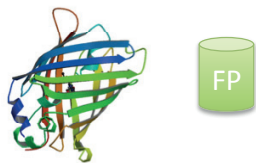
As shown in Figure 1A, the three electronic states (ground, first and second excited) have been highlighted as S_0 , S_1 and S_2 . Each one of them has vibrational energy levels in which the fluorophores can exist (0,1,2, etc). During illumination, an electron of the molecule absorbs a photon and the fluorophore is usually excited to a first or second excited electronic energy level (S_1 or S_2). Basically, the absorbed photon moves an electron into a different orbital that is further away from the nucleus. This process happens in femtoseconds.³ Prior to emission of a photon, the molecules usually rapidly relax to the lowest vibrational state of S_1 . This transition between electron orbital states (S_2 to S_1) is called internal conversion and takes picoseconds. Then, the remaining energy is emitted as a photon so that the electron can relax back to the ground state (Fluorescence).⁶

Important characteristics that define fluorophores are the absorption and emission maxima, the fluorescence quantum yield (Φ), the molar extinction coefficient (ϵ) and the fluorescence lifetime (τ). The absorption and emission maxima, are the wavelengths that correspond to maximum absorption or emission.³ They have to be taken into consideration especially in case of simultaneous labeling with different fluorophores. Moreover, since intrinsic fluorescence (autofluorescence) from cells or tissues reduces in longer wavelength excitation light, “red dyes” are preferred for live cell or *in vivo* imaging. The molar extinction coefficient defines the probability that a fluorophore will absorb a photon. The fluorescence quantum yield is the ratio of number of photons emitted through fluorescence to the number of photons absorbed. The fluorescence lifetime is the time a fluorophore remains in the excited state before returning to the ground state.² All these properties have to be considered before choosing the appropriate fluorophore for each experiment.

1.3 Fluorescence Labeling Strategies for Imaging

According to PubMed, 8,454 articles used the word “fluorescence imaging” in 2015. This highlights the importance of fluorescence microscopy that enables scientists to visualise biological processes inside living cells. A number of techniques for fluorescent labeling of molecules have been developed during the last years, including immunostaining, chemical tag-probe labeling and molecular labeling with fluorescent proteins. Since the use of fluorochrome-labeled specific antibodies (immunostaining) requires fixation of cells, we are going to focus only on techniques that can be applied for live cell imaging.

I. Fluorescent Proteins (i.e. GFP)



II. Chemical tag-probe labeling techniques

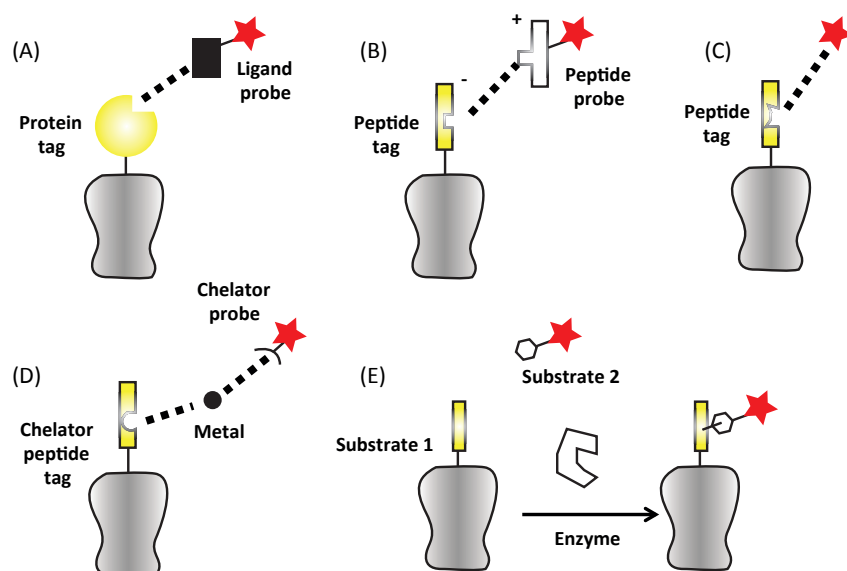


Figure 2: Fluorescence labeling techniques. (I) Fluorescent proteins: Protein structure of GFP (PDB ID: 1GFL)⁷. (II) Chemical tag - probe labeling techniques based on (A) Protein tag - ligand interactions, (B) Peptide tag - peptide interactions, (C) Peptide tag - fluorophore interactions, (D) Metal chelation and (E) Enzymatic reactions. Adapted from Yano *et al.*⁸

1.3.1 Genetically Encoded Fluorescent Proteins

The most popular technique for visualising molecular events and structural properties in live cells is the use of fluorescent proteins.⁹ Fluorescent proteins became very popular after the discovery and isolation of the Green Fluorescent Protein (GFP) from *Aequorea victoria* by Shimomura *et al.*¹⁰ and the demonstration that GFP can be fused to a protein of interest by Chalfie *et al.*¹¹ A lot of engineered colour variants of this protein have been developed by the Tsien lab and have been used for the visualisation of cellular organelles.^{12,13}

Being genetically encoded, fluorescent proteins have been widely exploited by the scientific community due to their "targeted use", since they can be expressed as fusions to almost any protein of interest in living cells. However, when compared to organic fluorophores, their larger molecular weight, their lower brightness and photostability and their narrower dynamic range due to absence of sensitivity to the surrounding environment have motivated scientists to develop alternative chemical labeling strategies.^{14,15}

1.3.2 Chemical Tag-Probe Labeling Techniques

Various chemical labeling techniques have been developed so far (Figure 2B). They can be based on different interactions that are mentioned in Table 1.

Table 1: Tag-probe labeling methods. Adapted from Yano *et al.*⁸

Interactions	Labeling method	Tag	Probe
Protein tag - ligand	LigandLink ¹⁶	<i>E. coli</i> dihydrofolate reductase (eDHFR)	TMP
	SNAP-tag ¹⁷	hAGT mutant	Benzylguanine
	CLIP-tag ¹⁸	hAGT mutant	Benzylcytosine
	Halo-tag ¹⁹	Haloalkane dehalogenase	Chloroalkane
Peptide tag - peptide	Coiled-coil ²⁰	E3 tag peptide	K3 probe peptide
Peptide tag - fluorophore	TR-binding peptide ²¹	TR512 peptide	Xanthene core or Texas Red
Metal chelation	Biarsenical-tetracysteine ^{22,23}	Tetracysteine peptides	Biarsenical fluorophores (fluorescein – FAsH Resorufin – ReAsH)
	NTA-His ^{24,25}	Oligo Histidine	NTA
Enzymatic reactions	BirA Labeling ²⁶	GLNDIFEAKIEWHE	Biotin
	LplA Labeling ²⁷	DEVLVEIETDKAVLEVPGE	Lipoic acid
	ACP-tag ²⁸	Acyl Carrier Protein (ACP)	CoA-fluorophore

Labeling techniques based on protein tag-ligand interactions can be covalent or non-covalent. Covalent methods allow very specific labeling with the use of self-labeling tags, like SNAP-tag, CLIP-tag and Halo-tag (Figure 2A). These tags have a size of 20 kDa, which is similar to the size of fluorescent proteins and therefore there are not so many concerns regarding the perturbation of the protein function due to the large size of the tag.²⁹ Moreover, these tags are multivalent and therefore, when combined, they allow the simultaneous labeling of different cellular compartments with different fluorophores.¹⁸ A limit of this labeling technique is that the excess of the dye that is unbound and present in the medium has to be removed with extensive washing steps before imaging. Non-covalent methods (e.g. LigandLink) have other advantages, like reduced photobleaching and longer-term imaging due to recycling of the fluorophore when the dissociation constant is not negligible (k_{off}).²⁹

Another non-covalent peptide based labeling method is based on metal chelation. This method ensures the small size of tag, but has other disadvantages. Since the probe must be present

during the whole process problems like metal toxicity and perturbation of the cellular process can arise.²⁹ In addition, the affinity of the probe has to be strong enough and preferably the latter has to be weakly or non-fluorescent in the unbound state in order to minimize background fluorescence (Figure 2B).^{8,29}

A balance between small size and specificity can be achieved by exploiting peptide tag-peptide (Figure 2C) or peptide tag-fluorophore (Figure 2D) interactions. Finally, with enzymatic reactions (Figure 2E) it is possible to ensure specificity of labeling with the trade of a longer labeling time procedure (Table 1).⁸

In order to achieve the perfect labeling result there should be a balance between high specificity of labeling, high brightness of the label, versatility of available fluorophores, short time and simplicity of the labeling technique, no toxicity on live cells and tissues and no perturbation of the target protein (small size of tag).⁸

Unfortunately, none of the above labeling techniques has all these characteristics simultaneously and therefore, the choice of the chemical tag depends on the question that needs to be answered in each case. Currently, efforts are made for improvement of these techniques and discovery of new interesting fluorophores.

1.4 Fluorogenic Protein Labeling

In fluorescence microscopy achieving a good signal to noise ratio is crucial for the quality of the image and the success of the experiment. In the recent years a lot of efforts have been made in order to develop fluorogenic probes – probes that become fluorescent only upon binding to the target we are interested in visualising.³⁰ The use of fluorogenic probes does not only allow avoiding the tedious and time-requiring washing steps. Most importantly, such probes are absolutely required in cases where the removal of the unbound probe with extensive washing steps is not possible, like for *in vivo* imaging or real-time monitoring of molecular events. For example, in *in vivo* imaging, removal of the probe is not possible and usually excess of label is eliminated via kidney or other excretion systems. Such probes are normally in a dark state and turn fluorescent only upon binding to the target.³¹ This ensures high specificity of labeling through fluorogenicity.²⁹

Several design strategies for fluorogenic probes have been described so far. Such strategies take advantage of the quenching of fluorescence due to:

1. Sensitivity of the fluorophore to its environment (pH, solvent polarity or temperature)³²

Environment-sensitive dyes change their fluorescence characteristics (intensity or absorption or/and emission maxima) in response to changes in the physicochemical properties of the surrounding environment.³³ Such probes are interesting for the biomembrane research and have been used for the development of fluorogenic probes:

- i. **Molecular rotors:** Molecular rotors have a very high rotational flexibility which is affected by the viscosity of their environment (Figure 3A); in viscous environment (i.e. lipid bilayer) their flexibility is restricted leading to an increased fluorescence quantum yield (QY), whereas in a non-viscous solution (i.e. water) they have a very low emission.^{31,34} A number of such viscosity sensing probes have already been developed (Figure 3B).³⁵ Moreover, recently, a fluorescent molecular rotor was designed for studying the molecular interactions between proteins involved in cancer.³⁶
- ii. **Solvatochromic dyes:** The absorption and emission maxima of solvatochromic dyes is strongly dependent on the polarity of the surrounding solvent. This is a result of intramolecular charge transfer from the electron donor to the electron acceptor and H-bonding interactions in protic solvents (“donor-acceptor” or “push-pull” chromophores).^{31,33,34,37} Studies have been made to optimize such polarity sensing probes³⁸ and several have already been developed for studying ligand-receptor interactions.³⁹ Typical examples of solvatochromic dyes are Nile Red (NR), Prodan⁴⁰ and 4-aminophthalimide (Figure 3C).³⁴

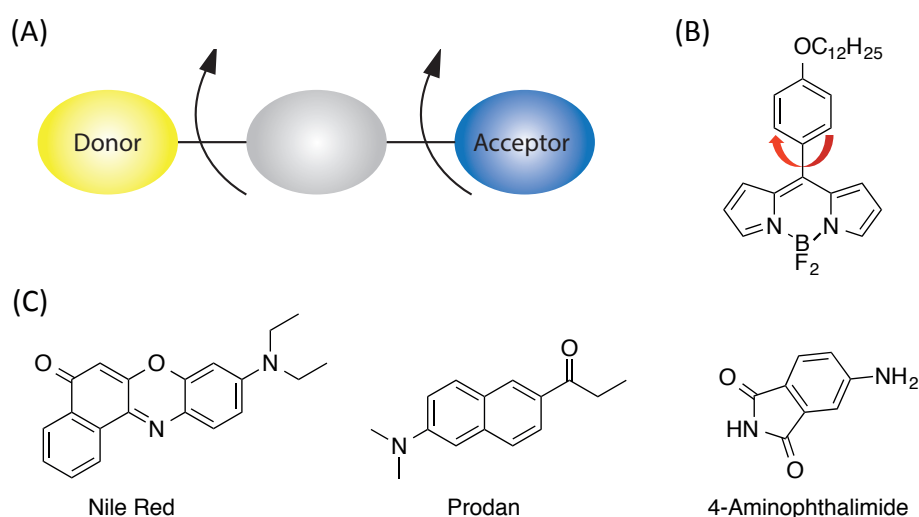


Figure 3: (A) Typical structure of molecular rotors with the electron donating group (yellow), the electron accepting group (blue) and the spacer between them (grey). (B) An example of a molecular rotor: viscosity sensing probe 4,4'-difluoro-4-bora-3a,4a-diaza-s-indacene. (C) Structures of the solvatochromic dyes NR, Prodan and 4-Aminophthalimide.

Fluorescent probes that are environment sensitive have been used for direct fluorogenic labeling of proteins⁴¹ and have also been a powerful tool for studying the biophysical properties of the membrane.

2. Quenching through energy transfer (Förster Resonance Energy Transfer - FRET)³²

FRET is the non radiative energy transfer between a donor molecule in its excited state and an acceptor molecule in its ground state.⁶

FRET has been exploited for the generation of ratiometric sensors for the detection of small molecules of interest, like metabolites or ions.^{42,43} In other applications, for example in FRET based fluorogenic probes, an acceptor quencher is linked to a fluorophore through a flexible linker which is cleaved after the labeling reaction leading to the “fluorescent-on” state.³⁰ In this case, three important factors have to be considered:

- (i) the absorption spectrum of the quencher relative to the emission spectrum of the donor
- (ii) the length of the spacer that links the donor-acceptor pair and
- (iii) the orientation of the two.⁶

FRET based fluorogenic probes have already been described for SNAP and CLIP-tag labeling (Figure 4A).^{44,45}

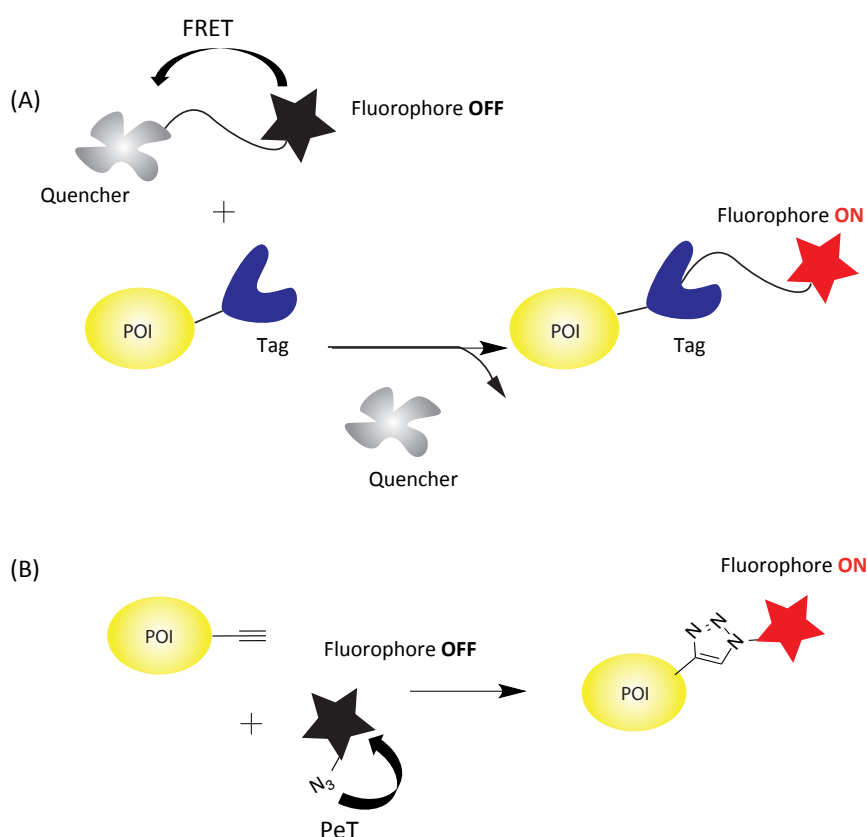


Figure 4: Examples of fluorogenic labeling based on (A) FRET from the fluorophore (donor) to the quencher (acceptor) and (B) PeT quenching. Adapted from Chen *et al.*³²

3. Quenching through electron transfer (Photoinduced Electron Transfer – PeT)³²

PeT is the electron transfer from an electron rich donor molecule to an electron deficient acceptor molecule following the absorption of light.⁶ PeT quenching can be either static or dynamic/collisional.⁴⁶ Both types of quenching require that the acceptor quencher and the fluorophore are in contact with each other. The difference between the two is that in dynamic quenching, PeT occurs through molecular collisions, whereas in static quenching the fluorophore and the quencher form a stable molecular complex which is non-fluorescent.⁶

In the PeT quenching mechanism, electron transfer can occur either from the excited donor fluorophore to the LUMO of the quencher (d-PeT) or from the HOMO of the quencher into the lower semi-occupied orbital of the excited fluorophore (a-PeT). In both cases the result is that the electron does not return to the ground state normally, prohibiting the emission of a photon (Figure 5).⁴⁷ This method of quenching is also distance dependent.

PeT based fluorogenic labeling techniques have already been developed, such as the alkyne-azide bioorthogonal pair (Figure 4B)⁴⁸ or the FIAsh-EDT₂ pair.⁴⁹

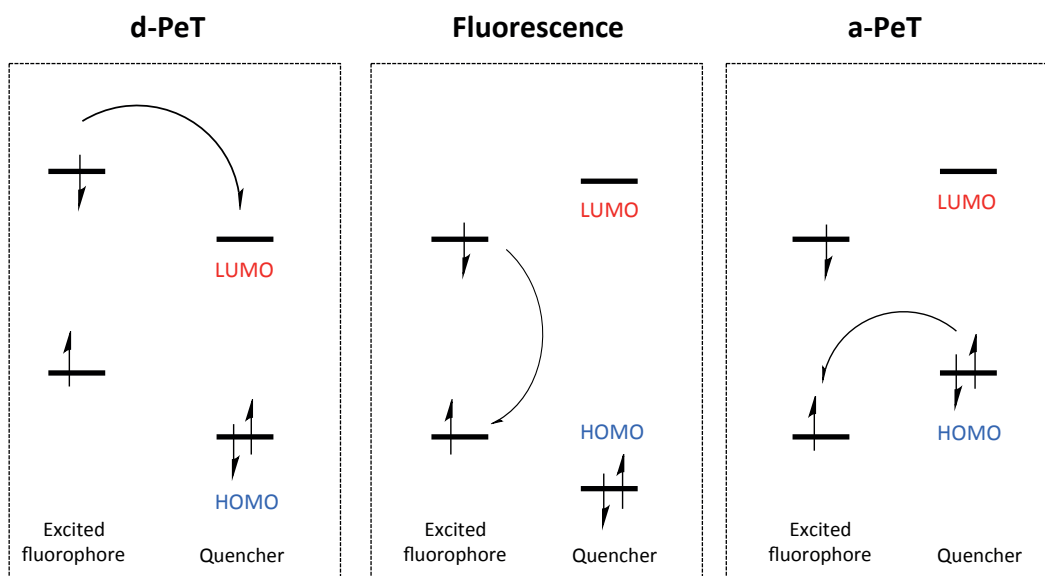


Figure 5: Photoinduced electron transfer (PeT) mechanisms. Adapted from Ueno *et al.*⁴⁷

1.5 Idea of the Project

As mentioned above, during the last years, optical microscopy and especially fluorescence imaging have evolved rapidly. This has underlined the importance of visualising cellular compartments and molecular events on living cells for understanding more the spatio-temporal dynamics of biological phenomena of interest. The drawbacks of using fluorescent proteins in imaging (large size, low sensitivity) led to the development of novel chemical labeling approaches that combine the specificity of the genetic targeting of fluorescent proteins and the sensitivity of small organic fluorophores.

At the time, we were collaborating with the laboratory of Howard Riezman at the University of Geneva. They were using a solvatochromic dye, Nile Red (NR), to study the membrane fluidity. Looking at the properties of this dye, we thought it would be a very good candidate for creating a fluorogenic probe for cell surface receptors.

More specifically, we were interested in the following properties of this dye:

- (i) its high affinity for the membrane,

- (ii) the sensitivity of its fluorescent characteristics to the polarity of the surrounding environment,
- (iii) its high fluorescence quantum yield in apolar environments, whereas in aqueous solution it is almost non fluorescent and
- (iv) its excitation in longer wavelengths ("red dye") which results in a minimal background from intrinsic fluorescence.^{50,51}

We hypothesized that tuning the membrane affinity of NR through chemical derivatization of the molecule would direct NR into the membrane only after it was bound to a specific target sitting close to or on the membrane (e.g. a receptor protein). This would enable us to create a specific and fluorogenic probe for this object. Only the NR molecules bound to the target of interest would have a high concentration near the lipid bilayer and therefore would be able to insert in the membrane, where - experiencing a very apolar environment - they would fluoresce. The excess of the dye present in the medium, being in an aqueous environment, would remain in its "dark state", thus allowing "no wash" experiments (Figure 6).

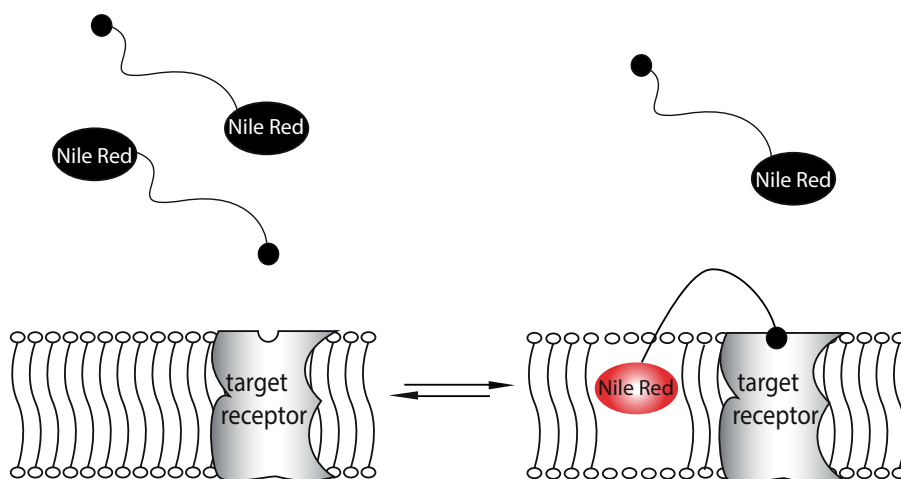


Figure 6: A NR derivative targeting a specific plasma membrane receptor turns fluorescent only upon binding to the target. The remaining excess of the dye, experiencing an aqueous environment, stays in its dark state, allowing "no wash" experiments.

Moreover, the charge separation of NR upon excitation that leads to an increase of the dipole moment of the latter by 7-10 D,⁵² could potentially suggest that NR is sensitive to changes of the membrane potential. Therefore, we suggested as a further application of our probes the generation of a voltage sensor based on this dye. More details on this matter are presented in Chapter 4.

1.6 Probe Design

Our approach is based on the solvatochromic dye NR and the self-labeling tag SNAP-tag, in order to demonstrate the generality of our approach.

1.6.1 SNAP-tag and CLIP-tag Labeling

SNAP- and CLIP-tag are self-labeling protein tags, introduced by our lab, permitting the specific covalent labeling of proteins with synthetic probes. They are mutants of O^6 -alkylguanine-DNA-alkyltransferase (AGT) that react specifically with O^6 -benzylguanine (BG) and O^2 -benzylcytosine (BC) derivatives respectively (Figure 7).^{17,18} Since SNAP and CLIP-tag possess orthogonal substrate specificities they allow simultaneous labeling with different substrates.^{53,54}

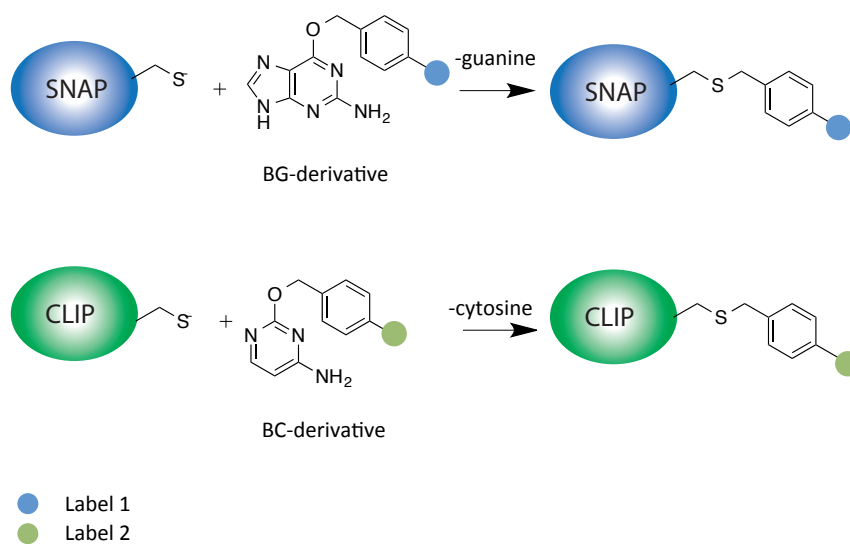


Figure 7: SNAP-tag and CLIP-tag are two protein tags that react specifically with BG- and BC-derivatives respectively, thereby covalently binding the label.

These tags can be expressed in different compartments of the cell and have been previously displayed on the extracellular surface of mammalian cells via a transmembrane (pDisplay) domain by Brun *et al.*⁵³ The labeling of these tags is irreversible, allowing a higher signal to noise (S/N) ratio by simply washing out the excess of substrate. These tags have become popular in the biological community for the specific labeling of proteins.¹⁷ Their main advantage is that they can be fused to any protein, allowing specific labeling of the latter in both cell imaging and *in vitro* applications.

1.6.2 Nile Red (NR)

NR is a benzophenoxazine dye (Figure 8A) which was used in 1985 by Greenspan and coworkers for the staining of intracellular lipid droplets.⁵¹ However, it was first studied by Thorpe in 1907, who observed that when the phenoxazine dye Nile Blue was applied on tissue lipids, the dye was staining acid lipids blue and neutral lipids red. While investigating this phenomenon, he realised that phenoxazine dyes (like Nile Blue) could be converted to phenoxazones (like NR) and therefore he came up with the conclusion that the basic Nile Blue was binding to fatty acids to form a soap, whereas the oxidation product – NR – was binding to neutral lipid droplets.⁵¹ We chose NR as a dye for our probe due to its very interesting spectroscopic properties and its environmental sensitivity.

1.6.2.1 Spectroscopic Properties of NR

NR is a chameleon. Like chameleons, animals that change their colour adapting to their environment, NR is an environmentally sensitive fluorophore.

(I) Solvatochromism:

NR belongs to the family of solvatochromic dyes and therefore, its absorption and emission shifts towards the red part of the spectrum as the solvent becomes more polar (Figure 8C).⁵⁵ This solvatochromic behavior is due to charge transfer (CT) between the diethylamino donor and the aromatic acceptor system in the excited state (Figure 8D).^{50,52,56–58} Upon excitation of the molecule, there is an increase in charge separation within the fluorophore: the electron donor becomes a stronger donor and the electron acceptor becomes a stronger acceptor in the excited state, resulting in stronger charge separation and therefore the creation of large dipole moments.⁵⁹ It has been shown that upon excitation of NR the dipole moment of NR increases by 7-10 D.⁵² This charge separation is favorable in polar solvents, due to solvation.

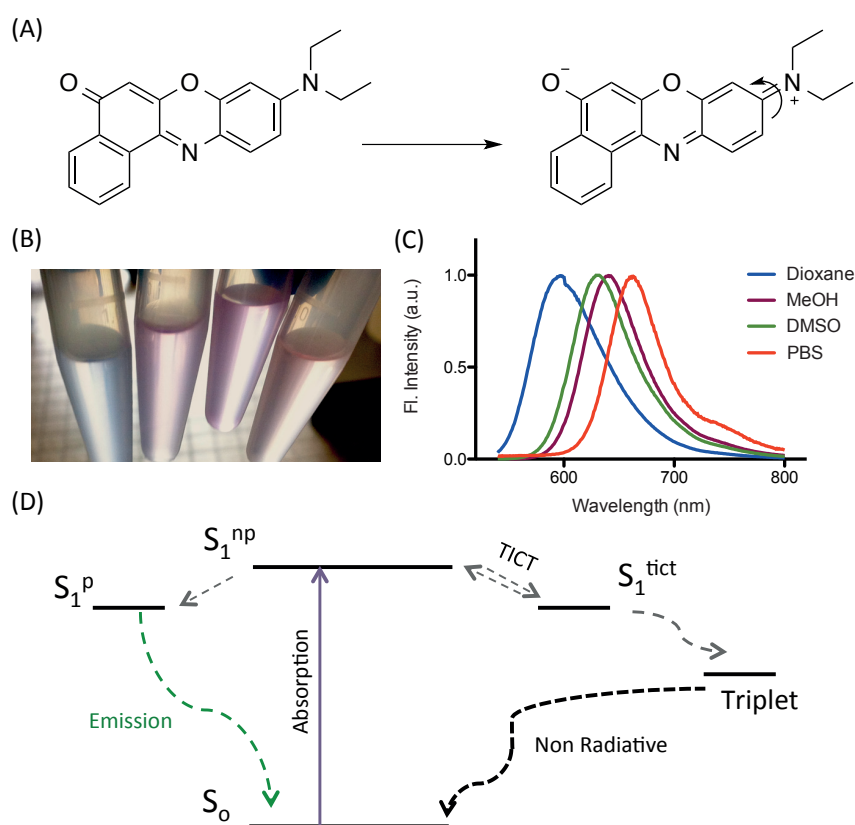


Figure 8: (A) TICT model for NR depending on the polarity of the solvent. (B) NR present in PBS, methanol, DMSO and dioxane (from left to right). (C) Emission spectrum of NR in solvents of different polarity (PBS, MeOH, DMSO and dioxane). (D) Polarity dependent TICT model for NR, where S_1^{np} and S_1^{tict} correspond to “Non polar” and “TICT” excited states respectively adapted from Sarkar *et al.*⁵⁸ and charge separation of NR that leads to the formation of a dipole and explains the solvatochromism of NR.

(II) Dependence of QY and Fluorescence Lifetime on the polarity of the solvent:

The QY of NR is also strongly depending on the environment. In aqueous solvents it is almost non-fluorescent, whereas in apolar environments its fluorescence QY reaches values close to unity.⁵⁰ There are different theories for this property of NR.

One of these theories supports that the low fluorescence QY of NR in aqueous solutions is due to hydrogen bonding that has been reported to provoke radiationless deactivation for anthraquinone and fluorenone derivatives.^{60–64} Others, support that this property of NR is due to the formation of aggregates that cause self-quenching.⁵⁷ Finally, Sarkar *et al.* suggested that the low QY and fluorescence lifetime in polar solvents is due to Twisted Intramolecular Charge Transfer (TICT).

TICT is a phenomenon that occurs in molecules that contain an electron-donating group (i.e. amino-groups) and an electron accepting group (i.e. carbonyl groups), which are usually located at the opposite sides of the molecule, thus inducing electronic polarization.⁶ According to this model, the molecules are first excited in a moderately “non-polar” state, in which the molecules undergo the electron transfer accompanied by a twist of the bond joining the donor with the acceptor and then transition to a highly polar TICT state. The TICT state is non emissive, probably due to rapid non-radiative transfer to triplets⁵⁸ (Figure 8A,D). It was demonstrated by Hicks *et al.* that the activation barrier for the TICT process decreases linearly with increase in polarity.⁶⁵

Apart from the QY, the fluorescence lifetime is also dependent on the surrounding environment. Fluorescence lifetime is the time the fluorophore spends in the excited state before returning to its ground state.⁶ It is known to be a useful indicator of the environment in which a fluorophore is localised.⁶⁶

Originally, it was suggested that the fluorescence lifetime of NR was strongly dependent on the polarity of the solvent NR was present in.^{58,67} More specifically, Sarkar *et al.* suggested that TICT is thermodynamically unfavorable in apolar solvents, with the consequence that both fluorescence lifetime and QY are significantly large in such media. The relation between the two can be shown in the following equations:

$$\Phi_f = k_r \tau_f$$

Equation 1: Relation between fluorescence QY and fluorescence lifetime, where Φ_f and τ_f are the fluorescence QY and fluorescence lifetime respectively.

$$k_r + k_{nr} = \tau_f^{-1}$$

Equation 2: Relation between kinetic radiative and non-radiative decay rate constants and fluorescence lifetime, where τ_f is the fluorescence lifetime and k_r and k_{nr} are the kinetic radiative and non-radiative decay rate constants respectively.⁵⁸

In contrast, Cser *et al.* supported recently that the fluorescence lifetime of NR is not dependent on the dielectric solvent-solute interactions.^{68,69} He showed that the fluorescence lifetime

decreases with the increase of the hydrogen bond donating ability in alcohols, which has been reported to be involved in radiationless deactivation from the excited state.⁶⁸

1.6.2.2 Applications of NR

Due to its particular spectroscopic properties and its environmental sensitivity, NR has had different applications so far. More specifically, NR - being a very hydrophobic molecule - has been used for studying the apolar environments in micelles⁷⁰ and for staining lipid droplets in membranes.⁷¹ Cholesterol is an important element of the plasma membrane that has a crucial role for the organisation and function of the latter.⁷² Mukherjee *et al.* have shown that the percentage of cholesterol in the membrane affects the spectroscopic properties and the fluorescence lifetime of NR,⁷³ and therefore Krishnamoorthy and coworkers decided to investigate the heterogeneity and organisation of membranes by studying the fluorescence lifetime distribution of NR in membranes with different levels of cholesterol.^{74,75} Also, recently, Yang *et al.* have described the development of a NR/BODIPY analogue for the study of viscosity and polarity changes at the ER.⁷⁶

Furthermore, NR has been used as a probe for the study of drug-protein interactions.⁷⁷ More specifically, Brown *et al.* applied NR to solutions of α_1 -acid glycoprotein and saw an enhancement of fluorescence QY and a blue shift in the emission maxima of NR, which suggested that the latter was binding to a non-polar part of the proteins. Upon addition of both acidic and basic drugs, the NR fluorescence reverted to its unbound form allowing the study of drug-protein interactions.⁷⁷

In addition, NR has been also used for the staining of proteins in SDS-polyacrylamide gels⁷⁸ and as a nucleoside fluorescent analog for monitoring the local polarity and dynamics of the inside of the DNA structure.⁷⁹

Interestingly, at the same time with our work, Karpenko *et al.* in Strasbourg, developed a fluorogenic probe for visualizing and quantifying GPCRs in living cells.⁸⁰ They also took advantage of the properties of NR in order to create a turn-on probe with which they then studied the oxytocin receptor in live cells. The same lab developed a NR derivative – NR12S - which has been used for studying cholesterol and lipid order in biomembranes.⁸¹

1.6.2.3 Compound NR12S

Compound NR12S (Figure 9) is a fluorescent probe, designed by Kucherak *et al.* to label only the outer leaflet of the plasma membrane. It consists of NR linked to a zwitterionic group and a long alkyl chain.^{81,82} The presence of a long alkyl chain allows strong interactions of the probe with the lipid membranes and at the same time the sulfonate group prevents the internalization of the dye in the cell.⁸¹

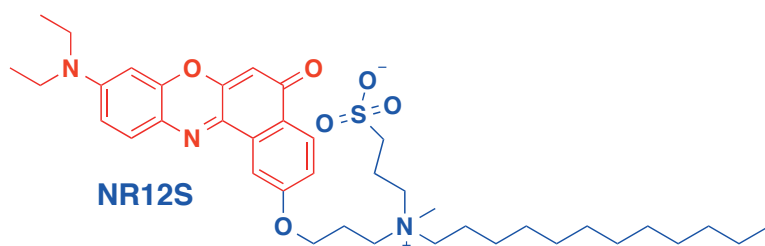


Figure 9: Structure of NR12S. NR is in red and the anchor group consisting of the zwitterionic group and the long alkyl chain is in blue.

The exact localisation of NR12S in the plasma membrane was studied by Saxena *et al.*,⁸³ using the parallax approach.⁸⁴ This method is utilising fluorescence quenching by spin-labeled phospholipids in order to define the penetration depth of the molecule in vesicles.⁸⁴ It was demonstrated that the fluorophore is localised in the membrane interfacial region, characterized by an average position of approximately 18 Å from the centre of the bilayer.⁸³

NR12S is localised in the outer leaflet of the bilayer and has been used for studying cholesterol and lipid order in biomembranes, since it changes its emission colour in the liquid order phase, which is enriched in sphingomyelin and cholesterol.^{81,85} Moreover, another application of this probe is the study of transmembrane asymmetry in small and giant unilamellar vesicles.^{86,87} Also, this probe was recently shown to be the first environmentally sensitive dye to detect apoptosis.^{88,89}

Finally, it has been shown that the fluorescence lifetime of NR12S is also dependent on the percentage of cholesterol present in the membrane. Apparently, there is an approximately 9% increase in fluorescence intensity from 3.5 ns to 3.8 ns as the percentage of cholesterol increases in DOPC vesicles up to 40 mol %.⁷³ Moreover, in another study performed in hippocampal membranes, it was pointed out that the fluorescence lifetime of NR12S was reduced as cholesterol was depleted due to water penetration.⁸⁵ This was supported by the theory of Saxena *et al.*,⁸³ according to which the fluorescence lifetime of NR12S decreases with the increase of polarity of the surrounding environment, as there is more TICT.

Chapter 2 Aim of the Project

The discovery of GFP from *Aequorea victoria*¹⁰ opened the way for the visualisation of proteins, cell compartments and organelles and for the monitoring of molecular events in the living cells with fluorescence imaging. Despite the power of targeted labeling of the genetically encoded fluorescent proteins, they present a number of disadvantages including a large molecular weight, low photostability and weak brightness. These drawbacks led to the development of novel chemical labeling approaches that combine the specificity of the genetic targeting of fluorescent proteins and the sensitivity of small organic fluorophores. Such probes have been used vastly in medicine and basic research.¹⁵

An ideal probe is specific to its target and turns fluorescent only upon binding to the target. In order to design such a probe, we took advantage of the interesting properties of NR. This dye is very sensitive to the polarity of its environment, turns fluorescent only when present in an apolar environment and has a high affinity for the membrane.^{50,90,91} Our idea was to tune the affinity of NR for the plasma membrane by chemical derivatization, so that it would insert in the membrane only after binding to a specific target receptor of interest. We hypothesized that only the NR molecules with a high concentration close to the lipid bilayer would insert into it and due to the apolar environment would fluoresce, whereas the rest of the NR molecules – being in an aqueous solution – would remain in their dark state. This would result in the development of a turn-on probe, which would allow the visualisation of the target receptor directly after labeling. We chose to anchor our NR derivatives to SNAP-tag in order to demonstrate the generality of our approach.⁹¹

Such a probe would be valuable for the imaging of interesting SNAP-fusions of plasma membrane proteins. Apart from this application, we envisioned using such probes as potential voltage sensors. We speculated that since NR has increased dipole moments upon excitation and is sensitive to the polarity of its environment, it could be that depolarization or hyperpolarization of the plasma membrane would result in changes of the fluorescent properties of the dye - a perfect readout for a voltage sensor. Designing a targeted voltage sensor for SNAP-tag would combine the specificity of genetically encoded voltage sensors with the sensitivity of organic voltage indicators.

Chapter 3 A Fluorogenic Probe Based on NR²

3.1 Introduction

3.1.1 Aim

We decided to design a fluorogenic probe for plasma membrane proteins based on NR. We chose to make BG-NR derivatives to label SNAP-tag because several proteins have already been expressed as fully functional fusion proteins with SNAP,^{42,43,92} allowing us to optimize the ligand. Most importantly, this would allow the general application of our approach to any plasma membrane receptor, which could be extracellularly fused to SNAP-tag.

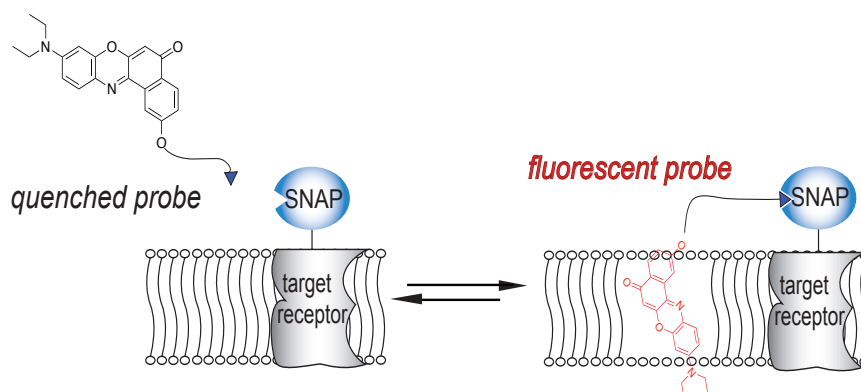


Figure 10: A cartoon of our idea for creating a fluorogenic probe for SNAP-tagged cell surface proteins. A BG-derivative of NR targeting SNAP was synthesized. We hypothesized that the probe on its own would not insert into membranes and therefore would be quenched. Upon reaction with SNAP, NR would be in very close proximity to the plasma membrane resulting in its subsequent membrane insertion. In the apolar environment the probe would turn fluorescent.

Furthermore, since the excess of the dye remaining in the medium would be in its dark state it would allow “no wash” imaging of the SNAP-tagged receptor. Imaging directly after labeling is an attractive property that has been pursued by others^{44,45,93,94} as it offers two important advantages apart from avoiding the time demanding and tedious washing steps. First, it allows real-time monitoring of molecular events, such as receptor trafficking. Second, it enables the use of the probe in cases where a washing procedure is not possible, like in *in vivo* experiments.

² Parts of this chapter have already been published. Adapted with permission from Prifti *et al.*⁹¹ Copyright (2014) American Chemical Society.

3.1.2 Design of the probe

As mentioned in Chapter 1.6, our probe design is based on SNAP-tag and NR. Our probe would have to bind to SNAP-tag and only then insert in the membrane specifically. Thus, we decided to chemically derivatize NR in order to decrease its high affinity for the membrane and make it react with SNAP-tag.

The NR derivatives should consist of:

- i) a benzylguanine moiety (BG), necessary for reacting with SNAP-tag and for reducing the hydrophobicity of NR,
- ii) a linker, necessary for allowing NR to reach the plasma membrane after binding to SNAP-tag and
- iii) the dye NR.

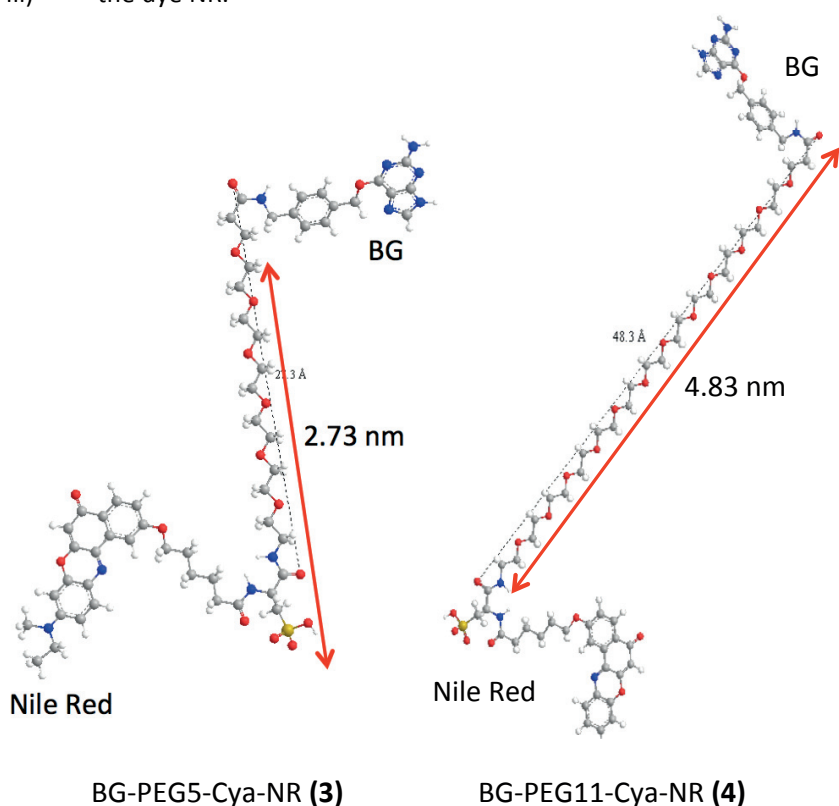


Figure 11: Approximate estimation of the length of PEG linkers in nm calculated for compounds **3** and **4** in Chemdraw.

We decided to use PEG linkers to anchor NR to BG for three reasons. First, they are hydrophilic and they can reduce the hydrophobicity of the probe in order to prevent unspecific insertion of the probe in the membrane. Second, it is easy to synthesize different linker lengths. Finally, they are quite flexible and can allow NR to reach the plasma membrane. According to Erickson⁹⁵ and his mathematical model for estimating the size of a protein, SNAP-tag (20 kDa) has an R_{\min} of 1.78 nm and therefore PEG5 and PEG11 linkers were chosen as a starting point for our experiments. As seen in Figure 11, the length of the PEG5 linker is approximately 2.78 nm and the one of the PEG11 linker is approx 4.83 nm.

3.1.3 Human Insulin Receptor (HIR)

We chose to label a pharmacologically interesting receptor, the HIR, via an extracellular SNAP-fusion. HIR belongs to the subfamily of receptor tyrosine kinases. It consists of two α and two β subunits (Figure 12).⁹⁶ The α subunit is primarily extracellular, whereas the β subunit has an extracellular, a transmembrane domain that anchors it to the plasma membrane and an intracellular domain.⁹⁷ The α subunit is known to be responsible for the binding of insulin, whereas the β subunit is thought to transduce the binding of the agonist into the activation of intracellular signaling cascades. HIR is activated by the binding of insulin⁹⁸ and has a very important role in regulating glucose homeostasis. Diseases such as diabetes are associated with HIR malfunction.⁹⁹

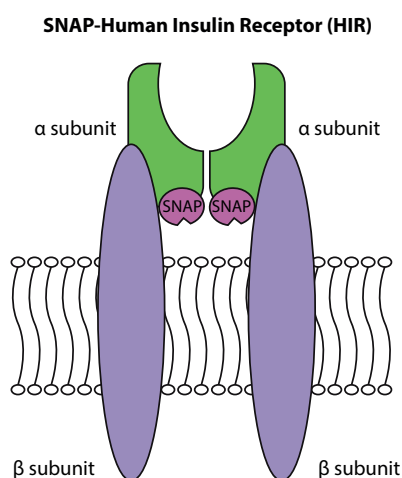


Figure 12: Schematic structure of SNAP-tagged Human Insulin Receptor (SNAP-HIR). It contains two α subunits for the binding of insulin and two β subunits that are involved in signal transduction. SNAP is positioned at the C-terminus of the α subunit of the receptor.

3.2 Results

3.2.1 Design of NR Derivatives 1-4

We synthesized compounds **1-4** that consist of (i) a benzylguanine moiety necessary for conjugation to SNAP-tag (blue), (ii) a polyethyleneglycol (PEG) linker that allows NR to reach the lipid bilayer and reduces the hydrophobicity of the molecule (black) and (iii) NR (red) (Figure 13). Compounds **1** and **2** differ from compounds **3** and **4** by the insertion of a negatively charged cysteic acid (Cya) (purple), which further reduces the hydrophobicity of the compounds and thereby further prevents non-specific insertion in the lipid bilayer. We chose to use PEG linkers to anchor NR to the BG moiety since it is easy to synthesize different lengths and they possess good aqueous solubility. We used two different PEG lengths: PEG5 (compounds **1** and **3**) and PEG11 (compounds **2** and **4**) (Figure 13). The synthesis of these compounds is presented in Chapter 7.1.

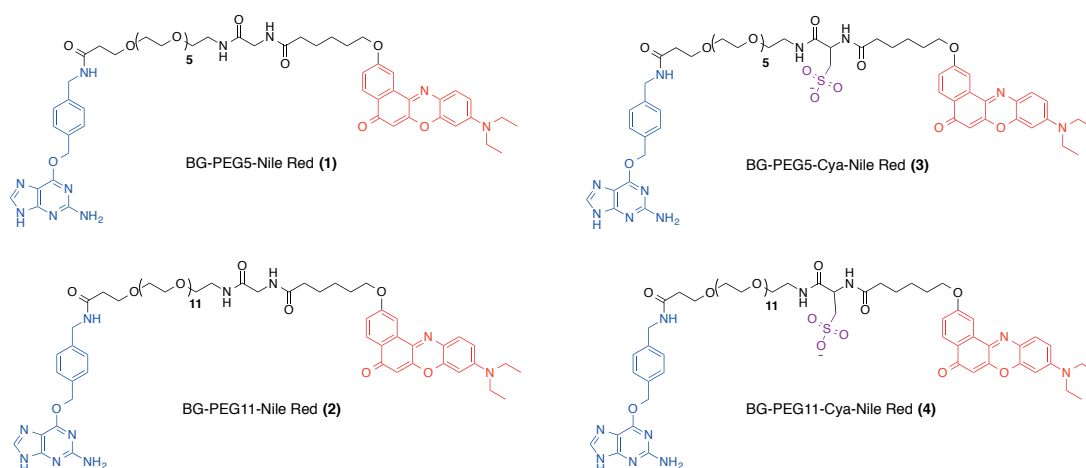


Figure 13: Structures of NR derivatives with different PEG linkers (compounds **1-4**). They consist of a benzylguanine moiety (blue), a linker (black), one or none negatively charged Cya (purple) and NR (red).

3.2.2 *In Vitro* Characterization of NR Derivatives 1-4

3.2.2.1 *Fluorescent Properties of NR Derivatives 1-4*

First of all, we were interested to test if the NR derivatives **1-4** maintained the solvatochromic properties of the parent NR. Therefore, the excitation and emission spectra, as well as fluorescence QY were determined in solvents of different polarity like dioxane, PBS and Dubelcco's modified Eagle medium (DMEM) + 10% fetal bovine serum (FBS) – the latter being the labeling and imaging medium on live cells (Table 2).

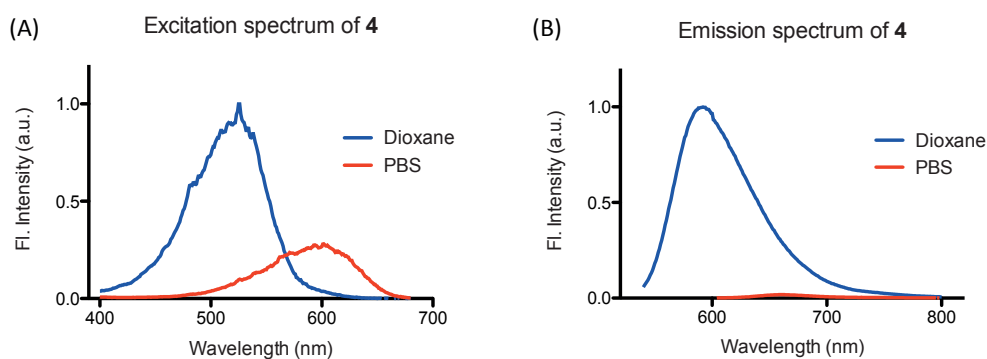


Figure 14: (A) Excitation and (B) emission spectra of the BG-derivative **4** in dioxane and PBS showing typical spectroscopic properties of NR. The intensities have been normalised to those of dioxane. Fluorescence emission was detected while exciting at 520 nm, and the excitation spectrum was recorded at 700 nm emission wavelength.

Fortunately, the NR derivatives indeed retained the solvatochromic properties of NR and were highly fluorogenic in the apolar dioxane compared to PBS (Figure 14).

Moreover, as shown in Table 2, there was a clear red shift of the λ_{abs} and λ_{fl} for all the NR derivatives in the more apolar solvent dioxane compared to PBS, which is a characteristic of NR (Figure 14).⁵⁰ In addition, looking at the fluorescence QY measured, we observed that compounds **1-4**, as NR, were also highly fluorescent in an apolar solvent like dioxane compared to PBS, where they were almost non-fluorescent (Figure 14, Table 2).

Table 2: Spectroscopic properties Including absorption and emission maxima and QY for compounds **1-4** and NR.

Derivative	Solvent								
	PBS			DMEM + FBS 10%			Dioxane		
	λ_{abs} , nm	λ_{fl} , nm	QY, %	λ_{abs} , nm	λ_{fl} , nm	QY, %	λ_{abs} , nm	λ_{fl} , nm	QY, %
BG-PEG5-C6-NR (1)	602	664	1.2	571	622	10.4	525	594	73.0
BG-PEG5-Cya-C6-NR (3)	601	664	2.0	572	624	8.4	526	591	73.0
BG-PEG11-C6-NR (2)	601	661	2.3	584	628	6.3	526	593	73.0
BG-PEG11-Cya-C6-NR (4)	602	661	2.7	595	645	6.0	526	592	73.0
Nile Red	571	657	5.0 ^a	563	619	n.d.	525	587	91.0 ^a

n.d.: not determined

a: corresponds to reference⁸¹

3.2.2.2 Kinetics of SNAP-tag Labeling with the NR Derivatives 1-4

Moreover, it was demonstrated that compounds **1-4** react with SNAP-tag with similar rate constants (Table 3). These values are in the same range of values that have been reported for other BG-substrates for SNAP-tag.⁴⁴

Table 3: Rate constants k and $t_{1/2}$ of labeling reaction of SNAP with compounds **1-4**, measured by SDS-page gel.

Kinetics of Labeling Reaction		
Derivative	Rate constant k , $M^{-1} sec^{-1}$	$t_{1/2}$ (sec)
BG-PEG5-C6-NR (1)	2253 ± 632	275 ± 66
BG-PEG5-Cya-NR (3)	1585 ± 461	311 ± 60
BG-PEG11-C6-NR (2)	2270 ± 926	305 ± 129
BG-PEG11-Cya-C6-NR (4)	1990 ± 521	310 ± 75

Our NR derivatives proved to be much faster when compared to other fluorogenic probes developed for SNAP-tag labeling in live mammalian cells. Sun *et al.* designed such probes based on the incorporation of a quencher on the guanine group in order to ensure that the probes will become fluorescent only upon binding to SNAP-tag.⁴⁴ As seen in Table 4, the rate constants and

$t_{1/2}$ of these fluorogenic probes are from 2 to 15-fold smaller compared to the ones measured for our NR derivatives.

Table 4: Rate constants k and $t_{1/2}$ of labeling reaction of SNAP as reported by Sun *et al.*⁴⁴

Kinetics of Labeling Reaction		
Derivative	Rate constant k , $M^{-1}sec^{-1}$	$t_{1/2}$ (sec)
CBG-488-DABCYL	162 ± 42	905 ± 272
CBG-488-TQ2	831 ± 549	213 ± 106
CBG-549-QSY7	152 ± 58	1027 ± 457
CBG-AF647-QC1	286 ± 61	499 ± 106
CBG-TF5-QSY21	284 ± 48	498 ± 90

3.2.3 Imaging of Live HEK 293T Cells with NR Derivatives 1-4

Having seen that the NR-derivatives are solvatochromic and fluorogenic *in vitro*, we decided to examine whether compounds **1-4** were suitable for live cell imaging. We transiently transfected HEK 293T cells with a fusion protein in which SNAP is fused via CLIP-tag and the human carbonic anhydrase (HCA) to a growth factor receptor transmembrane domain, which resulted in the expression of SNAP-tag on the extracellular side of the plasma membrane.⁵³ The reason for choosing this construct for proof-of-principle experiments was that it allowed the simultaneous labeling of SNAP-tag with the NR compounds and CLIP-tag with another fluorophore (in this case BC-AlexaFluor 488) in order to unambiguously identify the transfected cells and it also mimicked a fusion of SNAP-tag to a receptor protein by the presence of human carbonic anhydrase (HCA).

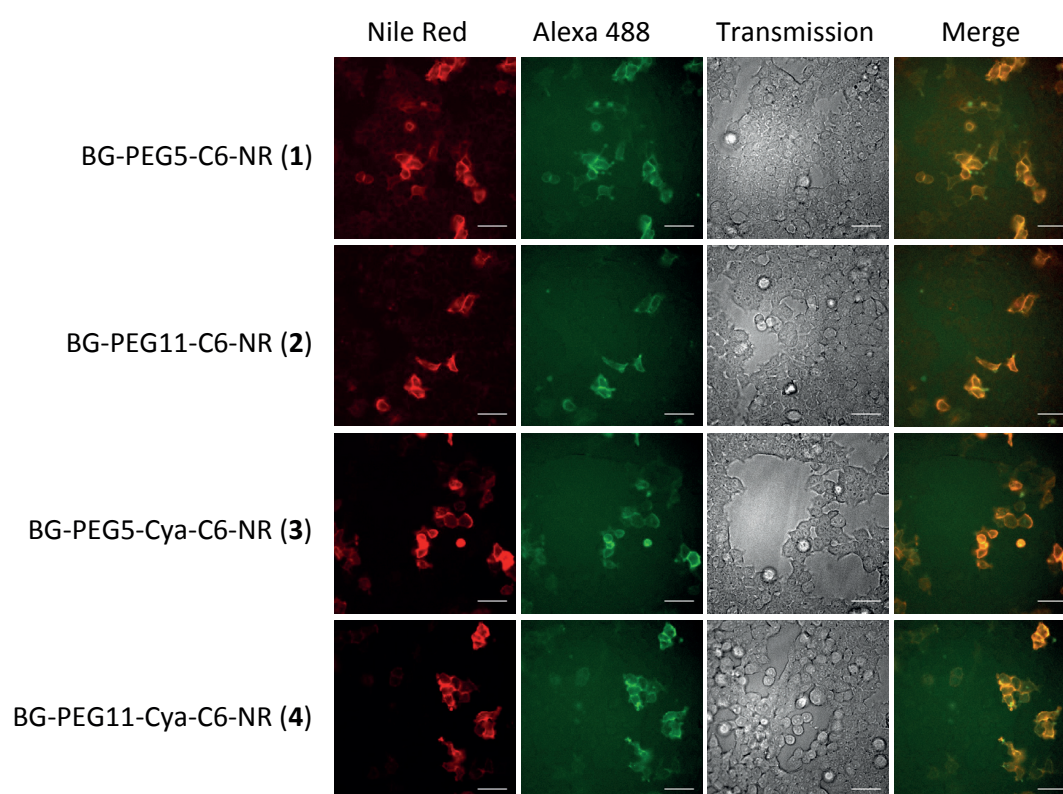


Figure 15: **Imaging after three washes in DMEM + FBS 10%.** HEK 293T cells transiently expressing pDisplay SNAP-CLIP-HCA labeled with BC-AlexaFluor 488 (10 μ M, 10 min incubation at 37 $^{\circ}$ C, three washes with DMEM + FBS 10%) and compounds **1-4** (500 nM, 30 min incubation at RT, DMEM + FBS 10%) imaged after three washes. Scale bar, 50 μ m. (N.B. The pictures in this figure have all been treated with the same settings. However, note that the settings between Figure 15 - Figure 18 are not the same.)

Transfected cells were labeled with BC-AlexaFluor 488, washed and treated with compounds **1-4** (500 nM, 30 min at RT). They were imaged after three washes in DMEM + FBS 10%. As shown in Figure 15, all compounds showed clear co-localization of the Alexa 488 and NR channels, suggesting that the NR derivatives were bound to SNAP-tag and that the NR was turned-on by experiencing a hydrophobic environment.

We then tested whether these compounds allowed “no wash” imaging of the transfected cells. Since NR is non-fluorescent in aqueous solution we expected the excess of the dye to be in its dark state, therefore allowing us to image the cells without necessarily removing the unbound dye with washing steps. We repeated the same procedure, but this time imaged the cells directly after labeling in DMEM + FBS 10%. In this case we observed a big difference in the behavior of the compounds.

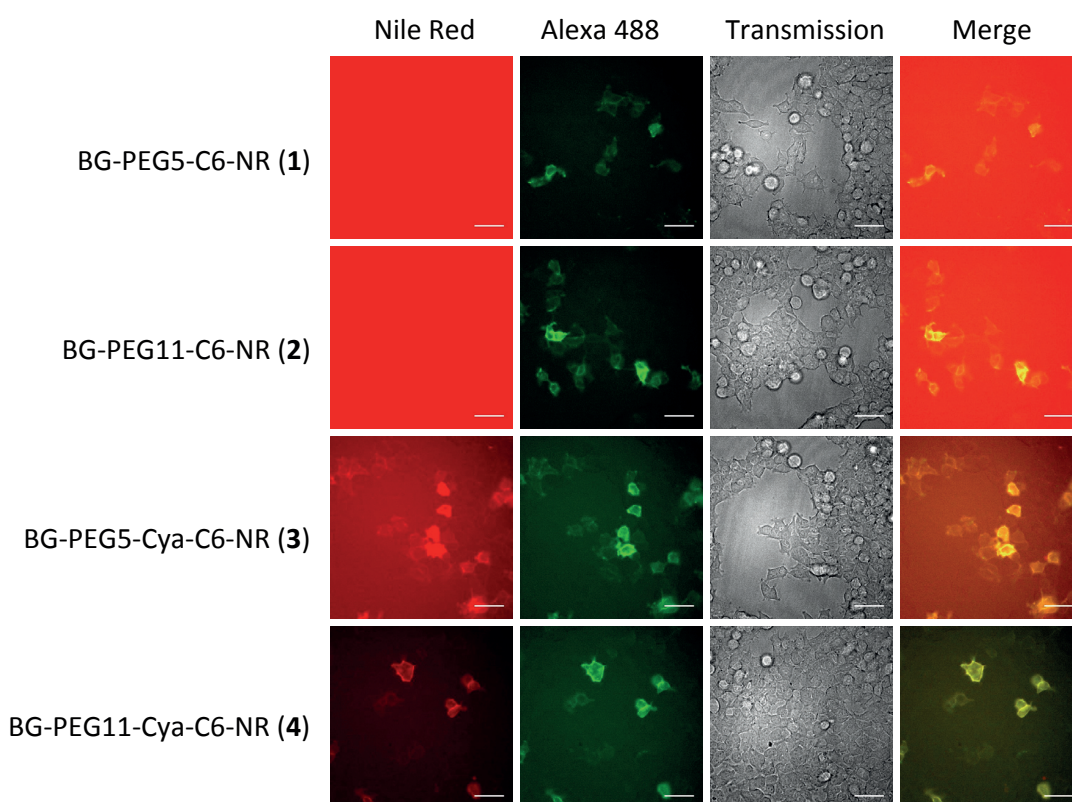


Figure 16: “No wash” imaging in DMEM + FBS 10%. HEK 293T cells transiently expressing pDisplay SNAP-CLIP-HCA labeled with BC-AlexaFluor 488 (10 μ M, 10 min incubation at 37 $^{\circ}$ C, three washes with DMEM + FBS 10%) and compounds **1-4** (500 nM, 30 min incubation at RT, DMEM + FBS 10%) imaged without wash. Scale bar, 50 μ m. (N.B. The pictures in this figure have all been treated with the same settings. However, note that the settings between Figure 15 - Figure 18 are not the same.)

As shown in Figure 16, there was a significant difference between compounds **1** and **2** and compounds **3** and **4** which differ structurally only by the presence of a negative charge (Cya). While with compounds **3** and **4** it is clearly possible to visualise transfected cells with a good (PEG11) to acceptable (PEG5) S/N ratio, compounds **1** and **2** are not fluorogenic. This suggests that the presence of the negative charge is necessary for reducing unspecific insertion of NR in the membrane or interactions of NR with BSA or other proteins present in the medium, which have been shown to dramatically increase the fluorescence QY of NR.¹⁰⁰ Compound **4** (PEG11 linker) showed a lower background compared to compound **3** (PEG5 linker). We hypothesize that this is due to the longer hydrophilic PEG11 linker, which reduces the overall hydrophobicity of the probe and therefore the unspecific interactions of NR with the membrane and BSA. This hypothesis is supported by the absorption and emission maxima of compound **3** which are approximately 20 nm blue shifted compared to compound **4** in DMEM + FBS 10% (Table 2).

In order to further understand the interactions of NR with BSA and other proteins present in the labeling and imaging medium, we decided to perform the same experiment in normal physiological medium (NPM), a salt buffer that contains neither FBS nor BSA.

HEK 293T transfected cells, expressing pDisplay-SNAP-CLIP-HCA, were labeled with BC-AlexaFluor 488, washed and treated with the NR compounds (500 nM, 30 min at RT) and imaged

with (Figure 17) or without (Figure 18) wash in NPM. NPM is a salt buffer consisting of (in mM): 1.8 CaCl_2 , 0.8 MgCl_2 , 10 glucose, 10 HEPES (pH 7.3), 5 KCl and 145 NaCl.

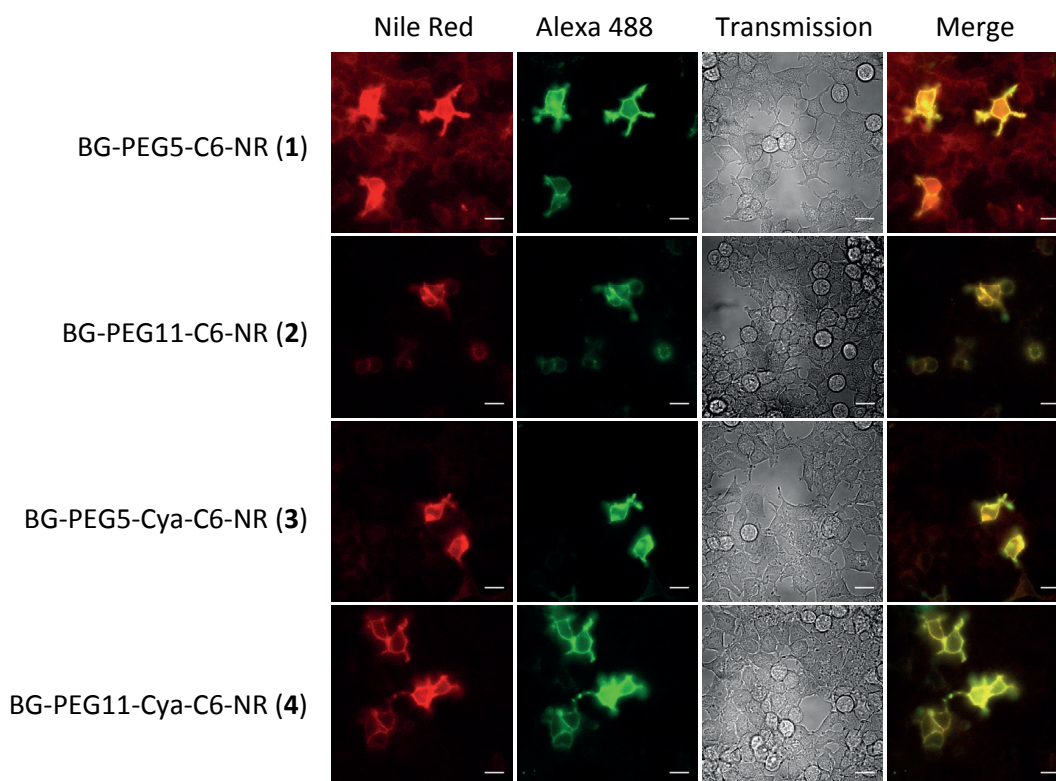


Figure 17: **Imaging after three washes in NPM.** HEK 293T cells transiently expressing pDisplay-SNAP-CLIP-HCA labeled with BC-AlexaFluor 488 (10 μM , 10 min incubation at 37 $^{\circ}\text{C}$, three washes with NPM) and compounds **1-4** (500 nM, 30 min incubation at RT, NPM) imaged after three washes. Scale bar, 20 μm . (N.B. The pictures in this figure have all been treated with the same settings. However, note that the settings between Figure 15 - Figure 18 are not the same.)

As it can be seen in Figure 17, there was clear co-localization between the channels of AlexaFluor 488 and NR for all compounds after three washes, suggesting the specific labeling of transfected cells. We observed a moderate unspecific signal from the membrane of non-transfected cells labeled with compounds **1** and **3** and we believe that this signal is due to residual affinities of these compounds for the membranes.

Interestingly, when cells were imaged without wash (Figure 18), the behavior of the NR derivatives was different compared to the one observed in DMEM + FBS 10%. First, in NPM, all compounds were fluorogenic (even compounds **1** and **2**). And second, it was possible to visualise transfected cells with very strong (compounds **1** and **3**) to acceptable (compounds **2** and **4**) background. These observations validated our hypothesis that the lack of fluorogenicity for compounds **1** and **2** in DMEM + FBS 10% was due to unspecific binding of NR to FBS and that the presence of the negatively charged Cya was necessary for preventing such interactions.

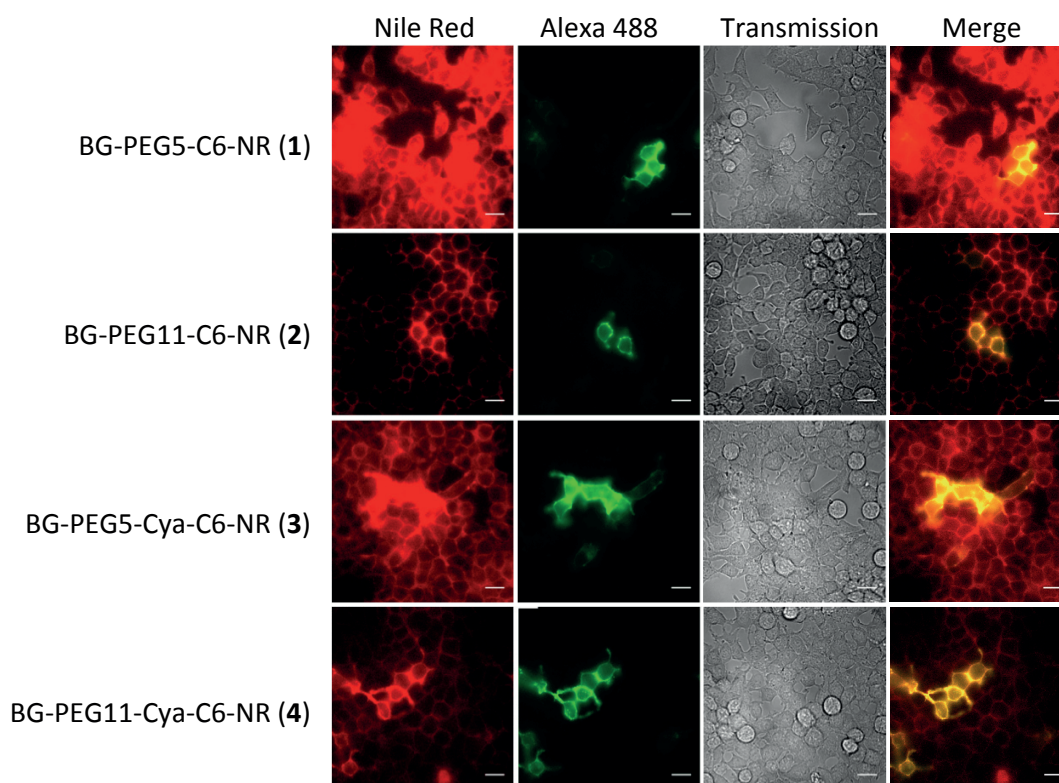


Figure 18: “No wash” imaging in NPM. HEK 293T cells transiently expressing pDisplay-SNAP-CLIP-HCA labeled with BC-AlexaFluor 488 (10 μ M, 10 min incubation at 37 $^{\circ}$ C, three washes with NPM) and compounds **1-4** (500 nM, 30 min incubation at RT, NPM) imaged without wash. Scale bar, 20 μ m. (N.B. The pictures in this figure have all been treated with the same settings. However, note that the settings between Figure 15 - Figure 18 are not the same.)

In addition, in “no wash” imaging, we observed a residual background from the membranes of non-transfected cells labeled with compounds **3** and **4** in NPM. This was not the case when the labeling was performed in DMEM + FBS 10%. We speculate that the residual background observed is due to the fact that in DMEM + FBS 10% the excess of the dye is interacting preferentially with FBS and not with the membranes. In the absence of FBS, this equilibrium is distorted and the dye enters unspecifically into all the membranes.

3.2.4 Visualisation of the SNAP-tagged HIR³

We decided to validate our proof-of-principle experiments with a pharmacologically interesting receptor: the HIR, expressed as a fusion protein with SNAP-tag on the extracellular part of the plasma membrane. We labeled CHO cells, stably expressing HIR-SNAP-tag fusion protein with the best performing compound **4** for 30 min at RT in F-12 HAM medium.

³ This experiment was performed by Dr Miwa Umebayashi, in Howard Riezman’s laboratory at the University of Geneva, Switzerland.

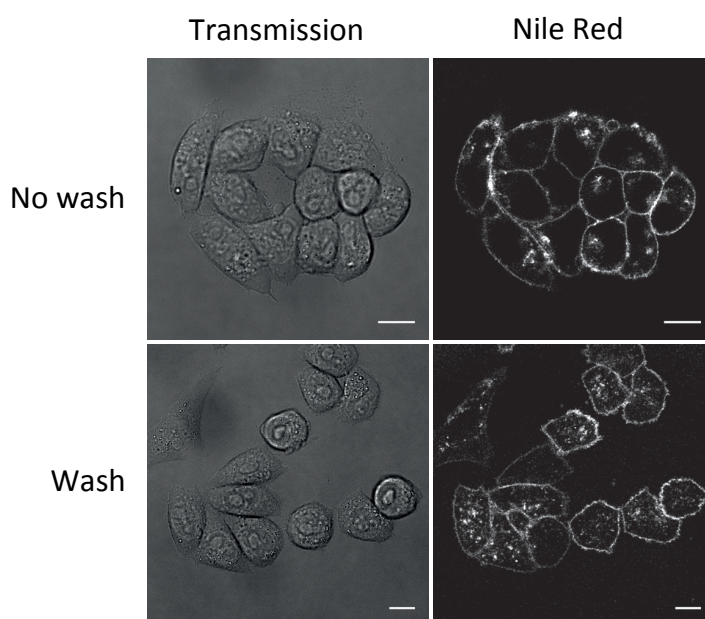


Figure 19: **Imaging of SNAP-HIR with compound 4.** CHO cells stably expressing extracellular SNAP-tagged HIR labeled with compound **4** (2 μ M, 30 min incubation at 37 $^{\circ}$ C in F-12 HAM medium), imaged before (no wash) and after three washes. Scale bar, 10 μ m.

Live cells were imaged using a confocal microscope directly after the labeling (no wash) or after three washes (Figure 19). We were happy to see that as with the artificial construct (SNAP-CLIP-HCA), compound **4** allowed the specific staining of all cells expressing the extracellular SNAP-tagged HIR, demonstrating that our strategy can be applied to a variety of other SNAP-tagged plasma membrane receptors. Moreover, a time-dependent internalization of the receptor was observed, highlighting the importance of the “no wash” property.

3.3 Conclusions

With the work described in Chapter 3, we have introduced a fluorogenic probe for SNAP-tagged plasma membrane proteins. We took advantage of the solvatochromic and fluorogenic character of NR in order to achieve specific labeling of cells expressing SNAP-fusion proteins.

NR derivatives were synthesized using two different PEG linkers (PEG5 and PEG11) and a negative charge or not (compounds **1-4**). For first experiments, we chose SNAP-CLIP-HCA expressed on the cell surface as a model fusion protein. We observed that indeed, when we labeled HEK 293T cells transiently expressing this fusion, NR was bound to SNAP-tag and due to the hydrophobic environment it was experiencing, it was turning fluorescent. Moreover, the importance of the linker length and the charge for “no wash” imaging was shown. Apparently, the longer hydrophilic PEG11 linker and the negatively charged Cya were necessary for imaging cells directly after labeling. Finally, we validated our proof-of-concept experiments by using the best performing ligand – compound **4** – for labeling HIR as a SNAP-fusion on the extracellular part of the plasma membrane.

Our choice of targeting our probe to SNAP-tag allows the generality of our approach, since after the optimization of the ligand, we could apply it to a variety of SNAP-fusion proteins. In addition, our “no wash” approach should make the real time monitoring of molecular events, like receptor trafficking, easier. We believe that this probe will prove to be a valuable tool for fluorescence imaging and study of cell surface receptors.

Chapter 4 A Voltage Sensor Based on NR

As a further application, we decided to study if our probes would be sensitive to changes of membrane potential. Monitoring potential changes has been a major challenge for scientists. Our probes based on NR and SNAP-tag would be an ideal candidate for creating a targeted voltage sensor for SNAP-tagged receptors (e.g. ion channels). These probes label specifically SNAP-tag, insert in the membrane and upon excitation, the increased dipole moment of NR could suggest that the dye could be sensitive to changes of the membrane potential.

4.1 Introduction

We chose voltage sensing as a second potential application of our probes. Cells are surrounded by the plasma membrane, which separates the cell from its external environment and regulates what ions enter and exit the cell.¹⁰¹ The membrane potential is the electrochemical difference that is observed between the external and the internal part of the cell (Chapter 4.1.2).¹⁰² Changes in membrane potential (or voltage fluctuations) are key events happening in important organs of our body, like the heart and the brain. For example, neurons communicate with each other with electrical signals that are manifested as rapid changes in membrane potential. Therefore, monitoring these potential changes has been a major challenge for scientists.¹⁰³ Traditionally, they used to measure these signals using electrodes, which proved to be a rather invasive method.¹⁰⁴ Voltage imaging was conceived in the late 60s and from the 70s until today, scientists have been trying to optimize organic voltage sensitive dyes.¹⁰⁵ In the last decades, many important improvements have been made in imaging electrical activity in invertebrate preparations.¹⁰⁶

4.1.1 Plasma Membrane

The cell is separated from its external environment by the plasma membrane, which consists of a variety of lipids and proteins. Some of the main roles of the proteins are to monitor the amount of molecules (e.g. ions) that enter or exit the cell, as well as transport the ions.¹⁰⁷ There are two types of ion transport: passive, where specific ions diffuse following electrochemical gradients; and active, where proteins transport ions across the membrane against those concentration gradients, using for example cellular energy (ATP). In this way, the cell maintains and restores specific concentration gradients across the plasma membrane.¹⁰⁷

4.1.1.1 Transport of Small Molecules Across the Membrane

Small molecules can pass across the plasma membrane, using different methods (Figure 20):

- 1) **Passive diffusion:** It is the simplest method of transport, since it does not involve the use of any proteins. Only small and hydrophobic molecules (i.e. not charged ions) diffuse into the lipid bilayer and flow down their concentration gradients (from higher to lower concentrations).¹⁰¹
- 2) **Facilitated diffusion:** As for passive diffusion, it does not require any additional external energy. However, in this case the molecules do not diffuse through the bilayer, but are transported via carrier or channel proteins. Thus, charged ions can also diffuse from the exterior to the interior part of the cell and vice versa.¹⁰¹
 - a. **Carrier proteins:** They bind specifically small molecules and then transfer them to the other side of the membrane by undergoing conformational changes.¹⁰¹
 - b. **Channel proteins:** They form aqueous pores allowing the free diffusion of molecules through the membrane. The best characterized channel proteins are the ion channels. They transport molecules rapidly, they are highly selective and their opening is regulated by gates that are responsive to specific stimuli:
 - (i) **voltage-gated channels:** They open and close depending on the membrane potential.
 - (ii) **ligand-gated channels:** They open and close depending on the binding of an external ligand.¹⁰¹

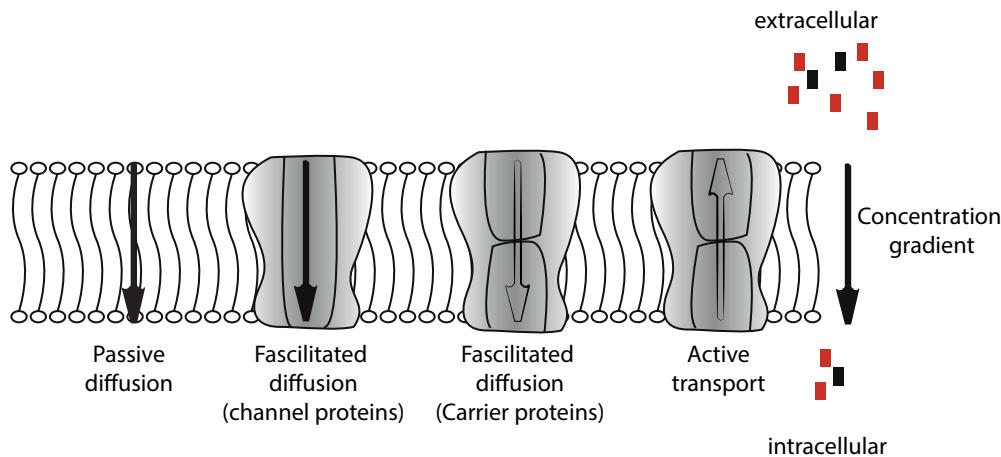


Figure 20: Methods to transport molecules through the plasma membrane: Passive transport (passive diffusion, facilitated diffusion by channel and carrier proteins) and Active transport.

- 3) **Active transport powered by ATP-hydrolysis (ion pumps):** Ion pumps facilitate the transport of ions against their concentration gradients, using energy coming from ATP-hydrolysis (e.g. Na^+/K^+ pump).¹⁰¹

- 4) **Active transport using pre-established ion gradients:** Active transport of molecules against concentration gradients, using energy which comes from the coupled transport of a second molecule in the energetically favorable direction (e.g. uptake of glucose).¹⁰¹

4.1.2 Membrane Potential

In animal cells, the absence of the cell wall around the plasma membrane suggests that they have to be protected from excessive osmotic forces by strict control of the osmolarity of the media inside and outside the cell. The media possess a gross distribution of ions and as a general rule, the concentration of K^+ ions is higher inside the cell than in the extracellular environment. On the other hand, Na^+ and Cl^- concentrations are higher outside than inside the cytosol.¹⁰⁸ Ions are charged, so the difference in ion concentration between the exterior and the interior milieu of a cell constitutes a difference of electrochemical potential – a synonym for membrane potential.¹⁰¹

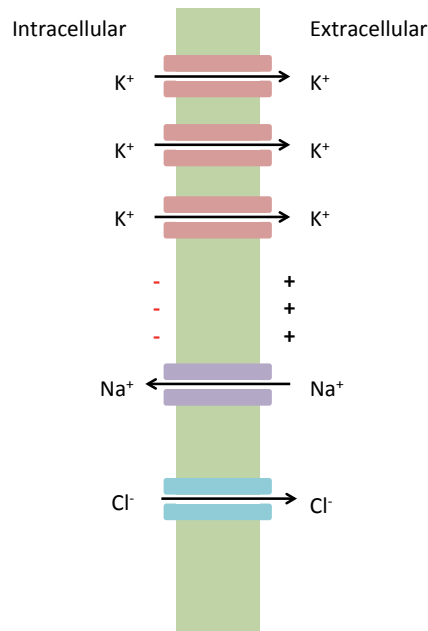


Figure 21: Ionic distribution in the extracellular and intracellular media. In resting conditions of the cell, there are 10 times more K^+ channels open than Na^+ or Cl^- , therefore the interior of the cell is negatively charged, leading to a resting membrane potential of -70 mV. These gradients of ions are maintained by the Na^+/K^+ pump. The figure is adapted from Cooper *et al.*¹⁰¹

These concentration gradients of each ion across the plasma membrane induce the diffusion of particles from higher to lower concentration.¹⁰⁸ In resting cells, there are ten times more open channels for the passive transport of K^+ than for Na^+ and Cl^- ions. At the same time, the higher concentration of K^+ ions inside the cell is mainly controlled by Na^+/K^+ ATPases, which are actively transporting the ions, using energy produced by ATP hydrolysis.¹⁰⁸ Due to the differences in ion concentrations across the plasma membrane, the resting membrane potential of cells is -70 mV, where the intracellular medium is negative relative to the extracellular.¹⁰⁷

4.1.3 Action Potential

In excitable cells (i.e. neurons and muscle cells) significant controlled fluctuations in membrane potential, such as depolarization (intracellular side less negative) and hyperpolarization (intracellular side more positive), play an important role in the propagation of action potentials in neuronal networks (i.e. signal transduction) and in muscle contractions.¹⁰⁷ These local and rapid reversals in membrane potential (i.e. transient action potentials) result from rapid ion redistributions, mainly of K^+ , Na^+ and Ca^{2+} ions, due to sequential opening and closing of voltage-gated ion channels (i.e. changes in membrane ion permeabilities). An action potential is a cycle that lasts 1-2 ms, characterised by membrane depolarization (opening of voltage-gated Na^+ channels), repolarization (opening of voltage-gated K^+ channels) and re-establishment of initial steady-state transmembrane potential (Figure 22).¹⁰⁷ Thanks to the axon conductance of these electric impulses (unidirectional propagation from the cell body to the axon terminus), a message can be propagated rapidly along the axon.¹⁰⁷

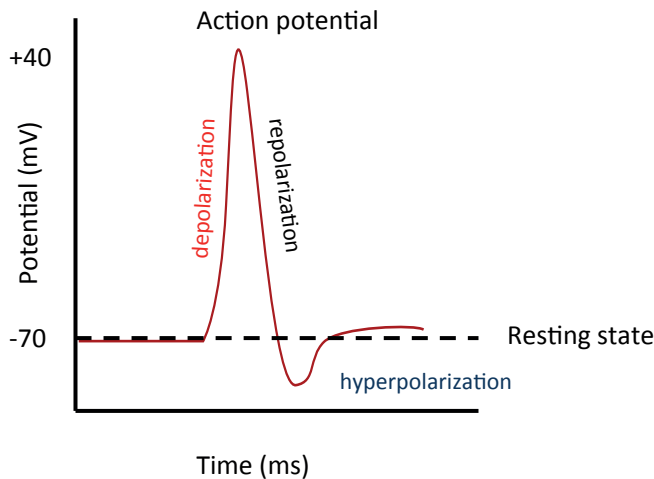


Figure 22: Changes in membrane potential during an action potential of excitable cells. The resting potential of the cell corresponds to the dashed line (-70 mV).

4.1.4 Patch Clamp Technique

Electrophysiologists interrogate the plasma membrane, the channels and the ions by electrical methods, in order to investigate the way excitable cells like neurons and muscle cells communicate with each other. The currents of ions flowing through single ion channels were recorded for the first time with the patch clamp method, which was developed by Erwin Neher and Bert Sackmann in 1976.¹⁰⁹ They received the Nobel Prize in Physiology or Medicine in 1991 for their work.

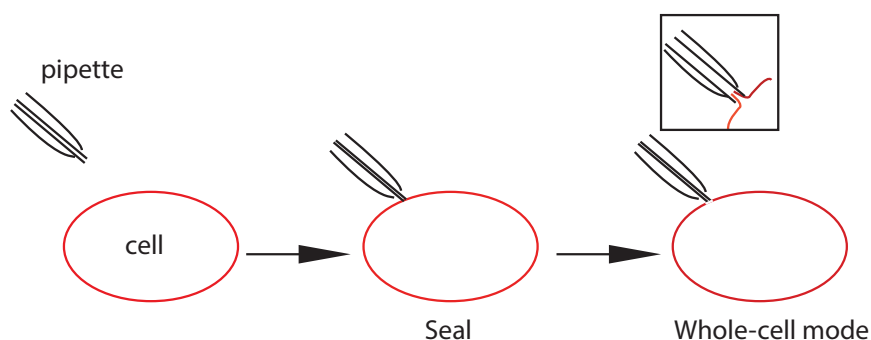


Figure 23: Patch clamp technique steps. A glass microelectrode is used to patch a cell. After seal formation, applying a strong pulse of suction ruptures the membrane of the cell and the microelectrode gets in contact with the intracellular medium of the cell.

In the whole-cell patch clamp method, the recording electrode is placed inside the glass micropipette and a reference ground electrode is put in the bath solution of the cell. The heat-polished micropipettes, that have an opening of 0.5-1 μm , are used to patch the cell membrane and with the application of a pulse of suction, a piece of the membrane is sucked into the pipette interior creating a seal. Then, the membrane is ruptured allowing the electrode to be in direct electrical contact with the interior of the cell (Figure 23).^{108,109}

4.1.5 Voltage Indicators

4.1.5.1 Genetically Encoded Voltage Indicators

Several attempts have been made to develop voltage sensitive fluorescent proteins. Most consist of a voltage sensitive domain of an ion channel that either fluoresces itself or it is connected to fluorescent protein(s) that does not sit on the plasma membrane and does not experience the membrane potential.¹⁰⁴

Different mechanisms of action have been reported so far. Some genetically encoded voltage indicators undergo a conformational change that alters their fluorescence spectra. In other cases, allosteric interactions change the environment or reorientate the fluorophore (e.g. FRET).¹¹⁰

The main advantage of voltage sensitive fluorescent proteins is that they can be targeted to a particular subset of cell-types, allowing like this the specific monitoring of cell-type populations. However, they show small fluorescence changes (<5%) per 100 mV change of membrane potential.¹⁰⁴

4.1.5.2 Organic Voltage Sensitive Probes

Voltage indicators constitute a non-invasive method for monitoring membrane potential fluctuations. They are normally chromophores with specific features. First, most voltage sensitive dyes are charged or have strong dipole moments in order to be electrically

sensitive.^{104,111} Second, they are inserted in the membrane or are localised to its surface in order to be able to “see” the electric field. Third they specifically bind on the plasma membrane (the external part of the cell membrane) and do not internalize, since internal membranes are not sensitive to the plasma membrane voltage. Finally, they have a high fluorescence QY and photostability, in order to avoid phototoxicity and damage of the plasma membrane by strong and longterm illumination.^{104,111}

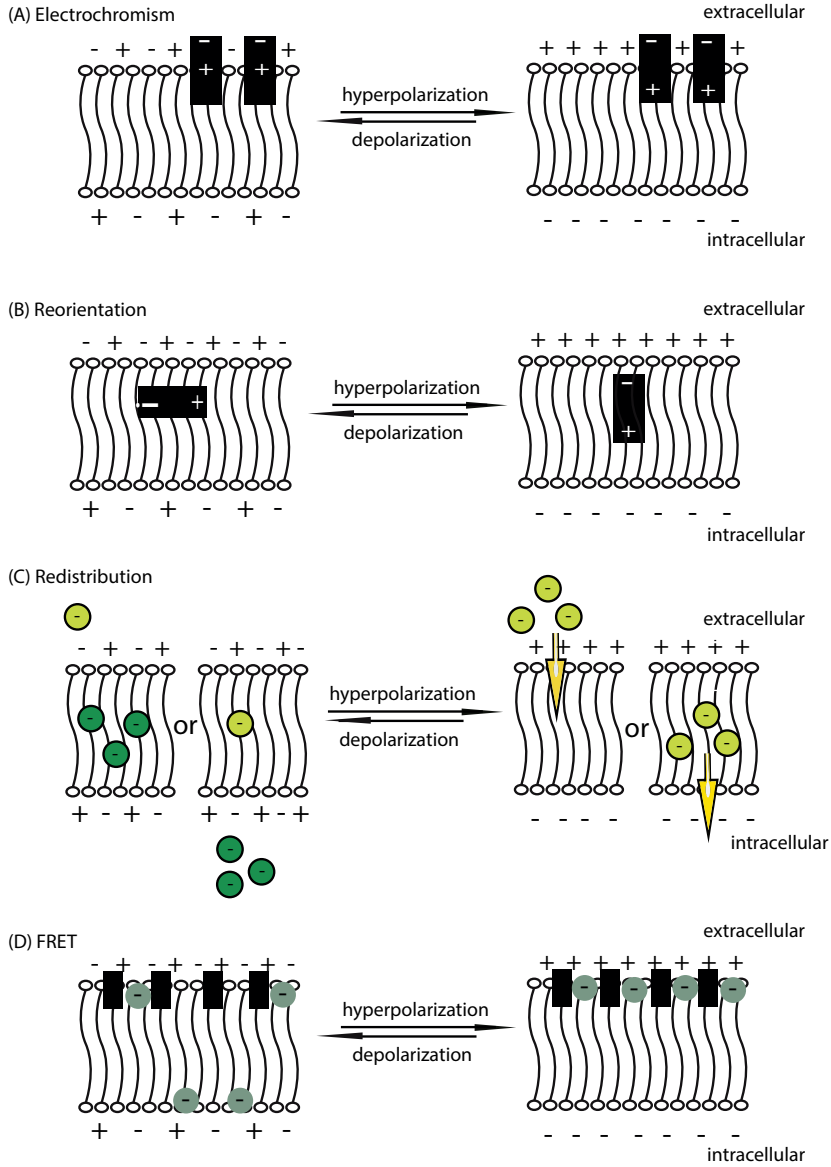


Figure 24: Four response mechanisms of membrane potential sensitive probes. (A) Electrochromic dyes change their electronic structure. (B) Dyes that reorient in the plasma membrane. (C) Dyes that redistribute upon change of the membrane potential. (D) Negatively charged fluorophores that act as FRET acceptors and move to the inner side of the lipid bilayer upon depolarization.

Voltage sensitive dyes can be divided into three categories based on their mechanism of action:

- 1) **Fast-response probes:** Probes that belong to this category can react to a change of the electric field with two mechanisms: reorientation and electrochromism.¹⁰⁵

In the **reorientation mechanism**, the dye is flipping from a perpendicular to a parallel orientation to the cell surface. This leads to a change of environment and therefore a change in the fluorescent properties of the molecule. Merocyanine dyes have been shown to have this mechanism of action (Figure 24B, Figure 25A).¹¹²

In the **electrochromic mechanism** the dyes change their electronic structure and therefore their fluorescent properties upon change of membrane potential (Figure 24A). Examples of such probes are the di-4-ANEPPS and di-8-ANEPPS dyes (Figure 25B).^{33,113} Di-4-ANEPPS has an electron π -rich system on one end and an electron deficient π -system on the other end and it is positioned with approximately a perpendicular orientation to the membrane. Upon change of the electric field, there is a redistribution of electrons, which results to a shift in the fluorescence properties of the dye.^{114–116}

These probes have a relatively fast optical response (millisecond range) and they show a moderate 2 – 10% fluorescence change per 100 mV. The typical electrochromic probes are polar, lipophilic and they are mostly derivatives of styryl or hemicyanine dyes.^{117,118}

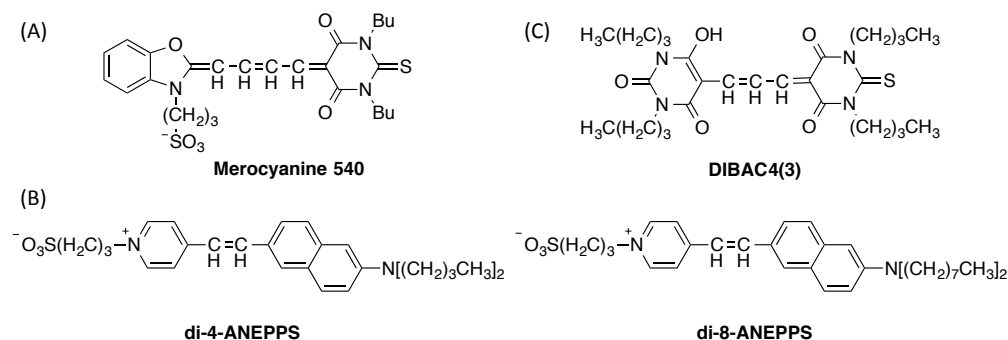


Figure 25: Chemical structures of examples of organic voltage sensitive probes. (A) Merocyanine 540 (fast-response probe, reorientation). (B) di-4-ANEPPS and di-8-ANEPPS (fast response probes, electrochromism). (C) DIBAC₄(3) (slow response probe, redistribution).

- 2) **Slow-response probes:** These probes change their distribution¹¹⁹ and therefore their fluorescence properties upon change of membrane potential (Figure 24C). Usually, most of the probes that belong in this category are dyes with cyanine and oxonol chromophores that move from the aqueous extracellular environment into the plasma membrane, leading to an increase in fluorescence intensity.¹²⁰ An example of a slow-response probe is DiBAC₄(3) (Figure 25C), an oxonol dye which translocates from the plasma membrane to the cell cytosol upon membrane depolarization, leading to an increased concentration in the cytosol and therefore an increased fluorescence intensity.¹²¹ These probes have a much more significant fluorescence change (1% per mV) compared to the fast-response probes.

- 3) **FRET mechanism:** A donor fluorophore is anchored to extracellular part of the plasma membrane. Upon excitation, the donor transfers its energy to an acceptor fluorophore that is nearby. Upon depolarization of the plasma membrane, if the acceptor is negatively charged, it will move to the inner part of the plasma membrane leading to resulting to a reduction of FRET (Figure 24D). This mechanism of action has been used by a FRET system of an oxonol acceptor (DPA) and a coumarin donor.^{122,123} This mechanism has a very high sensitivity.

4.1.6 NR as a Potential Voltage Sensitive Dye

NR has attractive properties that would make it an ideal candidate as a voltage sensitive dye.

First, it has a strong dipole moment upon excitation, which could suggest it is electrically sensitive.

Second, NR is an environment-sensitive dye: its fluorescent properties depend strongly on the polarity of its environment. Therefore, a change in the membrane potential could lead to a translocation of NR to a region with a different polarity and therefore could cause a change of its fluorescent properties, which would be a perfect readout for a voltage sensor.

Third, it has a high affinity for the membrane, where due to the apolar environment its fluorescence QY reaches values close to unity. Our approach would allow reducing this affinity of NR for the membrane and create a turn-on probe for specific plasma membrane receptors of interest. The specific anchoring of our probes to SNAP-tag would generate a targeted voltage sensor – an advantage that so far is a characteristic of genetically encoded voltage indicators.

Finally, the fluorogenic property of our probe would permit its use in cases where a washing step for the removal of the excess of the dye is not possible, like in *in vivo* experiments.

4.2 Results

4.2.1 Design of NR Derivatives with Additional Charges⁴

Most voltage-sensitive dyes are negatively or positively charged to enhance their sensitivity in detecting characteristic changes in electric field upon excitation.¹⁰⁴

⁴ The synthesis of compounds **5-9** was performed with the help of Nicole Vassali, during her master thesis under my supervision.

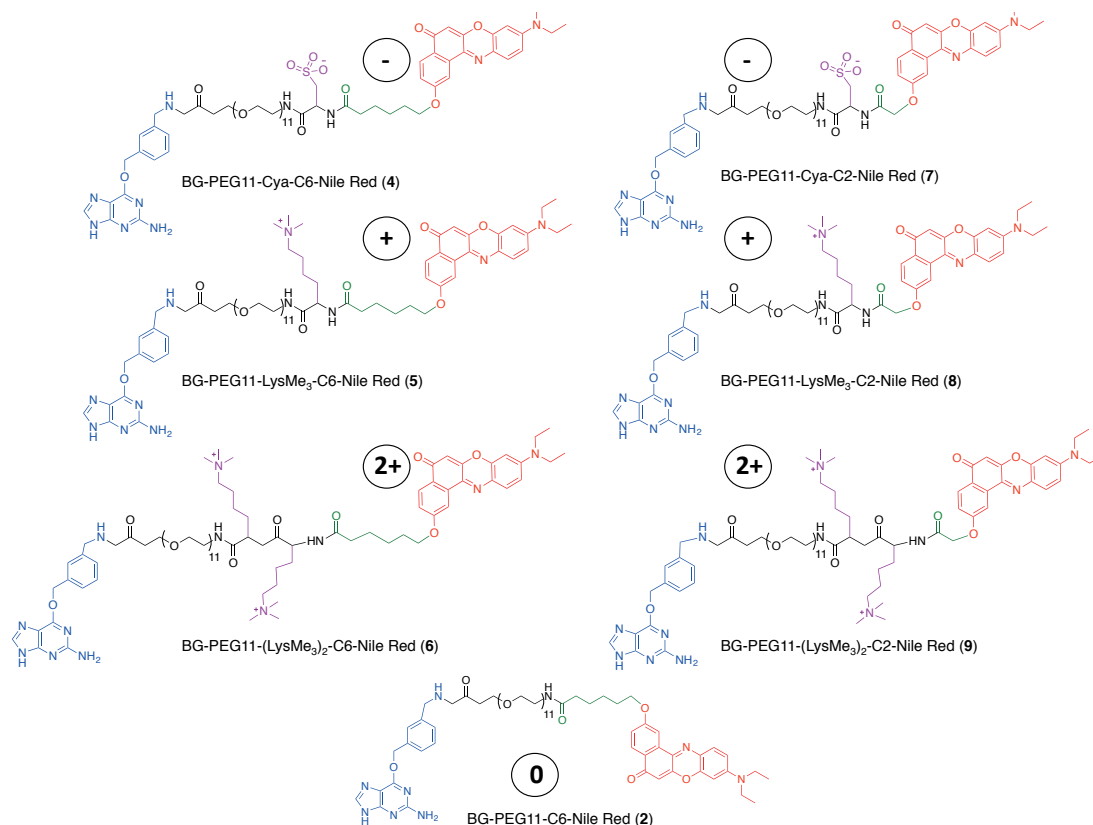


Figure 26: Structures of NR derivatives with multiple charges (compounds 4-9). They consist of a benzylguanine moiety (blue), a PEG11 linker (black), different charges (purple), a C-2 or C-6 linker between the charge and NR (green) and NR (red).

Therefore, we decided to expand the library of NR compounds by focusing on the PEG11 linker - the best performing one - and varying:

- the charges (one positive, one negative, or two positive charges) and
- the linker length between the charged moiety and NR (C-2 or C-6)

We synthesized compounds 5-9 (Figure 26). Compounds 4-6 have a C-6 linker between the charge and NR and compounds 7-9 a C-2 linker.

4.2.2 *In Vitro* Characterization of NR Derivatives 2 and 4-9.

We first tested whether all the NR derivatives maintained the solvatochromic properties of NR and if the linker length or the charge variation had an effect on the fluorescent properties of the dye. We measured the absorption and emission maxima, as well as the fluorescence QY in solvents of different polarity like dioxane, PBS and DMEM + FBS 10%, as before.

Table 5: Spectroscopic properties including absorption and emission maxima and QY for compounds **2** and **4-9**, measured in PBS, DMEM + FBS 10% and dioxane.

Derivative		Solvent								
		PBS			DMEM + FBS 10%			Dioxane		
		λ_{abs} , nm	λ_{fl} , nm	QY, %	λ_{abs} , nm	λ_{fl} , nm	QY, %	λ_{abs} , nm	λ_{fl} , nm	QY, %
BG-PEG11-C6-NR (2)	0	601	661	2.3	584	628	6.3	526	593	73.0
BG-PEG11-Cya-C6-NR (4)	-	602	661	2.7	595	645	6.0	526	592	73.0
BG-PEG11-LysMe3-C6-NR (5)	+	585	662	3.0	588	648	7.6	522	609	70.2
BG-PEG11-(LysMe3) ₂ -C6-NR (6)	2+	585	661	3.8	587	651	n.d.	524	609	79.0
BG-PEG11-Cya-C2-NR (7)	-	597	661	2.3	594	658	4.6	522	608	70.2
BG-PEG11-LysMe3-C2-NR (8)	+	600	662	2.3	602	661	5.3	528	614	61.4
BG-PEG11-(LysMe3) ₂ -C2-NR (9)	2+	597	662	3.0	602	661	3.8	526	611	61.4

n.d. Not determined

We observed that all the derivatives maintained the solvatochromic properties of NR and showed a hypsochromic shift in dioxane, compared to PBS (Table 5). Moreover, their fluorescence QY was significantly increased in an apolar solvent, like dioxane and they were almost non-fluorescent in PBS.

4.2.3 In Cellulo Characterization of NR Derivatives **2** and **4-9**

4.2.3.1 Imaging of live HEK 293T Cells with Compounds **2** and **4-9**

We then decided to test the new NR derivatives for live cell imaging. We used HEK 293T cells expressing the SNAP-CLIP-HCA fusion protein on the extracellular part of the plasma membrane, that again allowed co-staining of CLIP-tag with a different fluorophore to unambiguously identify the transfected cells. Thus, we labeled the cells with BC-AlexaFluor 488, washed and treated them with the NR derivatives (500 nM, 30 min at RT) and imaged them after three washes in DMEM + FBS 10% (Figure 27).

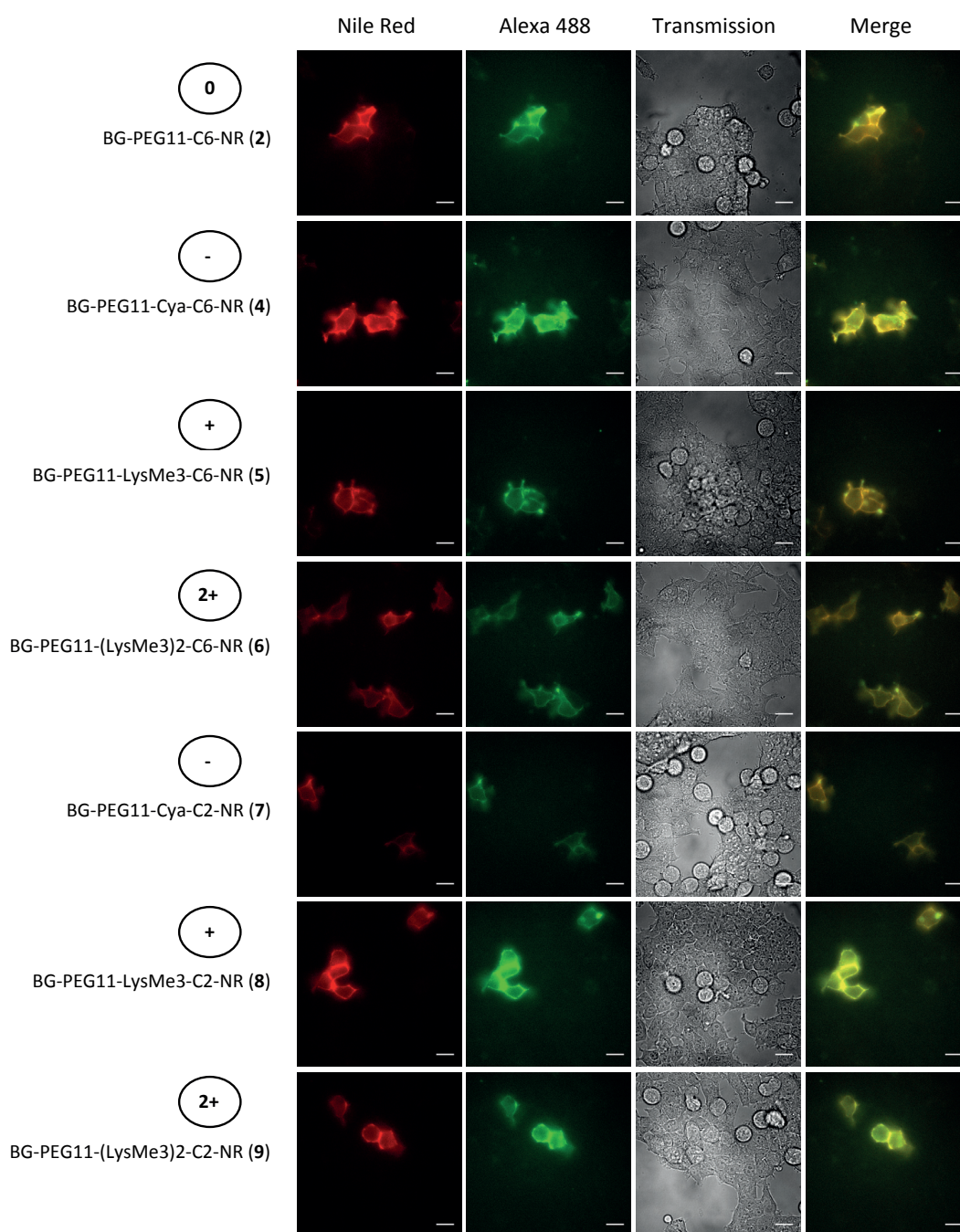


Figure 27: **Imaging after three washes in DMEM + FBS 10%.** HEK 293T cells transiently expressing pDisplay-SNAP-CLIP-HCA labeled with BC-AlexaFluor 488 (10 μ M, 10 min incubation at 37 $^{\circ}$ C, three washes with DMEM + FBS 10%) and compounds **2** and **4-9** (500 nM, 30 min incubation at RT, DMEM + FBS 10%) imaged after three washes. Scale bar, 20 μ m. (*N.B.* The pictures in this figure have all been treated with the same settings. However, note that the settings between Figure 27-Figure 30 are not the same.)

All compounds showed clear co-localization between the two channels, suggesting that the NR derivatives label specifically only the transfected cells after reaction with SNAP-tag and experiencing a hydrophobic environment that turns fluorescence on.

We then wanted to investigate if the different charges and linkers had an effect on the “no wash” property that we were able to observe for the previous NR derivatives we tested (Figure 16). Therefore, we imaged the HEK 293T cells directly after labeling with the NR derivatives without any prior washing steps (Figure 28).

Interestingly, there was a significant difference between compounds **4-6** (which have a C-6 linker between the charge and NR) and compounds **7-9** (which have a C-2 linker). Apparently, the shorter distance of the charge from NR leads to a higher S/N ratio presumably by reducing the unspecific interactions of NR with BSA or other proteins present in the medium. This is also supported by the *in vitro* data for these compounds (Table 5) that showed a red shift of approximately 10 nm between compounds **4-6** and **7-9** in DMEM + FBS 10%, suggesting stronger interactions of the first with FBS.

Moreover, we observed that the negatively charged compound **4** appeared to have a higher background compared to the positively charged compounds **5** and **6** (Figure 28). Based on the *in vitro* results (Table 5) we cannot conclude that this behavior is due to the fact that compound **4** has stronger interactions with FBS, than compounds **5** or **6**. We speculate that the higher background of compound **4** is due to unspecific binding of the derivative to poly-D-lysine, which is positively charged and is used for coating of the coverslips.

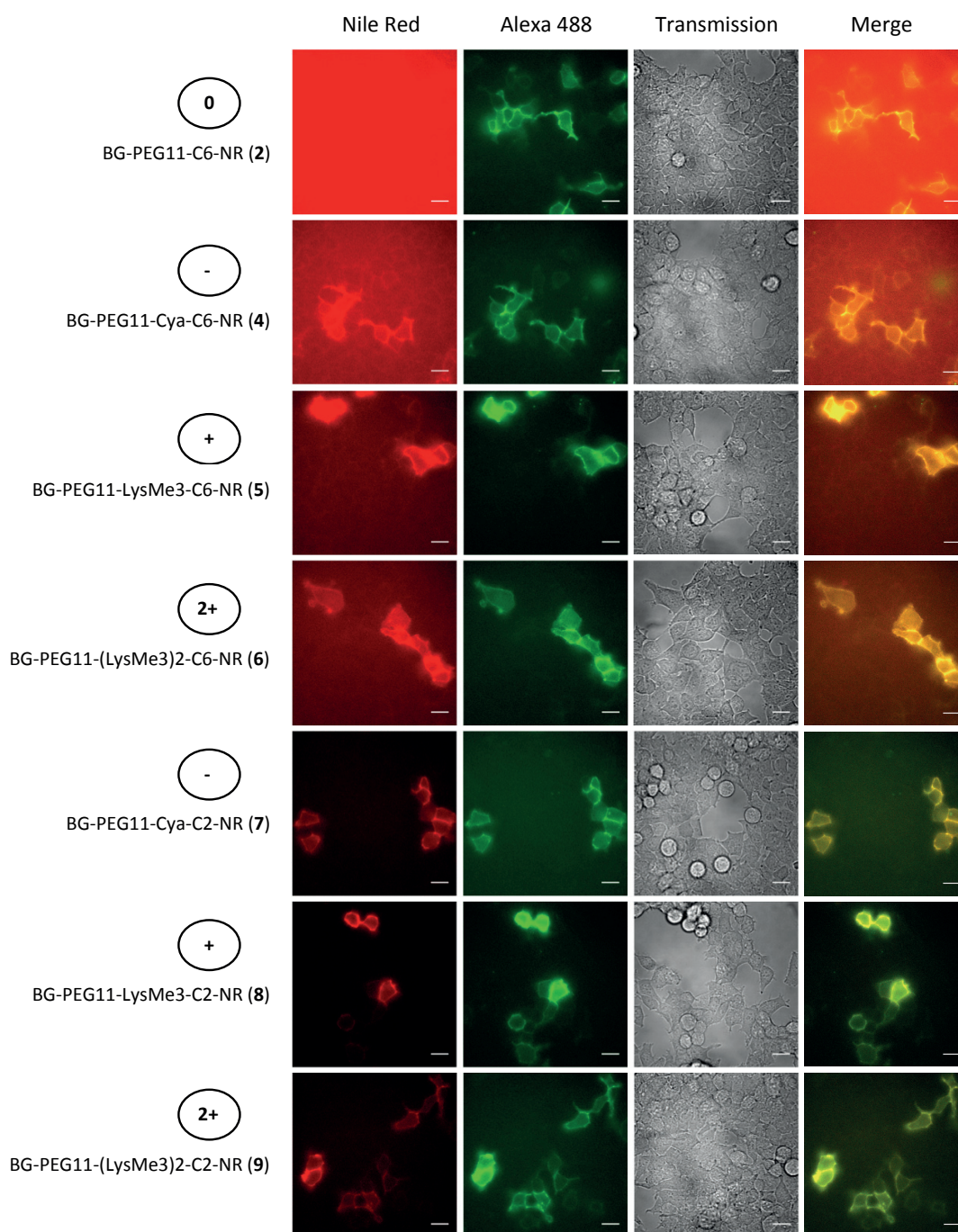


Figure 28: “No wash” imaging in DMEM + FBS 10%. HEK 293T cells transiently expressing pDisplay-SNAP-CLIP-HCA labeled with BC-AlexaFluor 488 (10 μ M, 10 min incubation at 37 $^{\circ}$ C, three washes with DMEM + FBS 10%) and compounds **2** and **4-9** (500 nM, 30 min incubation at RT, DMEM + FBS 10%) imaged without wash. Scale bar, 20 μ m. (N.B. The pictures in this figure have all been treated with the same settings. However, note that the settings between Figure 27-Figure 30 are not the same.)

In order to investigate the effect of FBS, as before, we decided to repeat the same experiment on live cells, but perform the labeling and imaging in NPM, a salt medium that does not contain FBS. NPM is a salt buffer consisting of (in mM): 1.8 CaCl_2 , 0.8 MgCl_2 , 10 glucose, 10 HEPES (pH

7.3), 5 KCl and 145 NaCl. We imaged the cells after three washes (Figure 29) or directly after labeling in NPM (Figure 30).

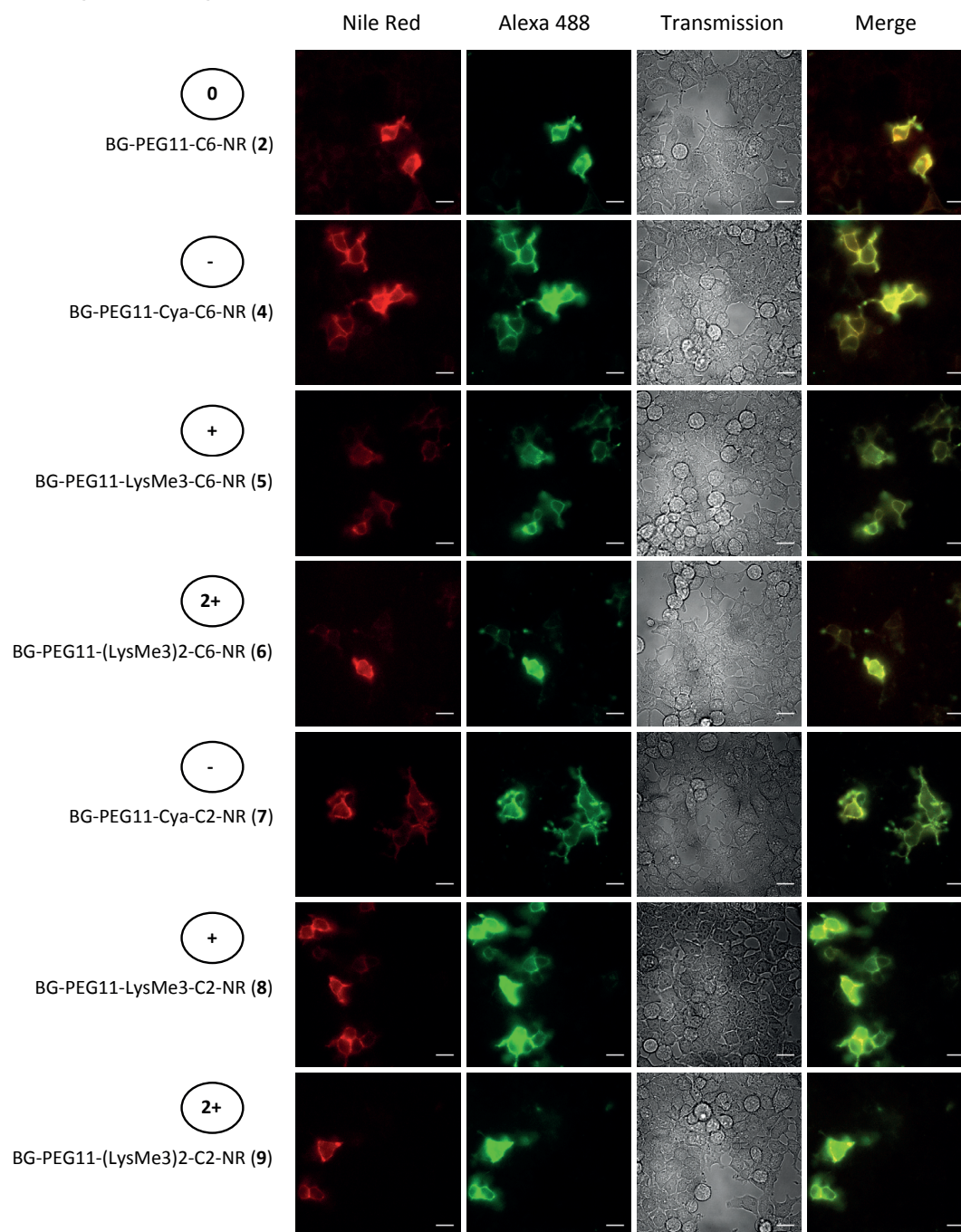


Figure 29: **Imaging after three washes in NPM.** HEK 293T cells transiently expressing pDisplay-SNAP-CLIP-HCA labeled with BC-AlexaFluor 488 (10 μ M, 10 min incubation at 37 $^{\circ}$ C, three washes with NPM) and compounds **2**, **4-9** (500 nM, 30 min incubation at RT, NPM) imaged after three washes. Scale bar, 20 μ m. (*N.B.* The pictures in this figure have all been treated with the same settings. However, note that the settings between Figure 27-Figure 30 are not the same.)

All compounds labeled specifically transfected cells when imaged after three washes (Figure 29). On the other hand, in “no wash” experiments the remaining of the excess of the dye resulted in visualising the cells with high (compound **4**) to moderate (compounds **5** and **6**) and low

(compounds **7-9**) background (Figure 30). We observed a slightly higher background for all compounds in NPM (Figure 30) than in DMEM + FBS 10% (Figure 28). As mentioned before, we hypothesize that the excess of the dye is interacting preferentially with FBS than with the membranes, and in absence of FBS this equilibrium is distorted leading to unspecific insertion of the dye in the membrane.

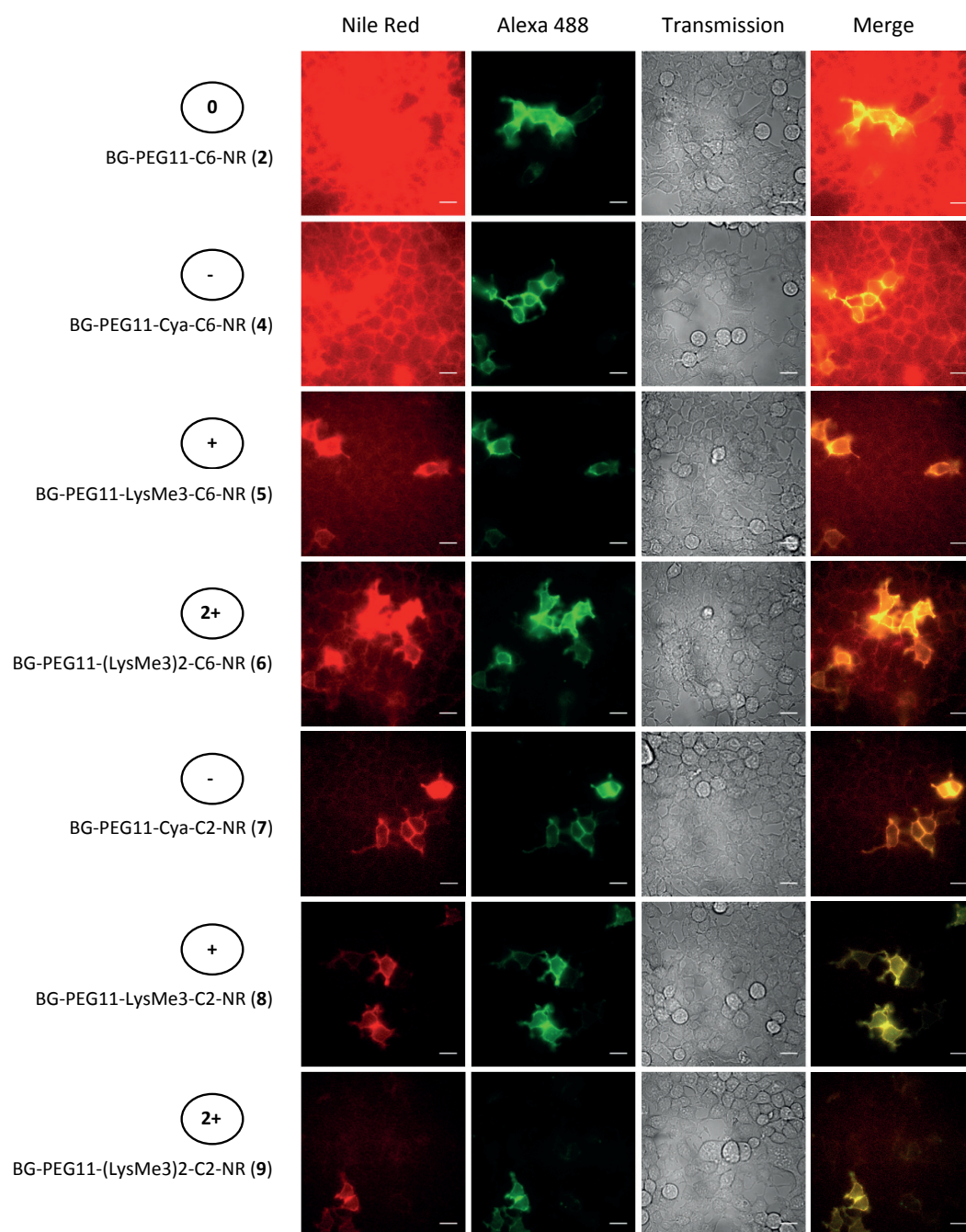


Figure 30: “No wash” imaging in NPM. HEK 293T cells transiently expressing pDisplay-SNAP-CLIP-HCA labeled with BC-AlexaFluor 488 (10 μ M, 10 min incubation at 37 $^{\circ}$ C, three washes with NPM) and compounds **2** and **4-9** (500 nM, 30 min incubation at RT, NPM) imaged without wash. Scale bar, 20 μ m. (N.B. The pictures in this figure have all been treated with the same settings. However, note that the settings between Figure 27-Figure 30 are not the same.)

In conclusion, from the *in cellulo* experiments, we observed that the presence of a charge and a short linker (C-2) between the latter and NR (compounds **7-9**) are essential for reducing the unspecific interactions of NR with membranes and other proteins present in the medium and therefore allow a good S/N ratio for “no wash” imaging.

4.2.3.2 Patch Clamp Experiments of Compounds 4-9 on Live HEK 293T Cells ⁵

Having studied the labeling efficiency and fluorogenicity of these probes on live cells and having assured that compounds **4-9** retain the fluorescent properties of parent NR, we decided to test if these probes were voltage sensitive. Therefore, the response of the NR derivatives **4-9** was established in whole-cell-patched, voltage clamped HEK cells.

Cells transiently expressing SNAP exposed on the extracellular side of the plasma membrane were labeled with the NR compounds (1 μ M, 30 min at RT) in extracellular buffer (EB) w/o FBS and washed three times with EB. EB is a salt medium (w/o FBS) consisting of (in mM): 150 NaCl, 5 KCl, 1 MgCl₂, 2 CaCl₂, 5 glucose, 10 HEPES; pH 7.4 adjusted with NaOH, 300 mOsm. Throughout the course of evaluation in HEK cells (45 to 60 min) at RT, we observed negligible dye internalization. Whole-cell voltage clamped HEK cells were held at -50 mV and then stepped to hyper- and depolarizing potentials in 50 mV steps (range \pm 100 mV, always returning to -50 mV after each 50 mV step as a control, Figure 31A).

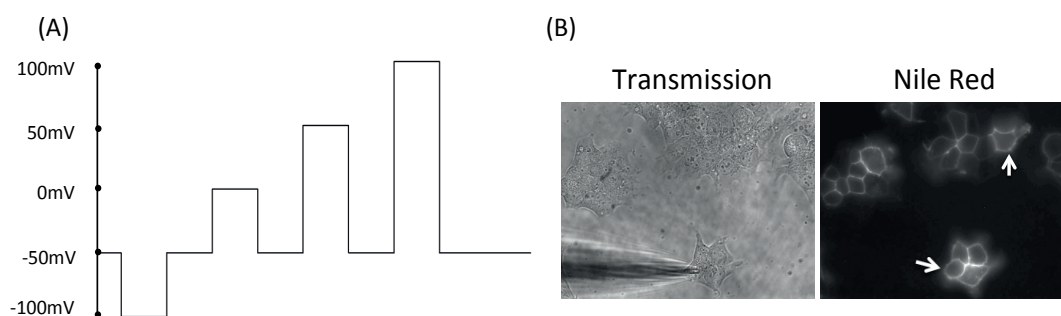


Figure 31: (A) Protocol of membrane potential change followed during the experiment. (B) HEK 293 T Cells expressing extracellular SNAP labeled with compound **4**. The white arrows indicate an example of patched and non-patched cells, which were analysed.

We investigated if the fluorescent properties of NR would be sensitive to the changes of membrane potential we applied and therefore we always analysed the fluorescence intensities of patched cells and non-patched cells as a control (Figure 31B). Unfortunately, as seen in Figure 32, there was no change observed upon 100 mV membrane potential changes for any of the NR compounds tested.

⁵ The patch clamp experiments were performed by me, with the help of Dr Mayya Sundukova, in Paul Heppenstall's laboratory at EMBL, Monterotondo.

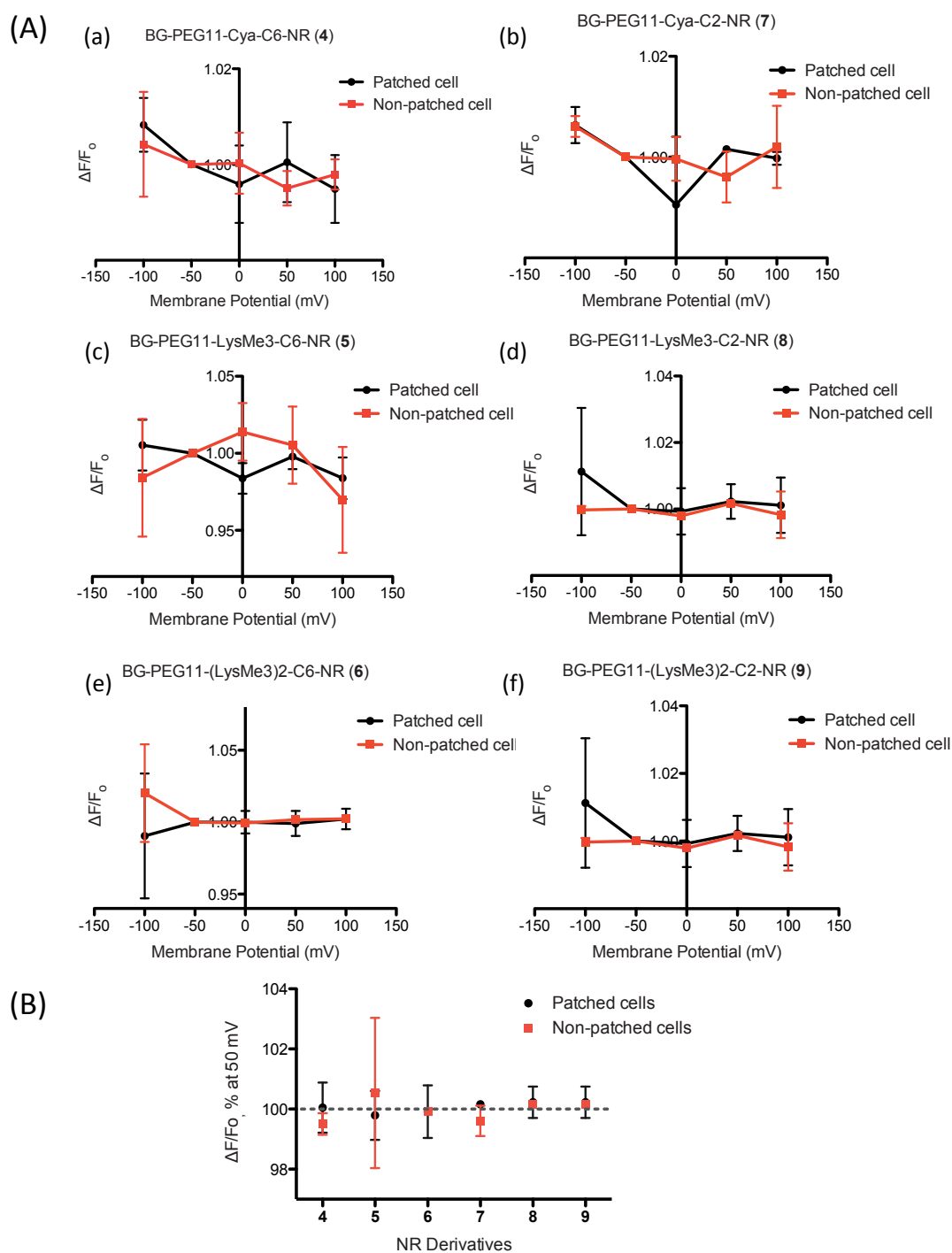


Figure 32: (A) Measurement of fluorescence intensity relative to the membrane potential of HEK 293T cells expressing extracellular SNAP and labeled with compounds **4-9** in EB for patched and non-patched cells using the patch clamp method. (B) Change of Fl. intensity of compounds **4-9** upon 100 mV membrane potential change for patched cells (black) and non-patched cells (red).

These results suggested different hypotheses:

- (i) Unlike to our expectations, NR was not voltage sensitive and
- (ii) NR was maybe experiencing a hydrophobic environment, which was not caused from insertion in the membrane,
- (iii) The orientation of NR in the membrane after binding to SNAP-tag was not optimal, resulting in a weak response to the electric field.

4.2.4 Compound NR12S as a Control for the Voltage Sensitivity of NR

In order to answer our questions, we decided to study the voltage sensitivity of compound NR12S. As mentioned in chapter 1.6.2.3 of the introduction, NR12S was designed by Kucherack *et al.* and is localised in the outer leaflet of the bilayer.⁸¹

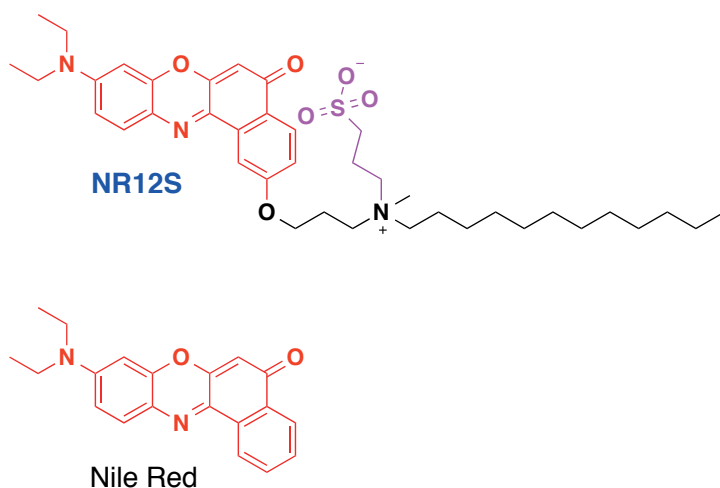


Figure 33: Structures of compound NR12S and NR.

Since it has been shown to be inserted in the membrane, we decided that NR12S would be the perfect control in order to understand if NR itself is voltage sensitive or not. Therefore, NR12S was synthesized as previously reported.⁸¹

4.2.4.1 *In Vitro* Characterization of NR12S

The spectroscopic properties of NR12S were studied in comparison to the ones of parent NR in solvents of different polarity like PBS, dioxane and DMEM + FBS 10%. As seen in Table 6, the λ_{abs} and λ_{fl} measured were similar to the values reported in literature⁸¹ and the two compounds behaved similarly in the different solvents. A small difference was observed in apolar solvents, like dioxane, probably due to close proximity of a charged polar group for NR12S.

Table 6: Spectroscopic properties including emission and absorption maxima and QY for compounds NR12S and NR measured in PBS, DMEM + FBS 10% and dioxane.

Derivative	Solvent								
	PBS			DMEM + FBS 10%			Dioxane		
	λ_{abs}, nm	λ_{fl}, nm	QY, %	λ_{abs}, nm	λ_{fl}, nm	QY, %	λ_{abs}, nm	λ_{fl}, nm	QY, %
NR12S	526	660	0.2 ^a	526	620	7.6	528	597	74.0 ^a
Nile Red	571	657	5.0 ^a	563	619	n.d.	525	587	91.0 ^a

n.d.: not determined

*a: corresponds to reference*⁸¹.

4.2.4.2 In Cellulo Characterization of NR12S

4.2.4.2.1 Imaging of Live HEK 293T Cells with NR12S

We tested the labeling of live cells with the compound NR12S and observed if it was also fluorogenic like our NR derivatives. We labeled live HEK 293T cells with compound NR12S (500 nM) in DMEM + FBS 10% (A) or in NPM (w/o FBS) (B) and recorded images directly after labeling (no wash) or after three washing steps. As seen in Figure 34, NR12S appears to be non-fluorogenic in DMEM + FBS 10%.

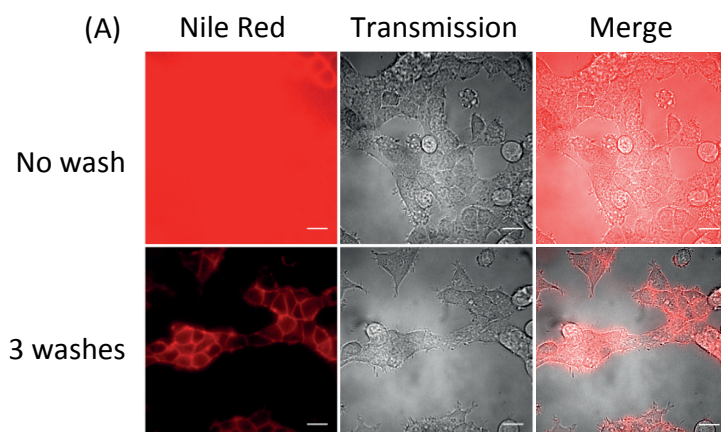
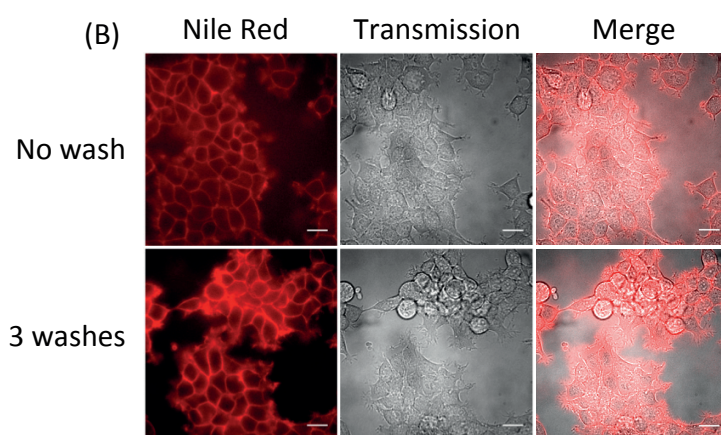
DMEM + FBS 10%**NPM**

Figure 34: **Imaging of live cells with NR12S.** HEK 293T cells, non-transfected, labeled with NR12S (500 nM, 7min at RT) and imaged directly after labeling (No wash) or after three washes (A) in DMEM + FBS 10%, and (B) in NPM (w/o FBS). Scale bar, 20 μ m. (*N.B.* The images in this figure have been treated with the same settings.)

We assume that the absence of fluorogenicity is due to interactions of NR12S with BSA or other proteins present in the labeling and imaging medium, a speculation which is also supported by the *in vitro* results (Table 6), where a blue shift of 40 nm is observed between the maximum emission measured in DMEM + FBS 10% and PBS. Moreover, as seen in Table 5 and Table 6, compound **4**, which is fluorogenic in DMEM + FBS 10% is 25 nm red shifted compared to NR12S, a fact which is supporting that the lack of fluorogenicity for NR12S is due to interactions of the dye with BSA.

4.2.4.2.2 Patch Clamp Experiments of NR12S on Live HEK 293T Cells⁶

Having tested the *in vitro* and *in cellulo* behavior of the compound NR12S, we decided to establish its voltage response in whole-cell voltage clamped HEK cells. Therefore, HEK 293T cells were labeled with the NR12S compound (500 nM, 7 min at RT). Throughout the course of evaluation in HEK cells (45 to 60 min) at RT, we observed negligible dye internalization. Whole-cell voltage-clamped HEK cells were held at -50 mV and then stepped to hyper- and depolarizing potentials in 50 mV steps (range ± 100 mV, always returning to -50 mV after each step as a control, Figure 35A).

Interestingly, we observed a 5% decrease in fluorescence intensity upon 100 mV increase of membrane potential (Figure 35B). We also analyzed non-patched cells and the background noise as a control, in order to be certain that the change in fluorescence intensity we observed was specific for the patched cells and only due to change of membrane potential (Figure 35B).

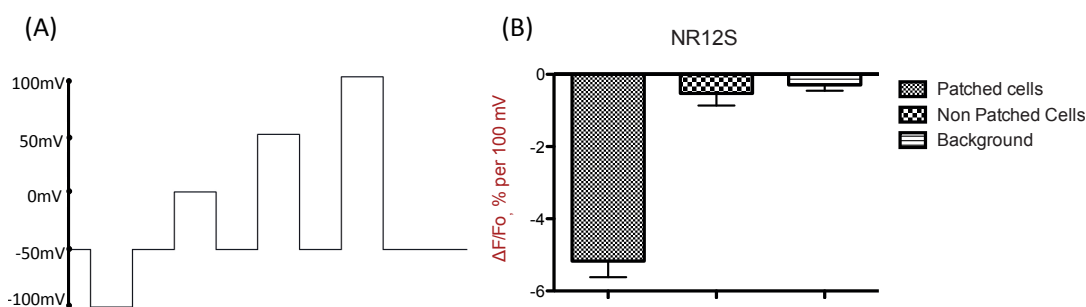


Figure 35: (A) Protocol of membrane potential change followed during the experiment. (B) Change of FI. intensity of compound NR12S upon 100 mV membrane potential change for patched cells (5% decrease), non-patched cells and background.

This result suggested that NR is indeed voltage sensitive, and thus eliminated our first hypothesis. Therefore, we speculate that the absence of voltage sensitivity observed for our probes **4-9** could be due to the wrong orientation or not full insertion of the NR in the membrane.

4.2.4.3 Targeting Compound NR12S to SNAP-tag

Our final aim was to create a targeted voltage sensor for SNAP-tag based on NR. Our first NR derivatives (compounds **4-9**) proved not to be voltage sensitive, so we decided to focus on the compound NR12S, which appeared to be more promising. Therefore, having seen that the compound NR12S is voltage sensitive, we decided to chemically derivatize it so that it would insert in the membrane only when bound to SNAP-tag. We designed compounds **10** and **11** (Figure 36), which consisted of: (i) a benzylguanine moiety, which was necessary for binding to SNAP-tag, (ii) a hydrophilic PEG11 linker, which would further reduce the hydrophobicity of the probe and allow NR to reach the plasma membrane and (iii) NR12S. Compound **10** differed from

⁶ The patch clamp experiments of NR12S on live HEK 293T cells were performed by Dr Mayya Sundukova (EMBL, Monterotondo), as part of a collaboration.

compound **11** from the addition of a negatively charged cysteic acid (Cya), which would further reduce the hydrophobicity and therefore the unspecific interactions of NR with the membrane or FBS.

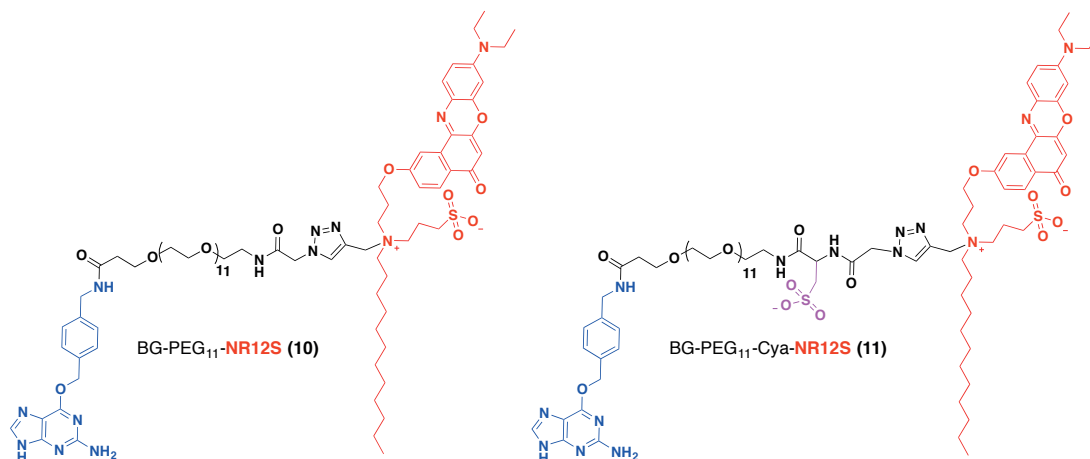


Figure 36: Structures of compounds **10** and **11**. They consist of a benzylguanine moiety (blue), a hydrophilic linker (black), negative charge (purple) and NR12S (red).

Compounds **10** and **11** were synthesized as reported in Chapter 7.1 and their fluorescence properties were studied *in vitro* and on live cells. Knowing the high affinity of NR12S for the membrane, we were curious to see if this chemical derivatization and the addition of an extra negatively charged Cya would reduce the hydrophobicity of the probe and allow its insertion in the plasma membrane only after binding to SNAP-tag.

4.2.4.3.1 *In Vitro* Characterization of Compounds **10** and **11**

We first measured the fluorescence properties of compounds **10** and **11** in solvents of different polarity, such as PBS, DMEM + FBS 10% and Dioxane, in order to see if they retained the solvatochromic properties of NR. As seen in Table 7 there is a blue shift observed in emission and absorbance maxima in a more apolar solvent, such as dioxane. This suggested that the two new compounds were also solvatochromic. Moreover, it appeared that the presence of a second negative charge (Cya) did not seem to affect the fluorescence properties, since both compounds behaved similarly in all solvents.

Table 7: Spectroscopic properties including absorption and emission maxima for compounds NR12S, **10** and **11** measured in PBS, DMEM + FBS 10% and dioxane.

Derivative	Solvent					
	PBS		DMEM + FBS 10%		Dioxane	
	λ_{abs}, nm	λ_{fl}, nm	λ_{abs}, nm	λ_{fl}, nm	λ_{abs}, nm	λ_{fl}, nm
NR12S	526	660	526	620	528	597
BG-PEG11- NR12S (10)	547	659	533	614	513	590
BG-PEG11-Cya- NR12S (11)	552	662	545	612	515	590

4.2.4.3.2 Imaging of Live HEK 293T Cells with Compounds **10** and **11**

We then decided to test the suitability of these two compounds for live cell imaging and observe if the chemical derivatization we performed was sufficient for specific labeling of only transfected cells expressing SNAP-tag. We transiently transfected HEK 293T cells so that they express a fusion protein, where SNAP is fused via CLIP and HCA to a transmembrane domain and is expressed on the external part of the plasma membrane. We chose this fusion protein, for the same reason as before: in order to identify the transfected cells with simultaneous labeling of CLIP-tag with another fluorophore.

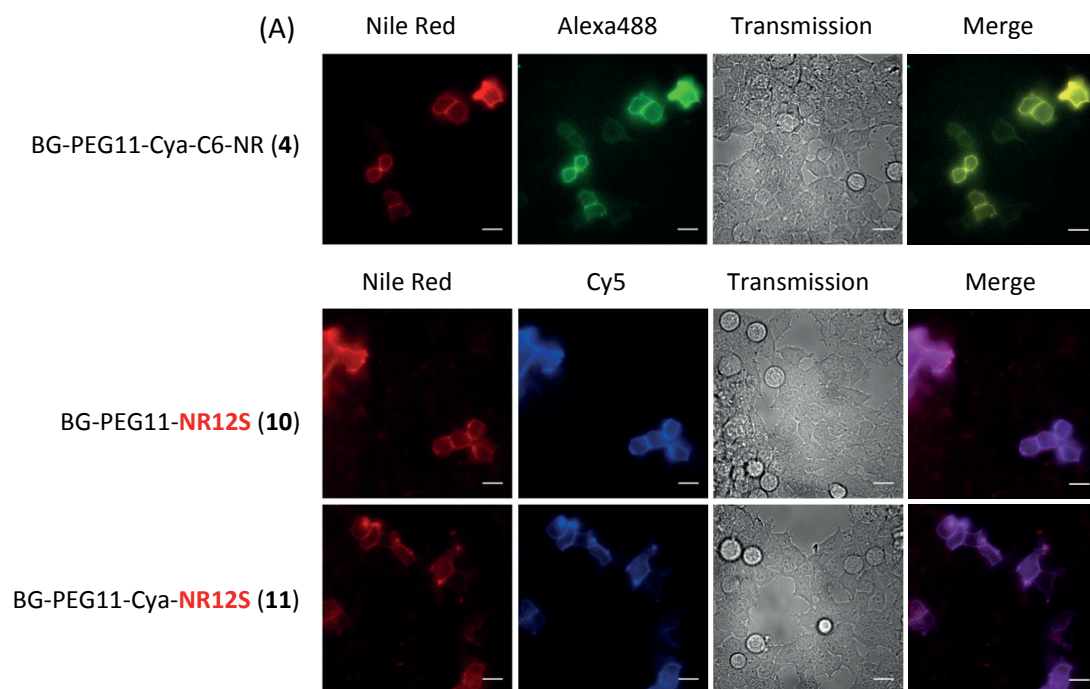
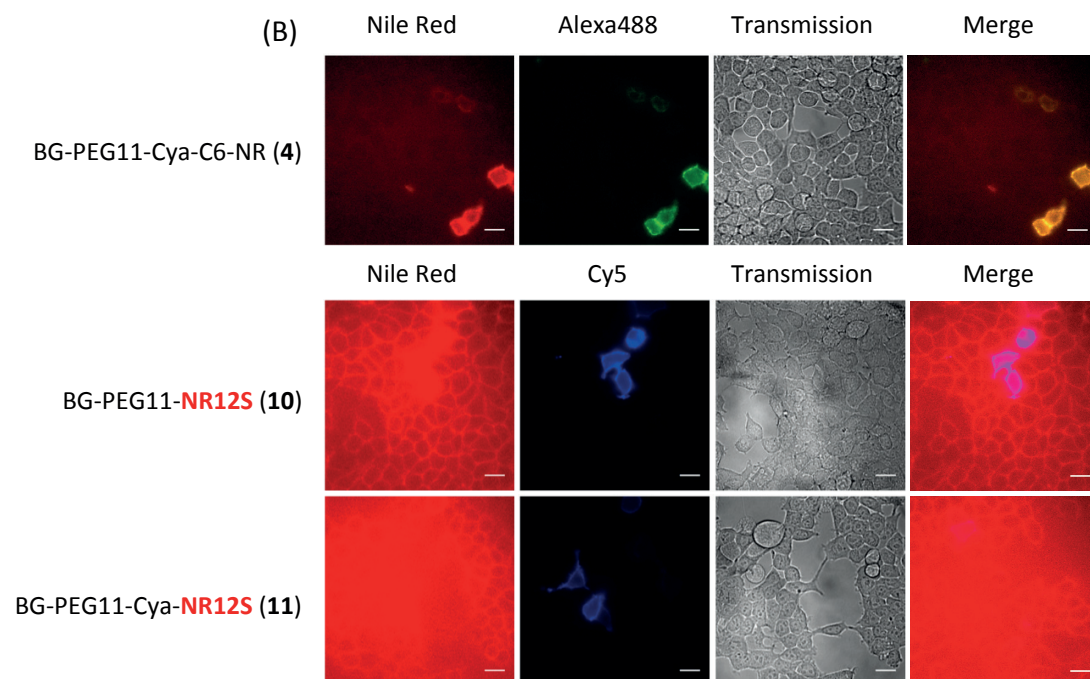
WASH**NO WASH**

Figure 37: **Imaging of transfected cells in DMEM + FBS 10%.** HEK 293T cells transiently expressing pDisplay-SNAP-CLIP-HCA labeled with BC-AlexaFluor 488 (10 μ M, 10 min incubation at 37 $^{\circ}$ C, three washes with DMEM + FBS 10%) or BC-Cy5 (10 μ M, 20 min incubation at 37 $^{\circ}$ C, three washes with DMEM + FBS 10%) and compounds **4**, **10** and **11** (500 nM, 30 min incubation at RT, DMEM + FBS 10%) imaged (A) after three washes and (B) directly after labeling. Scale bar, 20 μ m. (*N.B.* The pictures in this figure have been treated with the same settings in each subsection “wash” and “no wash”. However, note that the settings between Figure 37–Figure 40 are not the same.)

First, we labeled the HEK 293T cells with CLIP-Surface 647, or BC-Alexa488 in DMEM + FBS 10% (without phenol red), washed and treated them with compounds **10** and **11** (500 nM). We then imaged the cells after three washing steps or directly after labeling (Figure 37). We observed a low background coming from the membranes of non-transfected cells labeled with the new derivatives, when imaged after three washing steps (Figure 37, wash). We believe that this is probably due to residual affinity of these derivatives for the membrane.

Moreover, we observed that similar to compound NR12S, the new derivatives **10** and **11** were not fluorogenic in DMEM + FBS 10%. We believe that the reason for this are the unspecific interactions of NR12S with BSA or other proteins present in the medium (Figure 37, no wash).

In order to test how specific compounds **10** and **11** were, we decided to also treat non-transfected cells. We also compared them to compound **4**, which has been shown to label specifically only cells expressing SNAP-tag (Figure 38). We would expect that our chemically derivatized derivatives would not insert unspecifically in the membrane due to the absence of SNAP-tag – whose presence is necessary to bring them close to the lipid bilayer and lead to their insertion in the membrane.

We applied our derivatives on non-transfected HEK 293T cells and imaged under wide-field microscope directly after labeling (Figure 38, no wash) or after three washing steps in DMEM + FBS 10% (Figure 38, wash). As seen in Figure 38, after three washing steps contrary to **4**, compounds **10** and **11** showed a very low background coming from unspecific insertion of NR in the membrane.

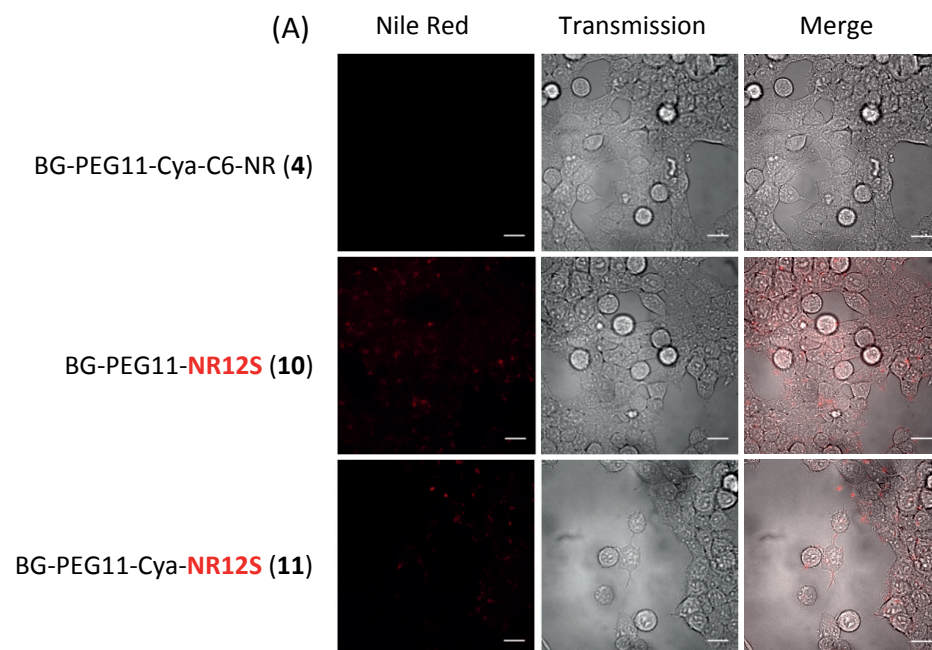
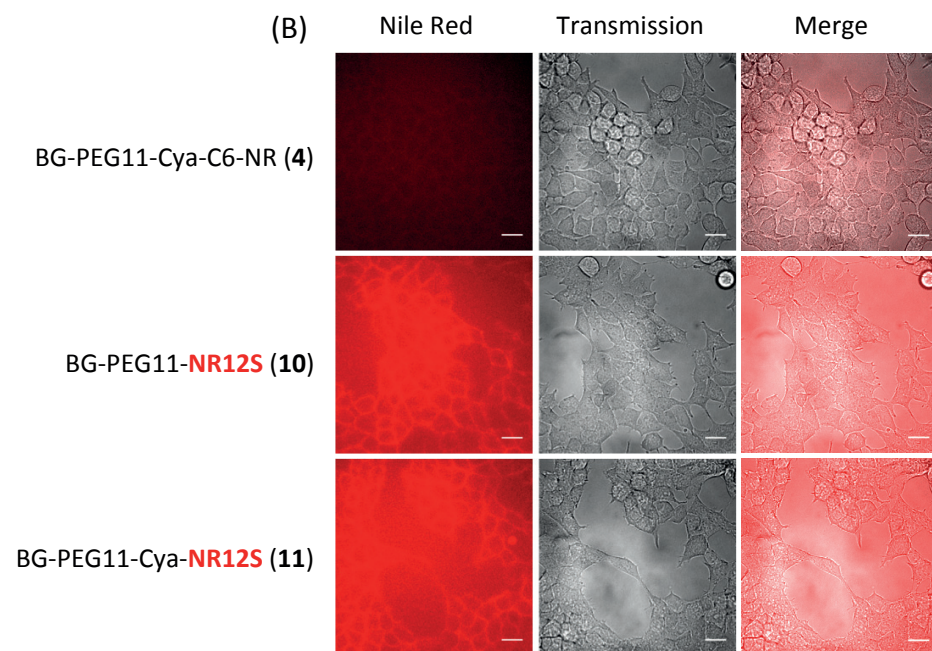
WASH**NO WASH**

Figure 38: **Imaging of non-transfected cells in DMEM + FBS 10%.** HEK 293T cells, non-transfected labeled with compounds **4**, **10** and **11** (500 nM, 30 min incubation at RT in DMEM + FBS 10%) imaged (A) after three washes and (B) directly after labeling. Scale bar, 20 μ m. (*N.B.* The pictures in this figure have been treated with the same settings in each subsection “wash” and “no wash”. However, note that the settings between Figure 37-Figure 40 are not the same.)

When the cells were imaged directly after labeling (Figure 38, no wash), as seen before (Figure 37, no wash), compounds **10** and **11** showed a strong uniform fluorescence throughout the whole imaging field.

To sum up, the new derivatives, contrary to compound **4**, were not fluorogenic and had a low residual background coming from the membranes of non-transfected cells when imaged in DMEM + FBS 10%.

On the other hand, the behavior of compounds **10** and **11** was different when they were applied on cells expressing the same fusion protein (pDisplay-SNAP-CLIP-HCA) and were imaged under wide field microscope in NPM (w/o FBS) (Figure 39). Apparently, in this salt medium that is lacking FBS the two compounds seemed to label unspecifically the membranes of all cells, regardless the expression of SNAP-tag.

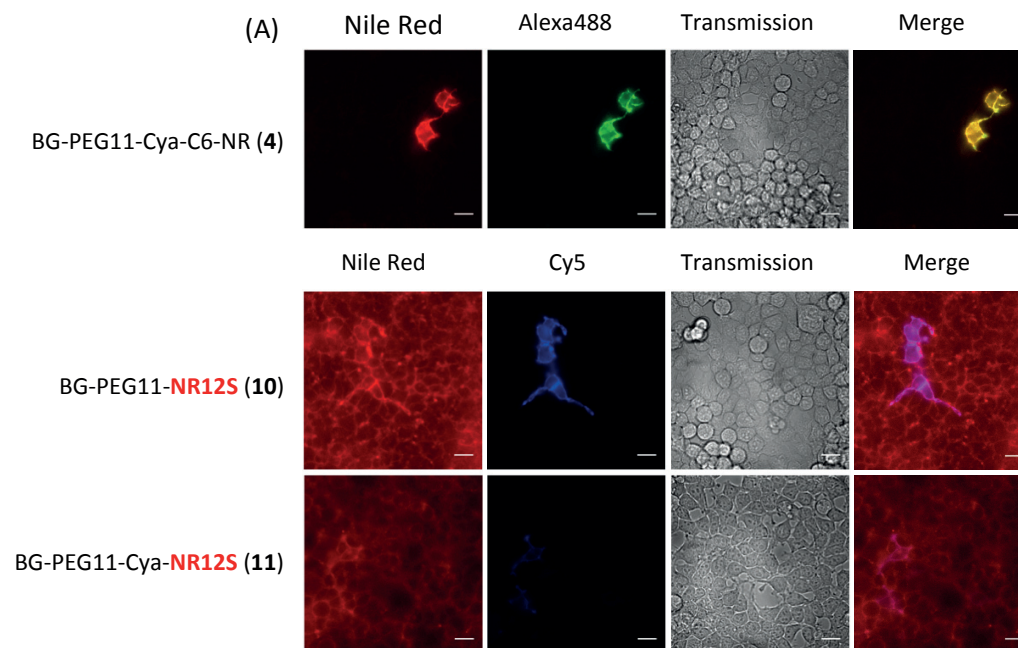
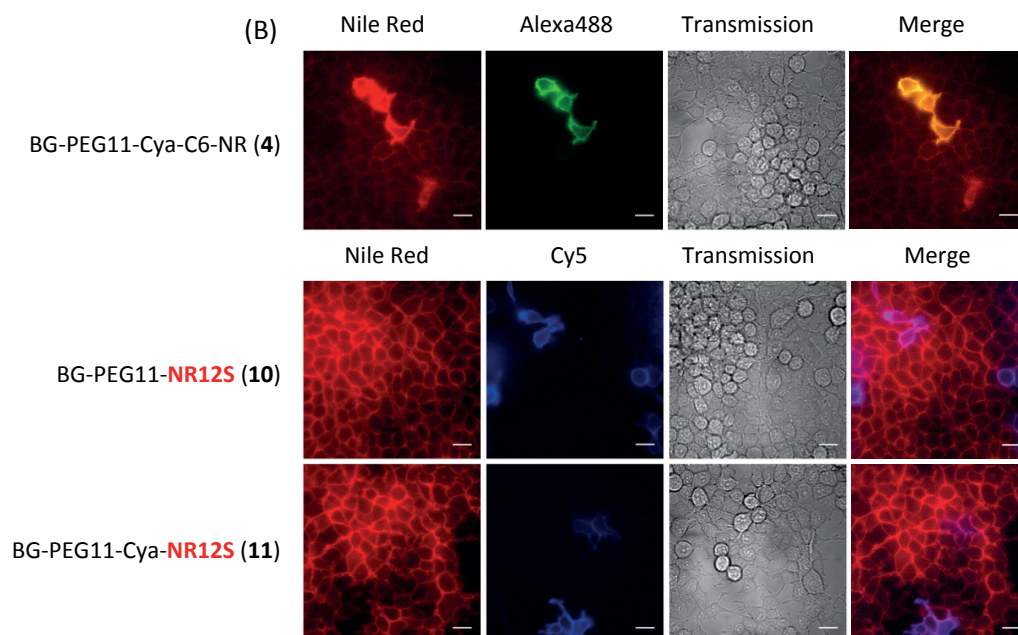
WASH**NO WASH**

Figure 39: **Imaging of transfected cells in NPM (w/o FBS).** HEK 293T cells transiently expressing pDisplay-SNAP-CLIP-HCA labeled with BC-AlexaFluor 488 (10 μ M, 10 min incubation at 37 $^{\circ}$ C, three washes with NPM) or BC-Cy5 (10 μ M, 20 min incubation at 37 $^{\circ}$ C, three washes with NPM) and compounds **4**, **10** and **11** (500 nM, 30 min incubation at RT, NPM) imaged (A) after three washes and (B) directly after labeling. Scale bar, 20 μ m. (*N.B.* The pictures in this figure have been treated with the same settings in each subsection “wash” and “no wash”. However, note that the settings between Figure 37-Figure 40 are not the same.)

We assume that this labeling behavior of compounds **10** and **11** observed in NPM (Figure 39) was due to the absence of FBS. We speculate that in presence of FBS, NR12S interacts preferentially with the latter over the membrane and thus prevents the unspecific insertion of

NR12S in the plasma membrane of non-transfected cells. In the absence of FBS, this equilibrium is distorted and NR12S inserts unspecifically in the membranes of non-transfected cells.

We validated this unspecific insertion of compounds **10** and **11** in the membrane of non-transfected cells by labeling non-transfected HEK 293T cells with compounds **4**, **10** and **11** and imaging under widefield microscope directly after labeling (Figure 40, no wash) and after three washing steps (Figure 40, wash).

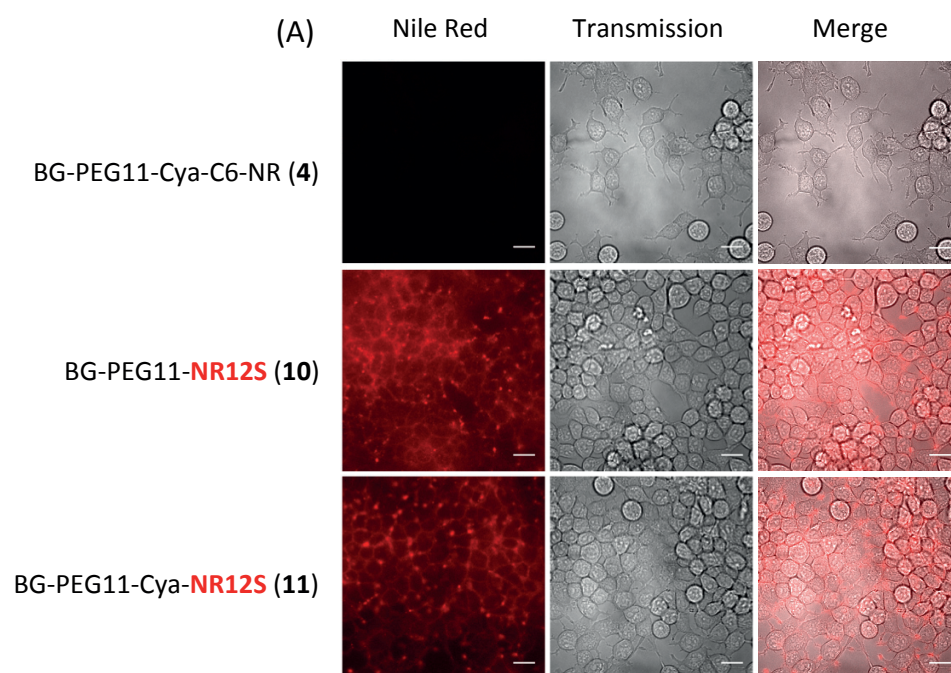
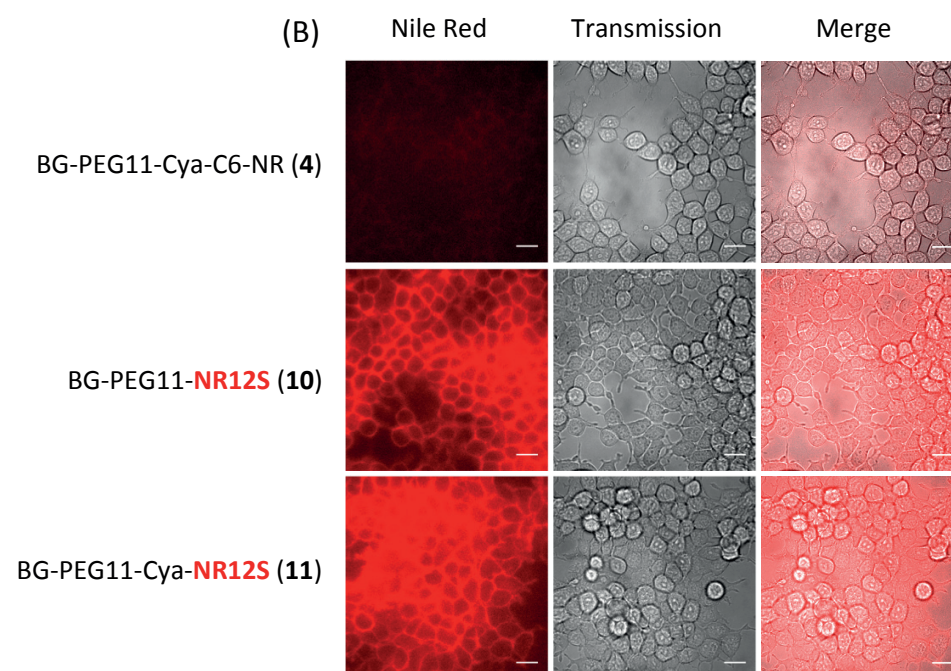
WASH**NO WASH**

Figure 40: **Imaging of non-transfected cells in NPM (w/o FBS).** HEK 293T cells, non-transfected labeled with compounds **4**, **10** and **11** (500 nM, 30 min incubation at RT in NPM) imaged (A) after three washes and (B) directly after labeling. Scale bar, 20 μ m. (*N.B.* The pictures in this figure have been treated with the same settings in each subsection “wash” and “no wash”. However, note that the settings between Figure 37-Figure 40 are not the same.)

As before (Figure 39, no wash), contrary to compound **4**, the two new compounds **10** and **11** appeared to insert unspecifically in the membranes of non-transfected cells, leading to a strong

(Figure 40, no wash) or low (Figure 40, wash) background, when imaged directly after labeling or after three washing steps respectively.

Therefore, to conclude, the presence of FBS in the labeling medium appeared to be necessary for the specific labeling of only the transfected cells by the two new NR derivatives (**10** and **11**).

4.2.4.3.3 Spectral Measurement of Compounds **10** and **11** on Live HEK 293T Cells⁷

In order to investigate whether compounds **10** and **11** inserted in the plasma membrane only after binding to SNAP-tag, and to understand the impact of the presence of FBS in the labeling medium more in depth, we decided to measure the emission maxima of these compounds:

- On HEK 293T cells expressing pDisplay-SNAP-CLIP-HCA, in order to unambiguously identify the transfected cells (Cells, Transfected) in EB with or w/o FBS.
- On non-transfected HEK 293T cells (Cells, Non-Transfected) in EB w/o FBS.
- Bound to SNAP-tag in PBS solution (SNAP)

Table 8: Measurement of $\lambda_{\text{max, emission}}$ of NR derivatives **10** and **11** (i) bound to SNAP-tag expressed on the surface of HEK 293T Cells in EB w/o FBS or EB + FBS 10% (Cells, Transfected), (ii) applied on non-transfected HEK 293T cells in EB w/o FBS (Cells, Non-Transfected) and (iii) bound to SNAP-tag in PBS solution (SNAP). The spectra were fitted using a Lorentzian fit to calculate the $\lambda_{\text{max, fit}}$.

Derivative	Cells		SNAP	
	Transfected		Non-Transfected	Solution
	EB (w/o FBS)	EB + FBS 10%	EB (w/o FBS)	PBS
NR12S	n.d.	n.d.	590.6 ± 1.6	627.6 ± 2.5
BG-PEG11- NR12S (10)	592.2 ± 1.4	604.2 ± 1.6	592.1 ± 1.5	625.0 ± 1.4
BG-PEG11-Cya- NR12S (11)	595.7 ± 1.3	607.1 ± 1.3	593.5 ± 1.4	624.6 ± 1.4

n.d. Not determined

N.B. EB is a salt buffer consisting of (in mM): 150 NaCl, 5 KCl, 1 MgCl₂, 2 CaCl₂, 5 glucose, 10 HEPES; pH 7.4 adjusted with NaOH, 300 mOsm.

As seen in Table 8, compound NR12S, when applied on non-transfected cells had an emission maximum at 590 nm - a value which is similar to the one measured for DPPC liposomes.⁸¹ Similar values were obtained for compounds **10** and **11** when applied on non-transfected cells.

Moreover, the emission maxima of compounds **10** and **11** were measured on HEK 293T cells transiently expressing pDisplay-SNAP-CLIP-HCA. Cells were labeled with CLIP-Surface 647 (1 μ M, 1 h at 37°C), were washed and treated with the NR derivatives (500 nM, 30 min at RT) in extracellular buffer (EB) with or w/o FBS. We observed that the spectra of the two compounds

⁷ This experiment was performed by Annalisa Bucci and Dr Mayya Sundukova (EMBL, Monterotondo) as part of a collaboration.

on transfected cells in EB w/o FBS showed a maximum peak at 592.2 nm and 595.7 nm respectively (which are coherent with insertion in the membrane).⁸¹ We also measured the emission maxima of compounds **10** and **11** when bound to SNAP-tag in solution, which corresponded to 630 nm, a value which is 35 nm red-shifted compared to the one of insertion in the membrane.

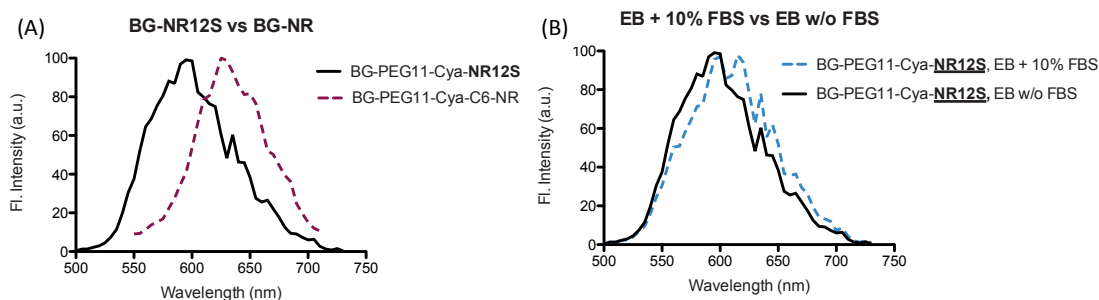


Figure 41: (A) Comparison of emission spectra of compounds **11** and **4** bound to SNAP-tag expressed on cells in EB w/o FBS. Compound **11** is blue shifted compared to **4**. (B) Comparison of emission spectra of compound **11** measured on cells in EB w/o FBS and in EB + FBS 10%.

Furthermore, as mentioned before, the compounds **10** and **11** appeared to behave in a different way when the labeling medium contained 10% FBS. Interestingly, the $\lambda_{\text{max,fl}}$ of the compounds bound to transfected cells was 10 nm red-shifted when measured in the presence of 10% FBS, suggesting less unspecific interactions with the membranes (Figure 41 no wash). Moreover, as we will see later (Table 9), NR12S, **10** and **11** were approximately 40 nm blue shifted compared to the NR-derivatives **1-9** (Figure 41A).

4.2.4.3.4 Patch Clamp Experiments of Compounds **10**, **11** on Live HEK 293T Cells⁸

The results of the spectral measurement mentioned above were confirmed from the patch clamp experiments.

In order to establish the response of compounds **10** and **11** in whole-cell-patched, voltage clamped cells, non-transfected HEK 293T cells were first labeled with the two compounds (500 nM, 7 min at RT) in EB w/o FBS. Whole-cell voltage clamped HEK cells were held at -50 mV and then stepped to hyper- and depolarizing potentials in 50 mV steps (range ± 100 mV, always returning to -50 mV after each 50 mV step as a control, Figure 31A).

Interestingly, the two compounds did not show the same response: for compound **10** we observed a 5% decrease in fluorescence intensity (same as for NR12S), whereas for compound **11** only a 2.5% decrease upon 100 mV change of membrane potential was observed (Figure 42). The two compounds differed only by the presence of an extra negative charge in compound **11** (Figure 36). According to the spectral measurement presented in Table 8, both compounds show an emission maximum at 592 nm - which is similar to the value measured for NR12S and in line

⁸ The patch clamp experiments of compounds **10** and **11** on live HEK 293T cells were performed by Annalisa Bucci and Dr Mayya Sundukova (EMBL, Monterotondo), as part of a collaboration.

with insertion of NR in the membrane.⁸¹ We speculate that this difference in voltage sensitivity is due to the presence of the negative charge, which reduced the insertion of **11** in the membrane compared to **10**.

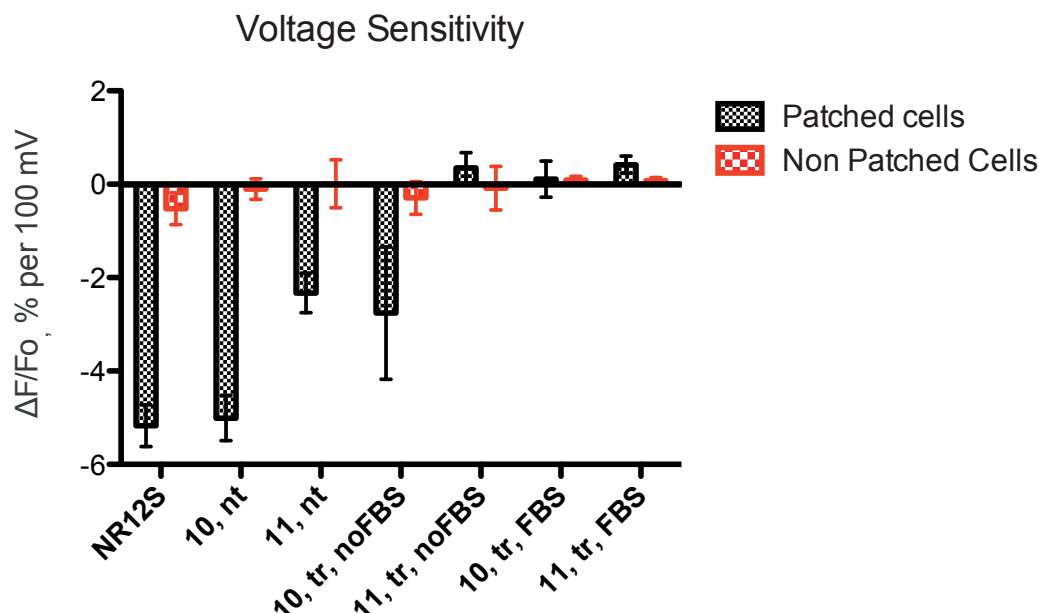


Figure 42: Change in fluorescence intensity of compounds (A) NR12S, **10** and **11** on non-transfected cells (nt) in EB (w/o FBS) and (B) **10** and **11** on transfected cells (tr) expressing pDisplay-SNAP-CLIP-HCA measured in EB (with 10% FBS or w/o FBS) per 100 mV change in membrane potential.

We then tested the voltage sensitivity of compounds **10** and **11** on HEK 293T cells transiently expressing the fusion protein SNAP-CLIP-HCA on the extracellular part of the plasma membrane. We first labeled the cells with CLIP-Surface 647 (1 μ M, 1 h at 37°C), washed them and treated them with compounds **10** and **11** (500 nM, 30 min at RT) in **EB w/o FBS**. We followed the same protocol as before (Figure 31A) and we observed that the response of the two compounds was smaller than the one observed in the non-transfected cells (Figure 42). We measured a 3% decrease in fluorescence intensity for compound **10** and no significant change for compound **11**. We attribute this behavior to the belief that there are two populations of the probe on the cells:

- (i) one that binds to SNAP and either gets “trapped” in its hydrophobic environment and fluoresces, or inserts in the membrane with a non-optimal orientation and
- (ii) one that inserts unspecifically in the membrane and enters a “fluorescent-on” state due to the apolar environment of the plasma membrane (Figure 43).

Therefore, we believe that the smaller change in fluorescence intensity per 100 mV observed was due to the smaller fraction of the dye inserted in the membrane or inserted in the optimal orientation. The presence of a negative charge in **11** did not allow its unspecific insertion in the membrane and therefore **11** was not voltage sensitive, whereas for **10** a part of the probe was inserted unspecifically in the membrane and thus there was a degree of voltage sensitivity.

Having seen the importance of FBS in the labeling medium for the specificity of the probes, we decided to repeat the same experiment in **EB supplemented with 10% FBS** (Figure 42). In this case, no significant change in the fluorescent properties of compounds **10** and **11** was observed per 100 mV. We have already shown that in presence of FBS, NR binds preferentially to the latter over the membrane. The excess of the dye bound to FBS is removed with the washing step and the majority of the NR molecules present are bound to SNAP-tag and not inserted unspecifically in the membrane. Therefore, it was no surprise to see that in presence of 10% FBS, the two compounds were not voltage sensitive, since there was no unspecific insertion and we speculate that most probably they were either not inserted into the membrane or they did not have the optimal orientation in the membrane.

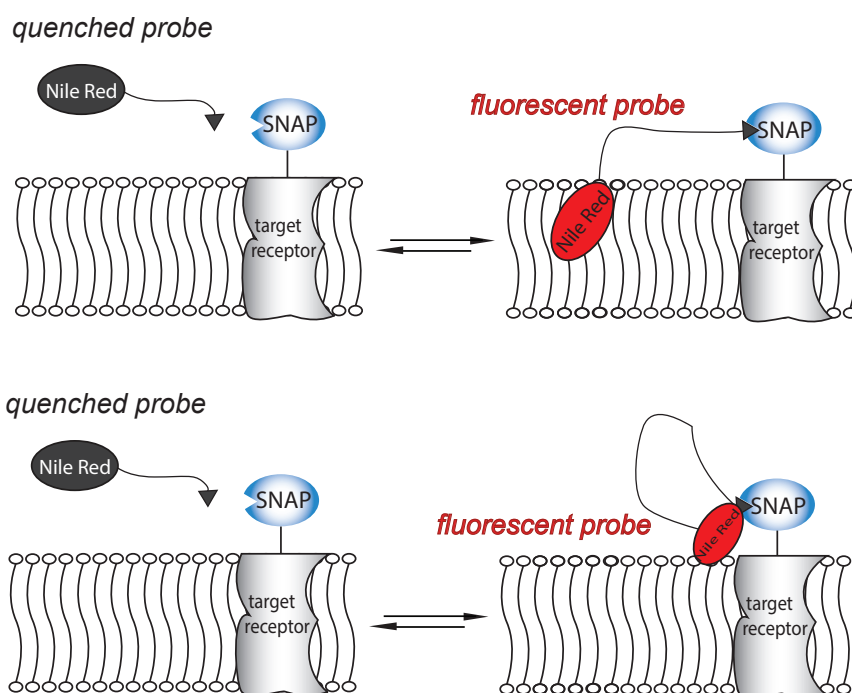


Figure 43: Speculations about the position of NR. It is not clearly defined yet if (A) the NR molecules bound to SNAP tag insert in the plasma membrane after binding to SNAP-tag and experiencing the apolar environment fluoresce, or (B) NR is “trapped” in the hydrophobic environment of SNAP-tag and due to its apolar environment turns into its “fluorescent-on” state.

4.3 Conclusions

Considering the environmental sensitivity of NR, its large dipole moment that is formed upon excitation, and its attractive fluorogenic property we decided to test this dye for voltage sensitivity. We anticipated that its fluorescent properties could be sensitive to changes of the membrane potential due to change of its electronic structure, reorientation or redistribution of the dye in other parts of the plasma membrane with a different polarity. Moreover, having seen that our NR derivatives labeled specifically SNAP-tag and only then turned fluorescent, we decided to use them in order to create a targeted voltage sensor for SNAP-tag. This sensor

would combine the specificity of the genetically encoded voltage sensors with the sensitivity of the organic voltage indicators.

First, we decided to enrich the repertoire of our NR derivatives with more charges and different linker lengths between the charged moiety and NR and synthesized compounds **5-9** (Figure 26). We saw that the best performing compounds in terms of “no wash” imaging were the ones with a shorter linker between the charge and NR (**6-9**), since this apparently reduced the unspecific interactions of NR with FBS present in the medium. Then, in collaboration with Paul Heppenstall’s laboratory at EMBL, Monterotondo, we tested our NR derivatives **4-9** for voltage sensitivity by doing whole-cell patch clamp experiments on live HEK 293T cells labeled with our compounds. Unfortunately, none of the derivatives appeared to be voltage sensitive (Figure 32).

This lack of sensitivity suggested that either NR was not voltage sensitive, or that the position/orientation of NR was not optimal. To answer our questions, we decided to use another NR derivative (NR12S) which was designed by Kucharak *et al.*⁸¹ NR12S was synthesized and proved to be non-fluorogenic in DMEM + FBS 10%, probably due to strong interactions of the dye with FBS. When tested with patch clamp experiments, it showed a 5% decrease in fluorescence intensity upon 100 mV increase of membrane potential (Figure 35B). This result indicated that NR was indeed voltage sensitive and that probably the lack of voltage sensitivity of our NR derivatives **4-9** was due to a wrong orientation of NR in the membrane or because the dye was not positioned entirely into the plasma membrane.

Going back to our original aim of designing a targeted voltage sensor, we decided to direct the voltage sensitive molecule NR12S to SNAP-tag and therefore, compounds **10** and **11** were synthesized (Figure 36). These derivatives appeared to label specifically HEK 293T cells expressing SNAP-tag only in DMEM + FBS 10%. Apparently, the presence of FBS in the medium was necessary for specific labeling of transfected cells with **10** and **11** (Figure 37, Figure 38). The whole-cell patch clamp experiments for these compounds suggested that there were two populations of the probe:

- (i) one inserted in the membrane unspecifically (voltage sensitive) and
- (ii) one that was bound to SNAP-tag, and was either “trapped” inside the hydrophobic environment of the protein or was inserted in the membrane with a different orientation (not voltage sensitive) (Figure 43).

The charge distribution has to occur parallel to the electrical field and therefore the orientation of the dipole moment is optimal for voltage sensitivity when it is perpendicular to the membrane surface. A poor orientation can lead to a weak response to the electric field.

With the work described in this chapter we have proved that NR is sensitive to changes in membrane potential. However, our results suggested that the position of our NR derivatives is not clearly defined yet. Therefore, we decided to perform spectral and FLIM measurements, in order to get more information about the environment of our BG-NR derivatives (Chapter 5).

Chapter 5 Position of the NR Derivatives

5.1 Introduction

The results observed for compounds **10** and **11**, suggested that the position of our NR derivatives was not clearly defined. In order to shed more light on the environment of our BG-NR derivatives (compounds **1-11**), we decided to perform fluorescence lifetime and spectral measurement experiments. Therefore, we measured the fluorescence lifetime and the emission maxima of our compounds when bound to SNAP-tag expressed on the extracellular surface of the plasma membrane of HEK 293T cells and compared them to the values obtained when our dyes were bound to SNAP-tag in solution. The fluorescence lifetime and emission maximum are two factors that are characteristic of the environment our dye is experiencing. Therefore, we anticipated that these experiments would give us information on the position of our probes.

5.2 Results

5.2.1 Spectral Measurements

5.2.1.1 Spectral Measurement of NR Derivatives Under Confocal Microscope

We measured the emission maxima of all our NR derivatives (compounds **1-11** and NR12S):

- when bound to SNAP-tag expressed on the outer leaflet of the plasma membrane in NPM or EB (w/o FBS) (Cells) (Figure 64)
- when bound to purified SNAP-tag in PBS solution (w/o BSA) (SNAP)
- when bound to BSA in PBS solution (BSA).

This experiment had the following aims:

- i. To understand if the differences in linker length, charge or linker between the charged moiety and NR had an effect on the environment NR was experiencing.
- ii. To understand if the apolar environment our dyes were experiencing was due to the membrane or SNAP-tag. To do this, we compared the values measured in cells to the ones measured in the presence of purified SNAP-tag in solution.
- iii. To study the interactions of our dye with BSA.
- iv. To compare our old NR derivatives (compounds **1-9**) with the new ones based on NR12S (compounds **10** and **11**).

Table 9: Measurement of $\lambda_{\text{max, emission}}$ of NR derivatives (i) bound to SNAP-tag expressed on the surface of HEK 293T Cells in NPM w/o FBS (or EB w/o FBS when indicated with ^{*}) (ii) bound to SNAP-tag in PBS solution (w/o BSA) and (iii) bound to BSA in PBS solution. The spectra were fitted using a Lorentzian fit for calculation of the $\lambda_{\text{max, fl}}$.

Derivative	Cells expressing pSNAP	SNAP in solution	BSA in solution
BG-PEG11-C6-NR (2) (nt)	607.3 ± 1.1	n.d.	n.d.
BG-PEG11-C6-NR (2)	632.4 ± 0.9	635.5 ± 1.3	635.6 ± 1.4
BG-PEG11-Cya-C6-NR (4)	632.8 ± 0.9	635.5 ± 1.2	635.8 ± 1.5
BG-PEG11-LysMe3-C6-NR (5)	632.5 ± 1.0	n.d.	n.d.
BG-PEG11-(LysMe3)2-C6-NR (6)	631.8 ± 0.7	n.d.	n.d.
BG-PEG11-Cya-C2-NR (7)	636.6 ± 1.2	n.d.	n.d.
BG-PEG11-LysMe3-C2-NR (8)	633.9 ± 1.1	638.4 ± 1.3	635.8 ± 1.5
BG-PEG11-(LysMe3)2-C2-NR (9)	636.6 ± 1.2	n.d.	n.d.
BG-PEG5-C6-NR (1)	631.8 ± 1.1	n.d.	n.d.
BG-PEG5-Cya-C6-NR (3)	634.2 ± 1.1	n.d.	n.d.
NR12S (nt)	[*] 590.6 ± 1.6	627.6 ± 2.5	619.9 ± 1.2
BG-PEG11- NR12S (10)	^{#,*} 592.2 ± 1.4	625.0 ± 1.4	614.9 ± 1.1
BG-PEG11-Cya- NR12S (11)	^{#,*} 595.7 ± 1.3	624.6 ± 1.4	623.2 ± 1.2
BG-PEG11- NR12S (10) (nt)	[*] 592.1 ± 1.5	n.d.	n.d.
BG-PEG11-Cya- NR12S (11) (nt)	[*] 593.5 ± 1.4	n.d.	n.d.
Nile Red	n.d.	652.4 ± 1.3	611.5 ± 1.5
BG-AlexaFluor 488	531.8 ± 1.5	532.6 ± 1.5	532.7 ± 1.6

n.d.: Not determined

(nt) Refers to measurement on non-transfected cells

^{*} Refers to measurement in EB (w/o FBS)

[#] Refers to measurement on transfected cells expressing pDisplay-SNAP-CLIP-HCA, co-stained with CLIP-Surface 647 for distinguishing the transfected cells in EB (w/o FBS).

N.B. **EB** is a salt buffer consisting of (in mM): 150 NaCl, 5 KCl, 1 MgCl₂, 2 CaCl₂, 5 glucose, 10 HEPES; pH 7.4 adjusted with NaOH, 300 mOsm and **NPM** is a salt buffer consisting of (in mM): 1.8 CaCl₂, 0.8 MgCl₂, 10 glucose, 10 HEPES (pH 7.3), 5 KCl and 145 NaCl.

HEK 293T cells, transiently transfected to express SNAP on the extracellular part of the plasma membrane, were labeled with compounds **1-9** for 30 min at RT in NPM w/o FBS. Fluorescence spectra of these compounds were recorded under confocal microscope in lambda mode. Apparently, all BG-NR derivatives (compounds **1-9**) had a similar environment in all cases regardless of the charge or linker length.

First, we defined the value of the emission maximum of our NR-derivatives in the membrane. To do this, we applied compound **2** - which inserts unspecifically in the membrane, due to the lack of charge - and measured the $\lambda_{\text{max,fl}}$ to be 607 nm; a value which is in accordance with the literature.⁸¹

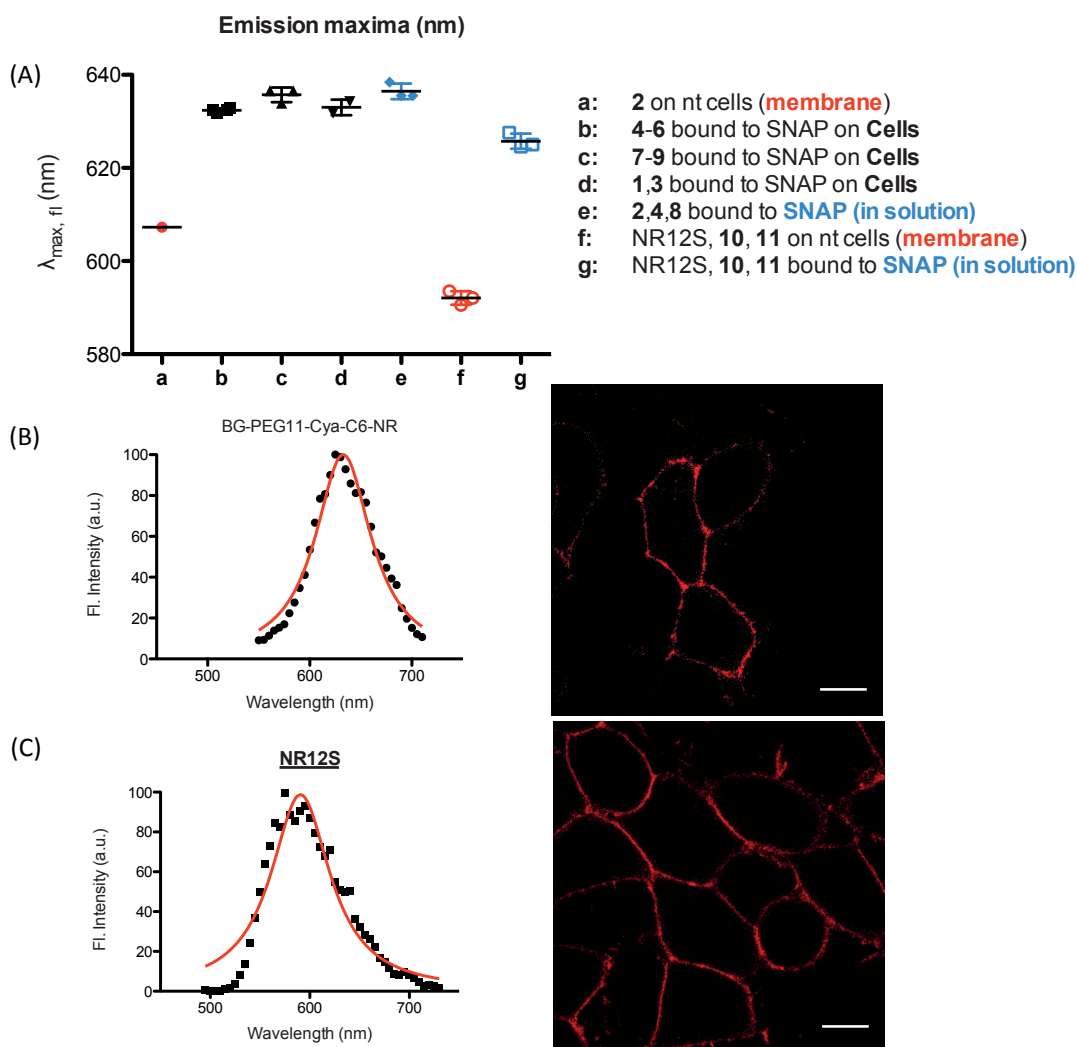


Figure 44: (A) Comparison of emission maxima measured for **a.** compound **2** inserted in the membrane, **b.** BG-NR compounds (PEG11, C2) bound to SNAP on cells, **c.** BG-NR compounds (PEG11, C6) bound to SNAP on cells, **d.** BG-NR compounds (PEG5, C6) bound to SNAP on cells, **e.** BG-NR compounds (**2**, **4** and **8**) bound to SNAP in PBS solution, **f.** Compounds NR12S, **10** and **11** inserted in the membrane of non-transfected cells and **g.** Compounds NR12S, **10** and **11** bound to SNAP in PBS solution. Each spot corresponds to one molecule. This figure corresponds to the results presented in Table 9. (B) Emission spectrum of compound **4** applied on HEK 293T cells expressing SNAP-tag on the extracellular part of the plasma membrane. (C) Emission spectrum of compound NR12S applied on non-transfected HEK 293T cells. (B) and (C) emission spectra were measured under confocal microscope on lamda mode (step: 5 nm). The spectra were fitted using a Lorentzian fit as a guide for the eye. Scale bars, 10 μm .

Then, as presented in Table 9, the emission maxima of compounds **1-9** were measured to be in the range of 630 nm - approximately 20 nm red shifted compared to the value of insertion in the membrane (Figure 44A). These values were similar to the $\lambda_{\text{max,fl}}$ of compounds **2**, **4** and **8** measured when bound to purified SNAP-tag in solution (approximately 630 nm). This result

could suggest that in both cases (Cells and SNAP), NR was experiencing the hydrophobic environment of SNAP-tag and not the one of the plasma membrane.

Moreover, NR is known to interact with BSA leading to an increase in fluorescence QY.¹⁰⁰ This has been shown in the *in vitro* (Chapter 3.2.2.1) and the *in cellulo* (Chapters 4.2.3.1 and 4.2.4.2.1) characterization of the NR derivatives so far. As a reminder, the NR-derivatives in PBS showed a maximum of fluorescence at 660 nm. With this experiment, we provided evidence that upon interaction of NR with BSA, NR experienced a more hydrophobic environment witnessed by the observed blue shift from 660 nm to 635 nm. This shift was attributed to interactions of NR with BSA. As a control, we used another dye – BG-AlexaFluor 488 – and showed that in this case, no shift in the fluorescence maximum was observed in the presence of BSA.

Finally, compounds based on NR12S, as mentioned in Chapter 4.2.4.3.3, were approximately 40 nm blue shifted compared to compounds **1-9** (Figure 41A, Figure 44A). Furthermore, the values measured for compounds **10** and **11** on cells were 40 nm blue shifted compared to the ones measured on purified SNAP-tag in solution (SNAP) in EB w/o FBS and 20 nm blue shifted in EB + FBS 10% (Table 8). This result suggested that the environment of these probes (**10**, **11**) was different in the two cases.

5.2.1.2 Spectral Measurement of NR Derivatives on DPPC Liposomes

In order to validate the above results, we decided to repeat the same experiment, using DPPC liposomes as a membrane model. We labeled a purified SNAP-tag protein containing a terminal hexahistidine tag (His-SNAP) with compounds **2**, **4**, **8**, NR12S and **11**. We then applied labeled His-SNAP on 1,2-dipalmitoyl-sn-glycero-3-phosphatidylcholine (DPPC) lipid vesicles containing Ni-NTA lipids (Figure 45A).¹²⁴ We performed several controls (Figure 45B), including:

- i. DPPC vesicles of the same composition, lacking the Ni-NTA lipids - to verify the effect of NTA-lipids on the dye.
- ii. DPPC vesicles with Ni-NTA lipids labeled directly with the compounds - to investigate the importance of the presence of SNAP for the labeling.
- iii. DPPC vesicles without Ni-NTA lipids labeled directly with the compounds – to investigate the importance of SNAP and Ni-NTA lipids for the insertion of NR in the membrane.

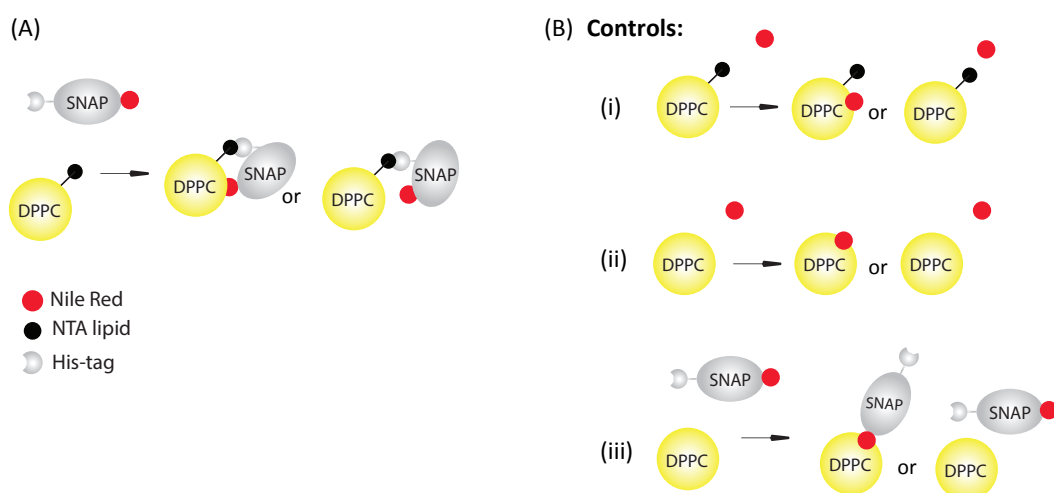


Figure 45: **Liposome experiment.** (A) A labeled SNAP-His with our NR derivatives is applied on DPPC liposomes containing Ni-NTA lipids leading to the anchoring of SNAP-tag on the surface of the liposomes. (B) Controls performed for the method.

We expected His-SNAP to bind to the Ni-NTA moiety at the surface of the vesicles, thereby anchoring it to the membrane. In control vesicles lacking the Ni-NTA lipids, we anticipated it would remain in solution.

Table 10: Measurement of $\lambda_{\text{max, emission}}$ of NR derivatives (i) after conjugation to His-tagged SNAP applied on DPPC lipid vesicles containing NTA-lipids and on control vesicles lacking the NTA lipids and (ii) directly on DPPC lipid vesicles containing NTA-lipids and on control vesicles lacking the NTA-lipids.

Derivative	Maximum emission on DPPC liposomes, $\lambda_{\text{max, emission}}$ (nm)			
	SNAP		No SNAP	
	NTA lipids	No NTA lipids	NTA lipids	No NTA lipids
BG-PEG11-C6-NR (2)	613.0 \pm 0.8	623.5 \pm 0.9	617.7 \pm 0.6	629.9 \pm 0.8
BG-PEG11-Cya-C6-NR (4)	611.8 \pm 0.8	621.7 \pm 0.9	618.8 \pm 0.7	628.8 \pm 0.8
BG-PEG11-LysMe3-C2-NR (8)	616.6 \pm 0.8	624.6 \pm 0.9	n.d.	n.d.
NR12S	606.1 \pm 0.8	615.2 \pm 1.1	610.9 \pm 0.9	620.1 \pm 1.2
BG-PEG11-Cya- NR12S (11)	607.8 \pm 0.8	616.7 \pm 0.9	n.d.	n.d.

Legend:
 ● Nile Red
 ● NTA lipid
 ○ His-tag

n.d.: Not determined

As presented in Table 10, the values observed when labeled SNAP-His was applied on DPPC liposomes with Ni-NTA lipids were in the range that corresponds to insertion of NR in the

membrane¹⁰⁰ and were more blue shifted compared to the values measured in the absence of Ni-NTA lipids. However, we also observed that there was a constant difference of 10 nm depending on the presence or absence of the NTA-lipids – regardless of SNAP-tag.

We believe that this anchoring system of labeled His-SNAP to the surface of DPPC liposomes containing Ni-NTA lipids cannot give us a clear explanation for the position of our NR derivatives, since it appears that the Ni-NTA lipids were interacting with our dye. This speculation is supported by the fluorescence lifetime results on the same liposome system that will be presented later (Table 12).

5.2.2 FLIM Measurements

Fluorescence lifetime is the average time the fluorophore spends in the excited state before returning to its ground state.⁶ It is known to be a useful indicator of the environment in which a fluorophore is localised, even more than the $\lambda_{\text{max,fl}}$ of the dye.⁶⁶ More specifically, it has been shown that the lifetime of NR12S is dependent on the percentage of cholesterol present in the membrane.⁷³ Also, it has been observed that NR12S has two lifetimes.^{73,125,126} In our experiments, we have measured the fluorescence lifetimes of the NR derivatives under confocal microscope in FLIM mode and presented the average of these two lifetimes based on the amplitude, calculated as reported in Chapter 7.2 of the method section.

5.2.2.1 FLIM Measurements of NR Derivatives Under Confocal Microscope

We measured the fluorescence lifetimes of all our NR derivatives (compounds **1-11** and NR12S):

- when bound to SNAP-tag expressed on the outer leaflet of the plasma membrane in NPM w/o FBS (Cells) (Figure 64)
- when bound to purified SNAP-tag in PBS solution w/o BSA (SNAP)
- when bound to BSA in PBS solution (BSA)

This experiment had the following aims:

- i. To understand if the difference in PEG linker length, charge or linker between the charged moiety and NR had an effect on the environment NR was experiencing.
- ii. To understand if the apolar environment our dyes were experiencing was due to the membrane or SNAP-tag. To do this, we compared the values measured in cells to the ones measured just in the presence of purified SNAP-tag in solution.
- iii. To study the interactions of our dye with BSA.
- iv. To compare our old NR derivatives (compounds **1-9**) with the new ones based on NR12S (compounds **10** and **11**)

Table 11: Measurement of fluorescence lifetime ($\tau_{ave, ampl}$) of NR derivatives bound to SNAP on the surface of HEK 293T Cells in NPM w/o FBS (Cells), bound to SNAP-tag in PBS solution (SNAP) and bound to BSA in PBS solution (BSA). Amplitude-averaged mean lifetimes for biexponential decays of fluorescence were calculated using Equation 4. For further details see Chapter 7.2.

Derivative	Fluorescence Lifetime, $\tau_{average, amplitude}$ (ns)		
	Cells	SNAP	BSA
BG-PEG11-C6-NR (2) (nt)	3.55 \pm 0.10	n.d.	n.d.
BG-PEG11-C6-NR (2)	2.99 \pm 0.10	3.67 \pm 0.13	1.59 \pm 0.59
BG-PEG11-Cya-C6-NR (4)	2.81 \pm 0.13	3.69 \pm 0.08	1.59 \pm 0.62
BG-PEG11-LysMe3-C6-NR (5)	2.75 \pm 0.12	n.d.	n.d.
BG-PEG11-(LysMe3)2-C6-NR (6)	2.59 \pm 0.11	n.d.	n.d.
BG-PEG11-Cya-C2-NR (7)	2.65 \pm 0.11	n.d.	n.d.
BG-PEG11-LysMe3-C2-NR (8)	2.32 \pm 0.31	3.38 \pm 0.16	1.10 \pm 0.62
BG-PEG11-(LysMe3)2-C2-NR (9)	2.07 \pm 0.10	n.d.	n.d.
BG-PEG5-C6-NR (1)	3.19 \pm 0.18	n.d.	n.d.
BG-PEG5-Cya-C6-NR (3)	2.98 \pm 0.07	n.d.	n.d.
NR12S (nt)	4.55 \pm 0.25	1.21 \pm 0.25	3.23 \pm 0.11
BG-PEG11- NR12S (10)	n.d.	4.44 \pm 0.14	2.99 \pm 0.12
BG-PEG11-Cya- NR12S (11)	n.d.	5.54 \pm 0.20	2.97 \pm 0.20
BG-PEG11- NR12S (10) (nt)	4.37 \pm 0.12	n.d.	n.d.
BG-PEG11-Cya- NR12S (11) (nt)	4.50 \pm 0.10	n.d.	n.d.
Nile Red	n.d.	1.22 \pm 0.06	3.14 \pm 0.14
BG-AlexaFluor 488	3.08 \pm 0.11	3.90 \pm 0.03	3.91 \pm 0.45

n.d.: Not determined

(nt) Refers to measurement on non-transfected cells

N.B. **NPM** is a salt buffer consisting of (in mM): 1.8 CaCl_2 , 0.8 MgCl_2 , 10 glucose, 10 HEPES (pH 7.3), 5 KCl and 145 NaCl

HEK 293T cells transiently transfected to express SNAP on the extracellular part of the plasma membrane were labeled with compounds **1-9** for 30 min at RT in NPM. Fluorescence lifetimes of these compounds were measured under confocal microscope in FLIM mode.

As seen in Table 11, the fluorescence lifetimes of compounds **1-9** ranged between 2.07 ns and 3.19 ns. Looking more closely at the measured values, we can see that the lifetimes of compounds with a C-6 linker between the charge and NR (compounds **4-6**) were slightly higher than the ones of compounds with a C-2 linker (**7-9**). Moreover, we observed that $\tau_{2+} < \tau_{+} < \tau_{-} < \tau_0$. This suggested that the fluorescence lifetime was somewhat sensitive to the

presence of the charge and the linker length (C-2 or C-6), contrary to the maximum fluorescence wavelength, which appeared to be similar for all compounds (Table 9).

In order to understand if the NR derivatives were experiencing the apolar environment of the membrane or of SNAP-tag, we first defined the fluorescence lifetime of our NR-derivatives in the membrane. Therefore, we applied compound **2** – which is known to insert unspecifically in the membrane - on non-transfected HEK 293T cells. This gave us the value of the fluorescence lifetime of NR in the membrane, which was measured to be 3.55 ns and is according to the value of fluorescence lifetime of NR measured in the membrane of DOPC vesicles in the literature.⁸³

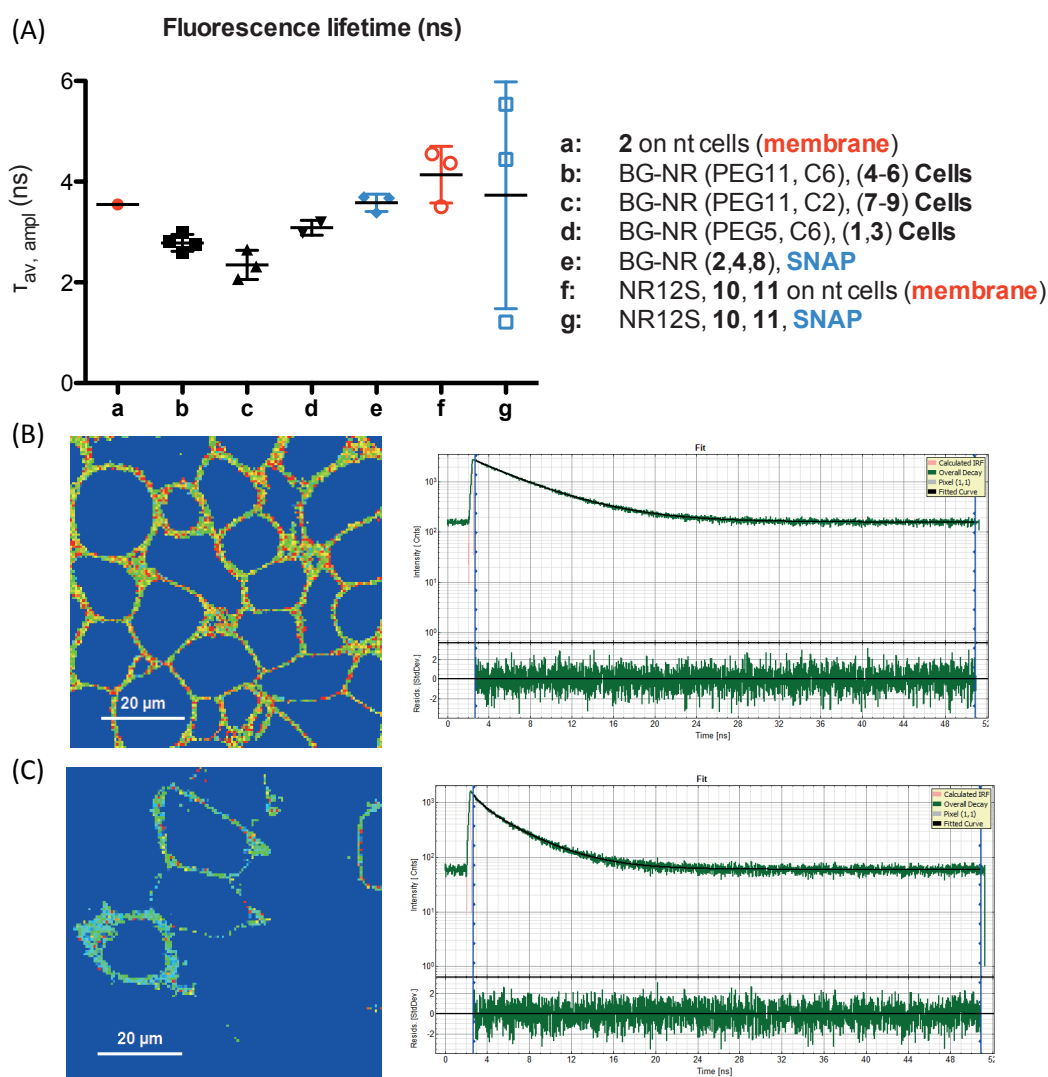


Figure 46: (A) Comparison of fluorescence lifetimes measured for **a**. Compound **2** inserted in the membrane, **b**. BG-NR compounds (PEG11, C2) bound to SNAP on cells, **c**. BG-NR compounds (PEG11, C6) bound to SNAP on cells, **d**. BG-NR compounds (PEG5, C6) bound to SNAP on cells, **e**. BG-NR compounds (**2**, **4** and **8**) bound to SNAP in PBS solution, **f**. Compounds NR12S, **10** and **11** inserted in the membrane of non-transfected cells and **g**. Compounds NR12S, **10** and **11** bound to SNAP in PBS solution. Each spot corresponds to one molecule. This figure refers to the results presented in Table 11. (B) Fluorescence decay of compound NR12S applied on non-transfected HEK 293T cells. (C) Fluorescence decay of compound **4** applied on HEK 293T cells expressing SNAP-tag on the extracellular part of the plasma membrane. Amplitude-averaged mean lifetimes for biexponential decays of fluorescence were calculated using Equation 4. For further details see Chapter 7.2.

Unfortunately, the lifetimes of our derivatives **1-9** were smaller than the one that corresponds to insertion in the membrane (3.55 ns) (Figure 46A). This could suggest that either our NR derivatives are not inserted in the membrane after the labeling reaction with SNAP or that the presence of a charge is affecting the lifetime of NR.

Furthermore, the lifetimes of compounds **2**, **4** and **8** were measured when bound to SNAP-tag in PBS solution w/o BSA (SNAP) and as shown in Table 11, they were slightly higher than the ones observed on cells. This was in contrast to the spectral measurement results (Table 9), where the

$\lambda_{\text{max,fl}}$ values of the derivatives on cells and the ones bound to SNAP-tag in solution were identical. This could be explained by the different consistency of NPM and PBS, which are solutions used in “Cells” and “SNAP” measurements respectively, since fluorescence lifetime is known to be very sensitive to the environment.

Moreover, it was interesting to see that the fluorescence lifetime of our NR derivatives **2**, **4**, **8**, **10** and **11** bound to BSA in PBS solution was always lower than the one observed when they were bound to SNAP-tag. The exact opposite behavior was shown for compounds NR12S and NR. This suggested that the presence of a benzylguanine moiety, PEG linker and charges reduced the hydrophobicity of the probe and further lowered the interactions of NR12S and NR with BSA.

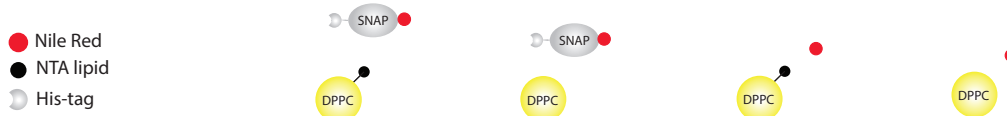
Finally, the lifetime of NR12S was measured to be 28.6% higher than the lifetime of compound **2** inserted in the membrane (Figure 46A). This suggested that these two derivatives were localised in different compartments of the membrane. Compounds **10** and **11** had similar fluorescence lifetimes with NR12S when applied on non-transfected cells.

5.2.2.2 FLIM Measurement of NR Derivatives on DPPC Liposomes

Finally, we also measured the fluorescence lifetimes of compounds **2**, **4**, **8**, **11** and NR12S, using DPPC liposomes as a membrane model, as described before (Chapter 5.2.1.2, Figure 45).

Table 12: Measurement of fluorescence lifetimes for NR derivatives (i) after conjugation to His-tagged SNAP applied on DPPC lipid vesicles containing NTA lipids and on control vesicles lacking the NTA lipids and (ii) directly applied on DPPC lipid vesicles containing NTA-lipids and on control vesicles lacking the NTA-lipids. Amplitude-averaged mean lifetimes for biexponential decays of fluorescence were calculated using Equation 4. For further details see Chapter 7.2.

Derivative	Fluorescence Lifetime on DPPC liposomes, $\tau_{\text{average, amplitude}}$ (ns)			
	SNAP		No SNAP	
	NTA lipids	No NTA lipids	NTA lipids	No NTA lipids
BG-PEG11-C6-NR (2)	1.520 ± 0.003	3.540 ± 0.020	1.650 ± 0.010	3.230 ± 0.030
BG-PEG11-Cya-C6-NR (4)	1.520 ± 0.020	3.660 ± 0.010	1.740 ± 0.010	3.280 ± 0.020
BG-PEG11-LysMe3-C2-NR (8)	1.370 ± 0.010	3.490 ± 0.020	n.d.	n.d.
NR12S	1.840 ± 0.010	3.910 ± 0.020	1.860 ± 0.010	3.770 ± 0.010
BG-PEG11-Cya- NR12S (11)	1.750 ± 0.004	3.810 ± 0.020	n.d.	n.d.



n.d.: Not determined

As presented in Table 12, the results of the spectral measurements that indicated the interaction of Ni-NTA lipids with our dye (Table 10) were confirmed. Indeed, regardless of the presence of SNAP, it appeared that the Ni-NTA lipids were quenching NR since in their presence; the fluorescence lifetimes of our derivatives were very small.

Therefore, we concluded that the Ni-NTA liposomes cannot be used as a membrane model and the results of these experiments could not be clearly used in order to interpret the position of our dyes.

5.3 Conclusions

We decided to investigate the environment our NR derivatives **1-11** were experiencing when they were applied on cells by performing spectral and FLIM experiments. The maximum emission and the fluorescence lifetime are two parameters of fluorophores that are very sensitive to the surrounding environment and indicative of the position of NR. Therefore, we measured the $\lambda_{\text{max,fl}}$ and the $\tau_{\text{av,ampl}}$ for all our NR derivatives when bound to SNAP tag expressed on cells and compared these values to the ones measured when bound to purified SNAP-tag in PBS solution.

These results suggested, that compounds **1-9** and **10,11** were positioned in different parts of the membrane. Moreover, according to the spectral measurement results, there seemed to be a correlation between the emission maxima of compounds **1-9** bound to SNAP on cells and in solution. This result could potentially suggest that compounds **1-9** were “trapped” in the hydrophobic environment of the protein and not inserted in the plasma membrane. This was not the case for compounds **10** and **11**, which were found to be 20-40 nm blue shifted in cells compared to purified SNAP in solution, suggesting that the dye was experiencing a different environment in the two cases (Table 8, Table 9). In addition, the Ni-NTA liposomes could not be used as a membrane model since the Ni-NTA lipids were quenching NR. Finally, the FLIM results could not give us a clear definition of the environment of NR derivatives.

Therefore, more experiments need to be done for investigating further the position of our compounds. This would be necessary in order to proceed with the voltage sensing application of our probes. However, regardless their mechanism of action, our probes are fluorogenic, allow the specific labeling of cells expressing SNAP-tag and thus can be used as a dynamic tool for the imaging of cell surface receptors.

Chapter 6

General Conclusions and Outlook

This thesis work focuses on the development of fluorogenic probes for plasma membrane proteins based on the solvatochromic molecule NR and its applications for

- (i) visualising SNAP-tagged membrane receptors (such as the Human Insulin Receptor) and
- (ii) developing a targetable voltage sensor

The award of the Nobel Prize in Chemistry to super-resolution microscopy in 2014 emphasized the importance of fluorescence microscopy. The rapid development of optical microscopy during the last years has enabled scientists to visualize biological processes inside living cells and organisms at almost molecular scale. Moreover, the use of fluorescent probes for tagging cell surface receptors has been of great importance in medicine as well as in basic research. The ideal probe would be a molecule that is both selective for its target and fluorescent only upon binding to its target molecule. To our knowledge, there is currently no generally applicable approach for the generation of such probes for cell surface receptors.

The high affinity of NR for the plasma membrane, its solvatochromic behavior and the sensitivity of its fluorescence QY to the polarity of the surrounding environment were exploited in order to design a specific and fluorogenic probe. Our idea was to reduce the affinity of NR for the plasma membrane with chemical derivatization. Then, only the chemically derivatized NR molecules bound to the target-receptor would have a high concentration close to the membrane and therefore insert in it and due to the apolar environment, fluoresce. The remaining NR molecules present in aqueous solution would remain in their dark state and thus would allow creating a fluorogenic and specific probe for interesting receptors. We decided to anchor our NR derivatives to SNAP-tag since it would ensure the generality of our approach.

We synthesized a large repertoire of chemically derivatized NR derivatives consisting of (i) a benzylguanine moiety, necessary for binding to SNAP-tag, (ii) a hydrophilic linker for further reducing the hydrophobicity of the probe and (iii) NR. We tried a variety of PEG linker lengths (PEG5 and PEG11), charges (no charge, one positive, one negative and two positive) and different linker lengths between NR and the charged moiety (C-2 and C-6). From the *in vitro* and the *in cellulo* experiments we performed, we validated our expectation that once the NR derivatives were bound to SNAP-tag they were experiencing a hydrophobic environment and were turning to their “fluorescent-on” state. Moreover, with the work described in this thesis we demonstrate the optimization of the structure of the NR derivatives in terms of fluorogenicity.

- 1) **PEG linker:** We showed that compounds **2** and **4** (PEG11) had a higher S/N in “no wash” experiments in DMEM + FBS 10% compared to compounds **1** and **3** (PEG5). We believe that the longer hydrophilic PEG11 linker reduced the hydrophobicity of the probe and therefore the residual affinity of the compounds for the membrane more than the PEG5 linker (compounds **1**, **3**) (Figure 16).
- 2) **Presence of a charge:** The presence of a charge in the linker was necessary for ensuring the fluorogenicity of the probe. We observed that compound **2**, that lacked a charge, was not fluorogenic in DMEM + FBS 10% (Figure 16). We attribute this to interactions of NR with FBS or BSA, which have been shown increase the fluorescence QY of NR.¹⁰⁰ The presence of the charge reduced these interactions and was necessary for guaranteeing the fluorogenicity of the probe.
- 3) **Different Charges:** We showed that in “no wash” experiments of compounds **4-6** (C-6 linker) the positively charged probes had a higher S/N ratio compared to the negatively charged. We believe that this was due to stronger interactions of the negatively charged molecules with the positively charged poly-D-lysine, which is used for coating of the coverslips, thus leading to a higher background noise (Figure 21).
- 4) **Linker length between NR and the charged moiety:** We observed that a short linker between NR and the charge (C-2, compounds **5-9**) achieved a higher S/N ratio in “no wash” experiments in DMEM + FBS 10%. We support that this is due to the closer proximity of the charge to NR, which further reduces the hydrophobicity of the probe and the unspecific interactions with BSA present in the medium.

We decided to validate our proof-of-concept experiments with a pharmacologically interesting receptor, the HIR. Indeed, cells expressing the SNAP-tagged HIR on the extracellular surface of the membrane were successfully imaged with or without a washing procedure. With this work we introduced a turn-on fluorogenic probe for “no wash” imaging of SNAP-tagged plasma membrane proteins, which should prove to be a powerful tool in bioimaging of membrane proteins.

As a second application for our probes, we chose to investigate if they could be used as voltage sensors. We were interested to see if the fluorescent properties of NR, being sensitive to the polarity of the environment, would also be sensitive to changes in membrane potential. This would allow us to design a targeted voltage sensor for SNAP-tag that would combine the specificity of genetically encoded voltage sensors with the sensitivity of organic voltage indicators. Thus, we performed patch clamp experiments in collaboration with EMBL (Paul Heppenstall's Group). Unfortunately, we saw that none of the NR derivatives **4-9** was voltage sensitive. This suggested that either NR was not voltage sensitive, or the position/orientation of our derivatives was not optimal.

The emission maximum and the fluorescence lifetime of NR are sensitive to its environment; therefore we anticipated that we would get valuable information from these experiments regarding the position of the derivatives. Thus, in order to shed light on where our NR

derivatives were positioned, we performed FLIM and spectral measurements of these compounds bound to SNAP-tag expressed on the plasma membrane of live cells or to purified SNAP-tag in solution. The results proposed that NR may be fluorescent not due to its insertion in the membrane, but rather due to the hydrophobic environment of SNAP-tag, where it is “trapped”. This hypothesis would also be supported by the work described by Karpenko *et al.* who designed a turn-on probe for GPCR oxytocin receptor based on NR, that was published in parallel with our work. In their work, they suggest that after the binding of the ligand to the receptor, the NR moiety protrudes into the lipid environment of the receptor and turns fluorescent.⁸⁰

In addition, we decided to use as a control for the voltage sensitivity another derivative of NR, that was introduced by Kucherak *et al.*⁸¹ and has been shown to be inserted in the membrane and be localized in the outer leaflet of the plasma membrane. This compound (NR12S) appeared to be non-fluorogenic in DMEM + FBS 10%, but in patch clamp experiments on HEK 293T cells it showed a 5% decrease in fluorescence intensity per 100 mV increase of membrane potential. This result was very encouraging since it confirmed our hypothesis about NR being voltage sensitive. As the final aim was to create a targeted voltage sensor for SNAP-tag, we decided to direct NR12S to SNAP-tag by chemical derivatization and synthesized compounds **10** and **11**. These compounds proved to label specifically cells expressing SNAP-tag only in the presence of FBS in the labeling medium (Figure 38, Figure 40). Apparently, in the presence of FBS, the NR derivatives bound preferentially to the latter than the plasma membranes of non-transfected cells. The excess of the dye bound to FBS was removed with the washing step and the remaining NR molecules were staining specifically cells expressing SNAP-tag, ensuring the specificity of labeling. When FBS was absent from the labeling medium, compounds **10** and **11** inserted unspecifically in all the membranes of cells (Figure 39).

As for the previous NR derivatives **1-9**, we observed that in the presence of FBS (specific labeling), compounds **10** and **11** were not voltage sensitive. On the other hand, when these probes were applied on non-transfected or transfected cells in EB (w/o FBS), there was a degree of voltage sensitivity. We believe that this result suggests that there was:

- (i) a fraction of the probe that inserted unspecifically in the membrane and was voltage sensitive and
- (ii) a fraction that was bound to SNAP-tag and was either “trapped” in the hydrophobic environment of the protein or had a different orientation in the membrane that led to lack of voltage sensitivity.

The optimal orientation of the dipole moment for voltage sensitivity is perpendicular to the membrane surface, since the charge distribution has to occur parallel to the electrical field. A poor orientation of the dye in the membrane can lead to a weak response to the electric field.

In addition, the results of our experiments imply that the position of our NR derivatives cannot be clearly defined based on the data we have at the moment. However, we would like to point out that the mechanism with which our probes turn fluorescent does not affect their use as effective fluorogenic probes for the imaging of cell surface receptors.

There are several experiments we could propose in order to further understand where our NR derivatives are positioned. First, we could derivatize NR with a longer hydrophilic PEG linker (e.g. PEG16 or PEG27) in order to bring NR further away from the binding site of SNAP-tag and direct it more towards the membrane. Another option would be to target the NR probe to another protein, like Halo-tag or ACP-tag and investigate if the behavior of the probes is different than the one observed for SNAP-tag. Moreover, checking the voltage sensitivity of our probes when applied on a different receptor (SNAP-HIR) could give us further information about their position. Finally, studying the interactions of BG-NR with SNAP-tag and obtaining a crystal structure of our derivatives bound to the protein, would give us more information about the potential binding pocket where NR may insert and allow us to come up with more strategies to direct the latter preferably to the membrane.

In short, we have successfully shown that, as we expected, NR is voltage sensitive. Patch clamp experiments on live HEK 293T cells showed a 5% decrease in fluorescence intensity of NR12S per 100 mV changes in membrane potential. This result will open a new path in the development of new voltage sensitive indicators and hopefully in the future we will be able to design a targeted voltage sensor based on this molecule which would combine the specificity of genetically encoded voltage sensors with the sensitivity of organic voltage sensitive dyes.

To conclude, with our work, we have introduced a new turn-on fluorogenic probe for “no wash” imaging of SNAP-tagged plasma membrane proteins. We identified a modified NR derivative that turns fluorescent only upon binding to SNAP-tag. The fluorogenicity of the probe is important not only due to the circumvention of tedious and time consuming washing steps, but mainly because it allows the application of this probe for monitoring molecular events in real time, or in *in vivo* experiments – where a washing procedure is not possible. This probe proved to efficiently label SNAP-tagged plasma membrane proteins with minimal background in “no wash” experiments with live cells and should thus become a powerful tool for bioimaging of plasma membrane proteins.

Chapter 7 Materials and Methods

7.1 Chemistry

General Information

All chemical reagents and dry solvents for synthesis were purchased from commercial suppliers (Sigma-Aldrich, Fluka, Acros) and were used without further purification or distillation. The composition of mixed solvents is given by the volume ratio (v/v). ^1H nuclear magnetic resonance (NMR) spectra were recorded on a Bruker DPX 400 (400 MHz), with chemical shifts (δ) reported in ppm relative to the solvent residual signals of CD_3CN (1.94 ppm) and DMSO-d_6 (2.50 ppm). Coupling constants are reported in Hz. High resolution mass spectra (HRMS) were measured on a Micromass Q-ToF Ultima spectrometer with electron spray ionization (ESI). Mass spectra were recorded on a Thermo Finnigan TSQ 7000 (ESI). Preparative RP-HPLC was performed on a Dionex system equipped with an UVD 170U UV- Vis detector for product visualisation on a Waters SunFireTM Prep C18 OBDTM 5 μm 10 \times 150 mm Column. Buffer A: 0.1% TFA in H_2O Buffer B: acetonitrile. Typical gradient was from 0% to 100% B within 30 min with 4 ml min⁻¹ flow.

Chemical Synthesis

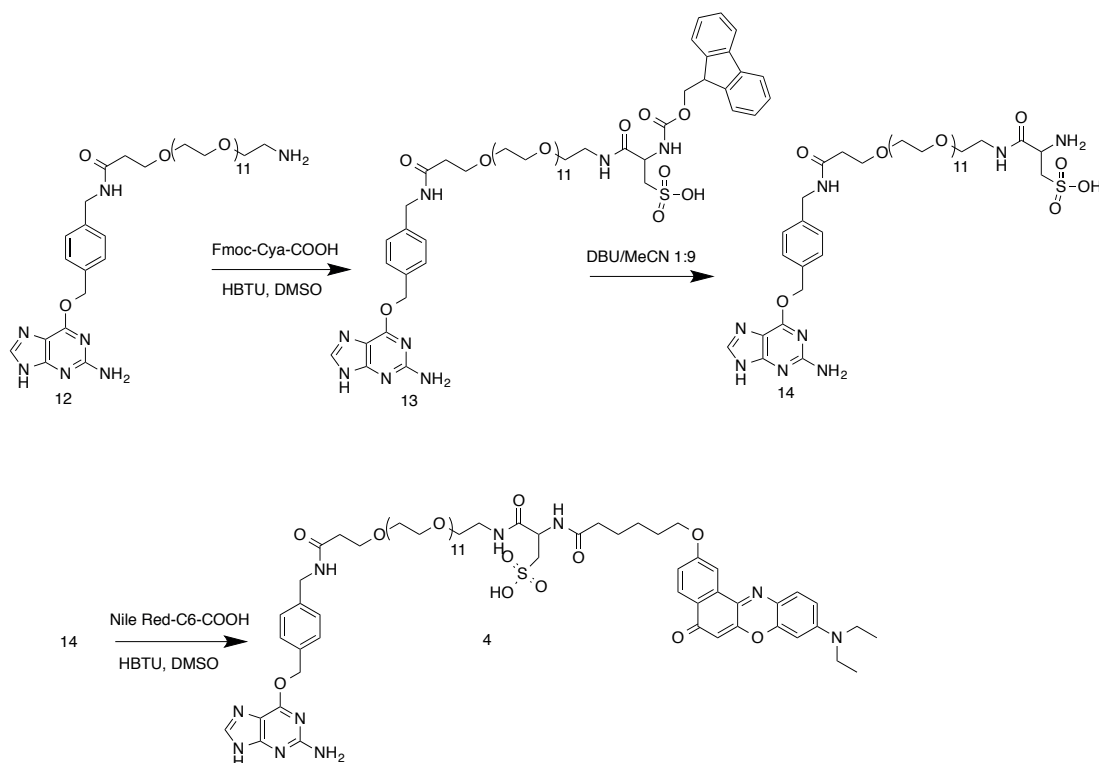


Figure 47: Synthesis of Compound 4 (BG-PEG11-Cya-C6-NR).

Compound 13: Fmoc-Cya-COOH (3.9 mg, 10 μ mol, 2 eq.) was dissolved in 0.1 ml DMSO. HBTU (3.8 mg, 10 μ mol, 2 eq.) and DIPEA (5 μ l, 29 μ mol, 4.8 eq.) were successively added. After 1 min, a 17 mM solution of **12*** (300 μ l, 5.1 μ mol, 1.0 eq.) was added. The reaction was let 45 min at room temperature. 300 μ l of H₂O were added and the reaction was purified by HPLC. The product was lyophilized (4.5 mg, yield 71%). MS (ESI, positive mode) calculated for C₅₈H₈₃N₈O₂₀S⁺ [M+H]⁺ 1243.5; found 1243.5. ¹H NMR (400 MHz, DMSO) δ 8.66 (br, s, 1 H), 8.40 (t, 1 H, J = 6.0 Hz), 7.87-7.95 (m, 3 H), 7.71 (m, 2 H), 7.50 (d, 2 H, J = 8.1 Hz), 7.39-7.44 (m, 3 H), 7.28-7.36 (m, 4 H), 5.55 (s, 2 H), 4.29 (d, 2 H, J = 5.9 Hz), 4.13-4.26 (m, 4 H), 3.63 (t, 2 H, J = 6.3 Hz), 3.49 (m, 44 H), 3.38 (t, 2 H, J = 6.1 Hz), 3.19 (m, 2 H), 2.81 (dd, 1 H, J = 5.0 Hz), 2.75 (dd, 1 H, J = 8.0 Hz), 2.39 (t, 2 H, J = 6.3 Hz).

* Compound **12** was synthesized as reported before¹²⁷.

Compound 14: Compound **13** (4.50 mg, 3.6 μ mol, 1 eq.) was dissolved in MeCN/DBU 9:1 (0.5 ml). After 5 min, 10ml Et₂O were added (precipitation). The solution was centrifuged, the supernatant was discarded, the pellet was washed with 10 ml Et₂O and dried under vacuum. The residue was dissolved in 1 ml H₂O (supplemented with 0.1% TFA) and purified by HPLC. The product was lyophilized (3.14 μ mol, yield 87%). MS (ESI, positive mode) calculated for C₄₃H₇₃N₈O₁₈S⁺ [M+H]⁺ 1021.5; found 1021.5. ¹H NMR (400 MHz, DMSO) δ 8.73 (t, 1 H, J = 5.4 Hz), 8.36-8.46 (m, 2 H), 8.09 (m, 3 H), 7.49 (d, 2 H, J = 8.1 Hz), 7.29 (d, 2 H, J = 8.1 Hz), 5.52 (s, 2 H), 4.29 (d, 2 H, J = 5.9 Hz), 4.02 (m, 1 H), 3.63 (t, 2 H, J = 6.4 Hz), 3.50 (m, 42 H), 3.44 (t, 2 H, J = 5.8 Hz), 3.18-3.37 (m, 4 H), 2.97 (dd, 1 H, J = 3.3, 14.0 Hz), 2.76 (dd, 1 H, J = 10.2, 14.0 Hz), 2.39 (t, 2 H, J = 6.3 Hz).

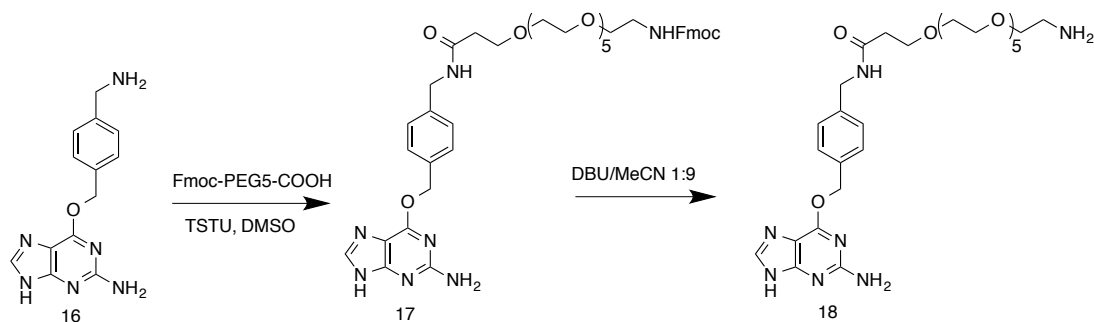


Figure 49: Synthesis of Compound 18.

Compound 17: To a solution of Fmoc-PEG₅-COOH (106 mg, 0.18 mmol, 1 eq.) in DMSO (0.8 ml) was added DIPEA (80 μ l, 0.46 mmol, 2.5 eq.) and TSTU (66 mg, 0.22 mmol, 1.2 eq.). After 10 min at r.t., a solution of BG-NH₂ **16*** (55 mg, 0.2 mmol, 1.1 eq.) in DMSO (0.2 ml) was added and the mixture stirred at r.t. for 20 min. The reaction was diluted with 0.5 ml H₂O and purified by HPLC and lyophilized (139 mg, yield 91%). MS (ESI, positive mode) calculated for C₄₃H₅₄N₇O₁₀⁺ [M+H]⁺ 828.4; found 828.2. ¹H NMR: (400 MHz, CD₃CN) δ 7.91 (s, 1 H), 7.82 (d, 2 H, J = 7.5 Hz), 7.63 (d, 2 H, J = 7.4 Hz), 7.41 (m, 4 H), 7.32 (m, 5 H), 5.87 (s, 1 H), 5.46 (s, 2 H), 4.38 (d, 2 H, J = 6.1 Hz), 4.35 (d, 2 H, J = 6.7 Hz), 4.20 (m, 1 H), 3.71 (t, 2 H, J = 5.9 Hz), 3.44-3.58 (m, 22 H), 3.24 (m, 2 H), 2.45 (t, 2 H, J = 5.9 Hz).

* **16** was synthesized as before ¹⁷.

Compound 18: Compound **17** (20 mg, 24.1 μ mol, 1.0 eq.) was dissolved in DBU/MeCN (1:9, 1.0 ml). After 5 min, the mixture was diluted with ether (10 ml), which resulted in the precipitation of an oil. The solution was centrifuged, the supernatant discarded and the oily residue was rinsed with 5 ml ether, dissolved in 0.1% TFA in water (1 ml), purified by HPLC and lyophilized (14.9 mg, yield 85% based on TFA salt). MS (ESI, positive mode) calculated for C₂₈H₄₅N₇O₈⁺ [M+H]⁺ 606.3; found 606.6. ¹H NMR: (400 MHz, DMSO) δ 8.42 (t, 1 H, J = 6.0 Hz), 8.33 (s, 1 H), 7.84 (br, s, 3 H), 7.49 (d, 2 H, J = 8.2 Hz), 7.29 (d, 2 H, J = 8.3 Hz), 5.53 (s, 2 H), 4.29 (d, 2 H, J = 5.9 Hz), 3.48-3.66 (m, 24 H), 2.98 (h, 2 H, J = 5.6 Hz), 2.39 (t, 2 H, J = 6.3 Hz).

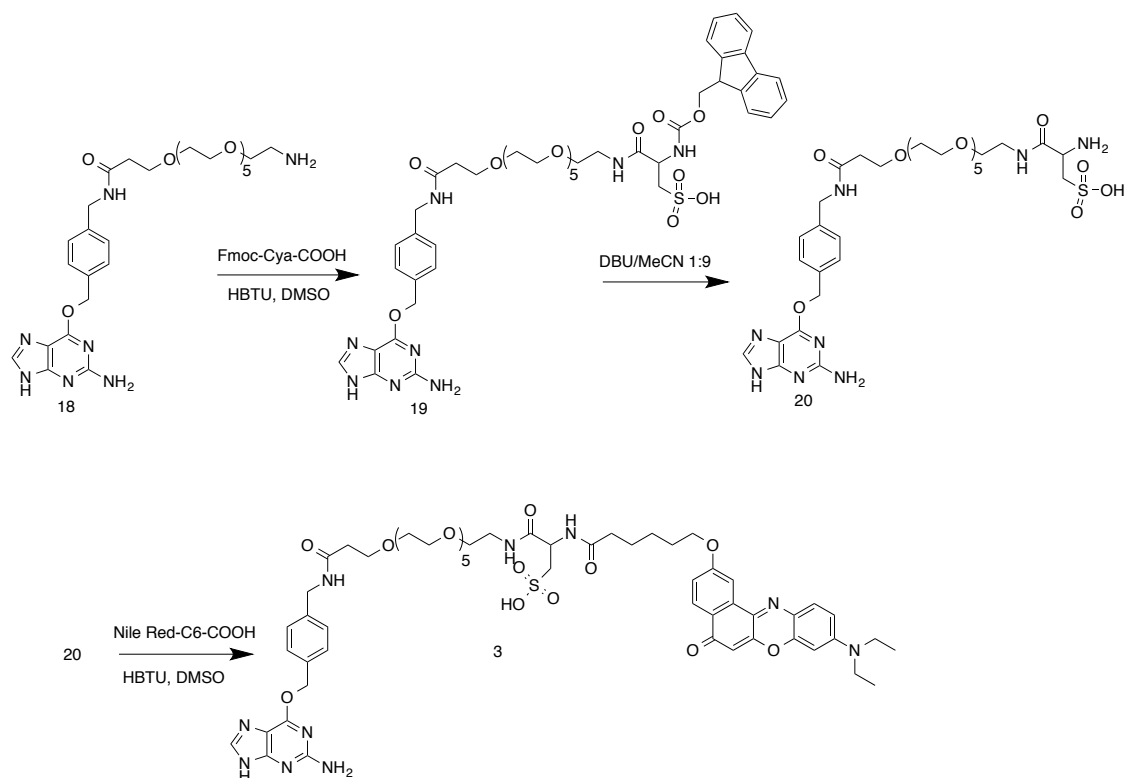


Figure 50: Synthesis of Compound **3** (BG-PEG5-Cya-C6-NR).

Compound 20: To a 0.1 M DMSO solution of Fmoc-Cya-COOH (60 μ l, 6 μ mol, 1.7 eq.) were added a 0.1 M solution HBTU (65 μ l, 6.5 μ mol, 1.8 eq.) and DIPEA (20 μ l, 115 μ mol, 32 eq.). After 1 min, a 36 mM solution of BG-PEG5-NH₂ (**18**) in DMSO (100 μ l, 3.6 μ mol, 1.0 eq.) was added. The reaction was let 45 min at room temperature and then 100 μ l H₂O were added. The reaction was roughly purified by HPLC. The product was lyophilized. The residue was then dissolved in MeCN/DBU 1:9 (1 ml) and after 5 min, 10 ml Et₂O were added (precipitation of an oil). The reaction was then centrifuged; the pellet was washed 3 times with 3 ml Et₂O. Finally the residue was dissolved in 0.5 ml water. After the addition of 10 μ l AcOH the product was purified by HPLC and lyophilized (2.1 μ mol, yield 58% over 2 steps). MS (ESI, positive mode) calculated for C₃₁H₄₉N₈O₁₂S⁺ [M+H]⁺ 757.3; found 757.7. ¹H NMR: (400 MHz, DMSO) δ 8.72 (t, 1 H, J = 5.3 Hz), 8.38 (t, 2 H, J = 5.6 Hz), 8.09 (bs, s, 3H), 7.49 (d, 2 H, J = 8.1 Hz), 7.30 (d, 2 H, J = 8.1 Hz), 5.53 (s, 2 H), 4.29 (d, 2 H, J = 5.8 Hz), 4.02 (m, 1 H), 3.64 (t, 2 H, J = 6.4 Hz), 3.48-3.54 (m, 22 H), 3.44 (t, 2 H, J = 5.8 Hz), 2.98 (dd, 1 H, J = 3.4 Hz), 2.77 (dd, 1 H, J = 10.1 Hz), 2.39 (t, 2 H, J = 6.3 Hz).

Compound 3: To a 20 mM DMSO solution of NileRed-C6-COOH **15*** (60 μ l, 1.2 μ mol, 1.1 eq.) were successively added a 0.1 M solution HBTU (15 μ l, 1.5 μ mol, 1.4 eq.) and DIPEA (10 μ l, 58 μ mol, 48 eq.). After 1 min, a 5.5 mM DMSO solution of compound **20** (200 μ l, 1.1 μ mol, 1 eq.) was added. The reaction was let 45 min at room temperature. 300 μ l H₂O were then added and the reaction was purified by HPLC. The product was lyophilized (0.54 μ mol, yield 48%). HRMS (ESI, positive mode) calculated for C₅₇H₇₆N₁₀O₁₆S²⁺ [M+H₂]²⁺ 594.2575; found 594.2569. ¹H NMR (400 MHz, DMSO) δ 8.64 (s, 1 H), 8.40 (t, 1 H, J = 5.9 Hz), 8.04 (d, 1 H, J = 8.7 Hz), 7.96 (m, 2 H), 7.77 (t, 1 H, J = 5.6 Hz), 7.67 (d, 1 H, J = 9.1 Hz), 7.50 (d, 2 H, J = 8.1 Hz), 7.24-7.33 (m, 3 H), 6.84 (dd, 1 H, J = 2.6 Hz), 6.67 (d, 1 H, J = 2.6 Hz), 5.54 (s, 2 H), 4.34 (m, 1 H), 4.28 (d, 2 H, J = 5.5 Hz),

4.16 (t, 2 H, J = 6.3 Hz), 3.62 (t, 2 H, J = 6.2 Hz), 3.48 (m, 28 H), 3.36 (t, J = 6.4 Hz), 3.18 (m, 3 H), 2.82 (m, 1 H), 2.73 (dd, 1 H, J = 7.5 Hz), 2.38 (t, 2 H, J = 6.2 Hz), 2.15 (t, 2 H, J = 7.3 Hz), 1.80 (m, 2 H), 1.59 (m, 2 H), 1.47 (m, 2 H), 1.17 (t, 6 H, J = 6.9 Hz).

* **15** was synthesized as reported before⁵⁷.

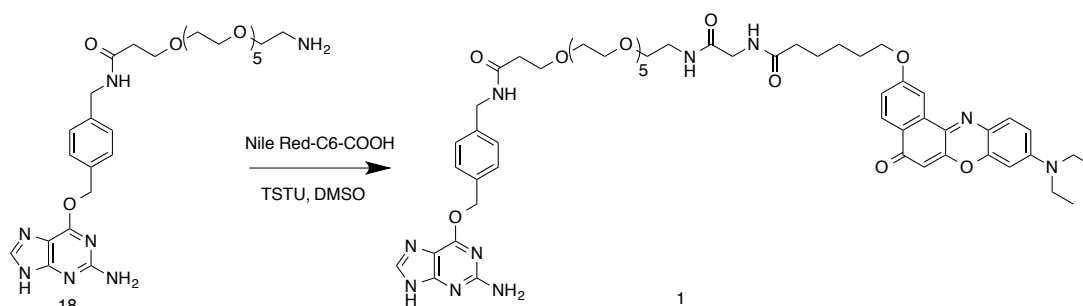


Figure S1: Synthesis of Compound **1** (BG-PEG5-C6-NR).

Compound 1: To a 62 mM DMSO solution of **15*** (88 μ l, 5.5 μ mol, 1.3 eq.), were added successively a 0.1 M TSTU solution in DMSO (60 μ l, 6.0 μ mol, 1.4 eq.) and DIEA (10 μ l, 77 μ mol, 18.0 eq.) The reaction was let 5 min at room temperature and a 50 mM DMSO solution of **18** (85 μ l, 4.25 μ mol, 1.0 eq.) was added. The reaction was let 15 min at r.t. and the product was purified by HPLC. The product was lyophilized (0.28 μ mol, yield 7.1%). HRMS (ESI, positive mode) calculated for $C_{54}H_{70}N_9O_{12}^+$ $[M+H]^+$ 1036.5138; found 1036.5137. (400 MHz, DMSO) δ 8.39 (m, 2 H), 8.03 (d, 1 H, J = 8.7 Hz), 7.93 (d, 1 H, J = 2.5 Hz), 7.87 (t, 1 H, J = 5.6 Hz), 7.63 (d, 1 H, J = 9.1 Hz), 7.47 (m, 2 H), 7.23-7.30 (m, 3 H), 6.82 (m, 1 H), 6.66 (d, 3 H, J = 2.5 Hz), 5.50 (s, 2 H), 4.26 (d, 2 H, J = 5.9 Hz), 4.14 (m, 2 H), 3.61 (t, 2 H, J = 6.3 Hz), 3.44-3.53 (m, 28 H), 3.38 (t, 2 H, J = 5.8 Hz), 3.18 (m, 2 H), 2.36 (t, 2 H, J = 6.3 Hz), 2.10 (t, 2 H, J = 7.2 Hz), 1.78 (m, 2 H), 1.58 (m, 2 H), 1.43 (m, 2 H), 1.15 (t, 6 H, J = 7.0 Hz).

* **15** was synthesized as reported before⁵⁷.

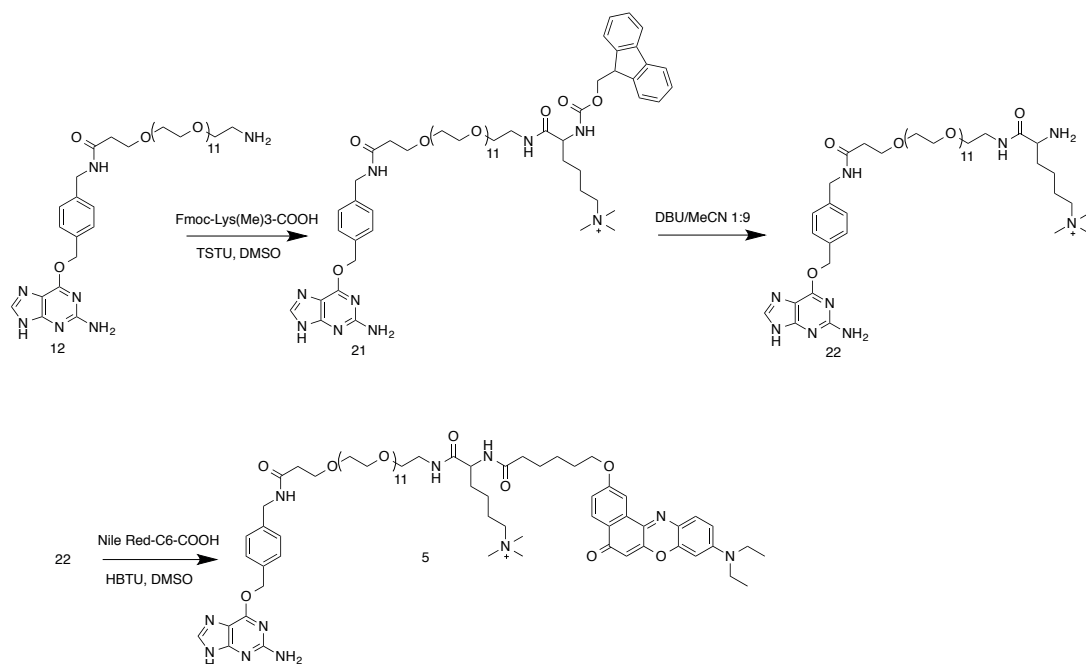


Figure 52: Synthesis of Compound **5** (BG-PEG11-LysMe3-C6-NR).

Compound 22: To a solution of Fmoc-Lys(Me)₃-COOH (61.52 mg, 137.93 μ mol, 1.2 eq.) in DMSO (0.5 ml) was added DIPEA (74.14 μ l, 574.7 μ mol, 5 eq.) and TSTU (69.2 mg, 229.89 μ mol, 2 eq.). After 15 min at r.t., a 120 mM solution of **12*** (957.85 μ l, 114.94 μ mol, 1 eq.) was added and the mixture stirred at r.t. for 1 h. After the addition of AcOH (74 μ l) the product was roughly purified by HPLC and lyophilized. The residue was then dissolved in MeCN/DBU 1:9 (1 ml) and after 5 min, 10 ml Et₂O were added (precipitation of an oil). The reaction was then centrifuged; the pellet was washed 3 times with 3 ml Et₂O. Finally the residue was dissolved in 1 ml water supplemented with 0.1% TFA and was purified by HPLC. The product was lyophilized (57.6 μ mol, yield 50% over 2 steps). MS (ESI, positive mode) calculated for C₄₉H₈₇N₉O₁₅⁺² [M+H]⁺² 520.81; found 520.80 ¹H NMR (400 MHz, MeOD) δ 8.39 (s, 1 H), 7.54 (d, 2 H, J = 8.1 Hz), 7.38 (d, 2 H, J = 8.1 Hz), 5.67 (s, 2 H), 4.43 (s, 2 H), 3.94 (t, 1 H, J = 6.6 Hz), 3.78 (t, 3 H, J = 6.0 Hz), 3.66-3.58 (m, 51 H), 3.46 (t, 2 H, J = 4.9 Hz), 3.16 (s, 10 H), 2.52 (t, 2 H, J = 6.0 Hz), 1.97-1.92 (m, 2 H), 1.89-1.83 (m, 3 H), 1.49 (m, 2 H).

***12** was synthesized as before¹⁷.

Compound 5: To a 100 mM DMSO solution of NileRed-C6-COOH **15*** (11.53 μ l, 1.15 μ mol, 1.2 eq.) were successively added TSTU (0.4 mg, 1.34 μ mol, 1.4 eq.) and DIPEA (0.8 μ l, 4.8 μ mol, 5 eq.). After 5 min, a 100 mM DMSO solution of compound **22** (9.6 μ l, 0.96 μ mol, 1.0 eq) was added. The reaction was let 45 min at room temperature. AcOH (0.8 μ l) was then added and the reaction was purified by HPLC. The product was lyophilized (0.7 μ mol, yield 67.7%) HRMS (ESI, positive mode) calculated for C₇₅H₁₁₃N₁₁O₁₉⁺² [M+H]²⁺ 735.9102; found 735.9109. ¹H NMR (400 MHz, MeOD) δ 8.39 (s, 1 H), 8.17 (d, 1 H, J = 8.8 Hz), 8.14 (d, 1 H, J = 2.5 Hz), 7.72 (d, 1 H, J = 9.2 Hz), 7.52 (m, 2 H), 7.37 (d, 2 H, J = 8.2 Hz), 7.26 (dd, 1 H, J = 2.6, 8.8 Hz), 6.96 (d, 1 H, J = 2.5 Hz), 6.72 (d, 1 H, J = 2.6 Hz), 6.33 (s, 1 H), 5.64 (s, 2 H), 4.40-4.43 (m, 3 H), 4.24 (t, 2 H, J = 6.2 Hz), 3.77 (t, 2 H, J = 5.9 Hz), 3.64-3.54 (m, 48 H), 3.51 (t, 2 H, J = 1.6 Hz), 3.16 (t, 2 H, J = 1.6 Hz), 3.13 (s, 9

let 45 min at r.t. Then, after addition of AcOH (0.5 μ l), the reaction was purified by HPLC. The product was lyophilized (0.6 μ mol, yield 64.6%). HRMS (ESI, positive mode) calculated for $C_{71}H_{105}N_{11}O_{19}^{+2}$ $[M+H]^{+2}$ 707.8789; found 707.8807. 1H NMR (400.08 MHz, MeOD) δ 8.34 (s, 1 H), 8.15-8.23 (m, 2 H), 7.69 (d, 1 H, J = 9.2 Hz), 7.51 (d, 1 H, J = 8.1 Hz), 7.35-7.38 (m, 4 H), 6.94 (dd, 1 H, J = 2.7, 9.2 Hz), 6.70 (d, 1 H, J = 2.7 Hz), 6.70 (d, 1 H, J = 2.7 Hz), 6.33 (s, 1 H), 5.63 (s, 2 H), 4.56 (m, 1 H), 4.42 (s, 1 H), 3.76 (t, 2 H, J = 5.9 Hz), 3.56-3.62 (m, 50 H), 3.39-3.43 (m, 2 H), 3.19-3.25 (m, 2 H), 3.09 (s, 9 H), 2.51 (t, 2 H, J = 6.0 Hz), 1.92-2.01 (m, 2 H), 1.71-1.86 (m, 2 H), 1.33-1.39 (m, 2H), 1.29 (t, 6 H, J = 6.9 Hz).

* **23** was synthesized as before⁵⁷.

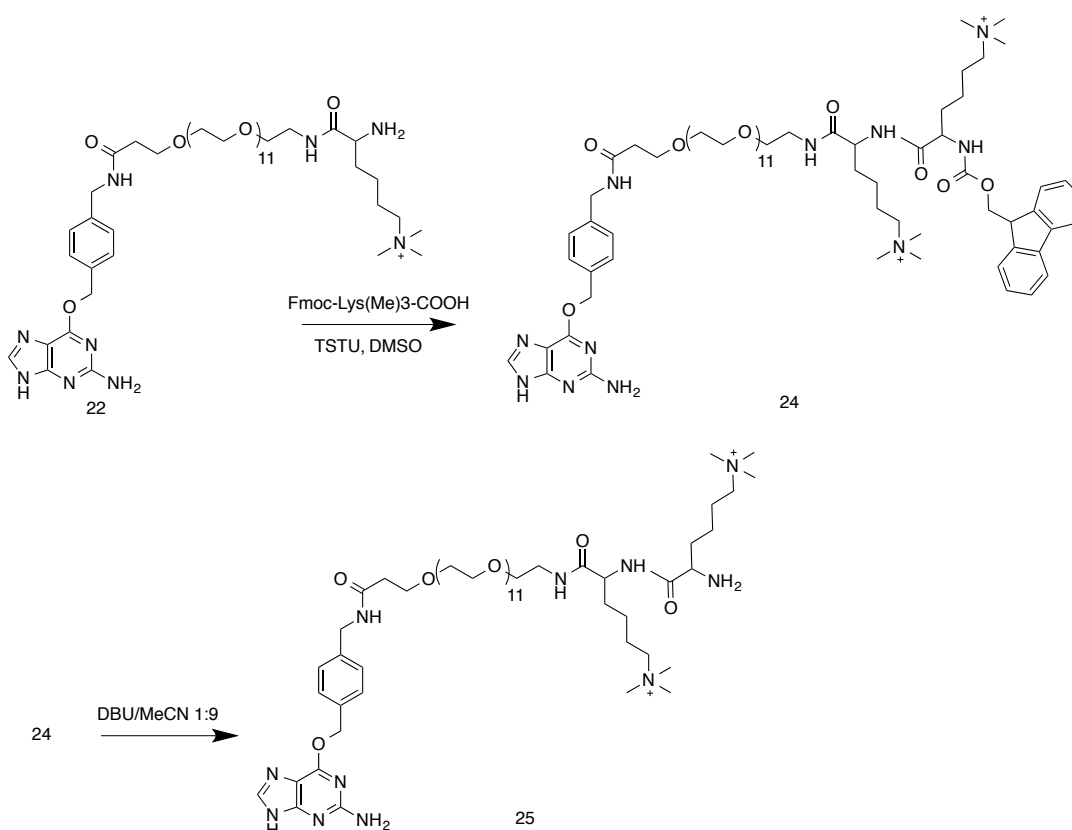


Figure 55: Synthesis of Compound **25**.

Compound 25: To a solution of Fmoc-Lys(Me)₃-COOH (30.8 mg, 69.2 μ mol, 1.2 eq.) in DMSO was added DIPEA (47.6 μ l, 288.1 μ mol, 5 eq.) and TSTU (34.7 mg, 115.3 μ mol, 2 eq.). After 15 min at r.t., a 100 mM solution of **22** (576.4 μ l, 57.6 μ mol, 1 eq.) was added and the mixture stirred at r.t. for 1 h. After the addition of AcOH (47.6 μ l) the product was roughly purified by HPLC and lyophilized. The residue was then dissolved in MeCN/DBU 1:9 (1 ml) and after 5 min, 10 ml Et₂O were added (precipitation of an oil). The reaction was then centrifuged; the pellet was washed 3 times with 3 ml Et₂O. Finally the residue was dissolved in 1 ml water supplemented with 0.1% TFA and was purified by HPLC. The product was lyophilized (4.3 μ mol, yield 7.5% over 2 steps). MS (ESI, positive mode) calculated for $C_{58}H_{106}N_{11}O_{16}^{+2}$ $[M+H]^{+2}$ 606.26; found 606.15. 1H NMR (400 MHz, MeOD) δ 8.42 (s, 1 H), 7.55 (d, 2 H, J = 8.1 Hz), 7.39 (d, 2 H, J = 8.2 Hz), 5.69 (s, 2 H), 4.44 (s, 2 H), 4.41-4.39 (m, 1 H), 4.02 (t, 1 H, J = 6.4 Hz), 3.78 (t, 2 H, J = 6.0

let 45 min at r.t. Then, after addition of AcOH (0.7 μ l), the reaction was purified by HPLC. The product was lyophilized (0.4 μ mol, yield 54.9%). HRMS (ESI, positive mode) calculated for $C_{80}H_{123}N_{13}O_{20}$ [M^+] 792.9498; found 792.9526. 1H NMR (400 MHz, MeOD) δ 8.16 (s, 1 H), 8.05 (d, 1 H, J = 8.8 Hz), 8.01 (d, 1 H, J = 2.5 Hz), 7.58 (d, 1 H, J = 9.2 Hz), 7.40 (d, 2 H, J = 8.1 Hz), 7.24 (d, 2 H, J = 8.1 Hz), 7.14 (dd, 1 H, J = 8.8, 2.6 Hz), 6.80 (dd, 1 H, J = 9.2, 2.7 Hz), 6.59 (d, 1 H, J = 2.7 Hz), 6.19 (s, 1 H), 5.51 (s, 2 H), 4.30 (s, 2 H), 4.23-4.19 (m, 1 H), 4.12 (t, 2 H, J = 6.2 Hz), 3.65 (t, 2 H, J = 6.0 Hz), 3.51-3.42 (m, 48 H), 3.38 (m, 1 H), 3.35-3.24 (m, 4 H), 3.19-3.16 (m, 1 H), 3.01 (d, 15 H, J = 3.8 Hz), 2.39 (t, 2 H, J = 6.0 Hz), 2.22 (t, 2 H, J = 7.3 Hz), 1.93 (s, 1 H), 1.82-1.77 (m, 3 H), 1.75-1.62 (m, 9 H), 1.53-1.47 (m, 2 H), 1.37-1.30 (m, 4 H), 1.17 (t, 6 H, J = 7.1 Hz).

* **23** was synthesized as before⁵⁷.

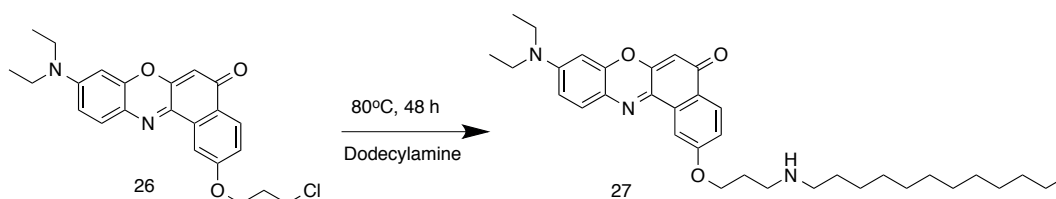
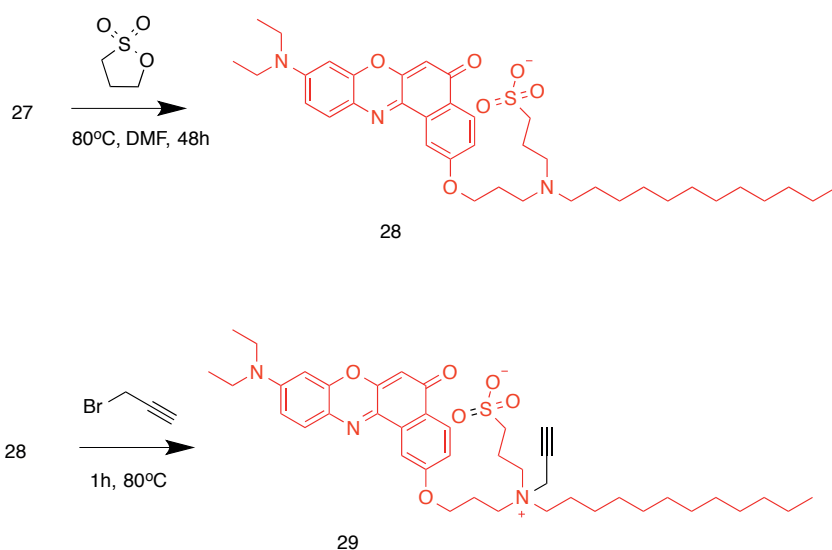


Figure 58: Synthesis of Compound **27**.

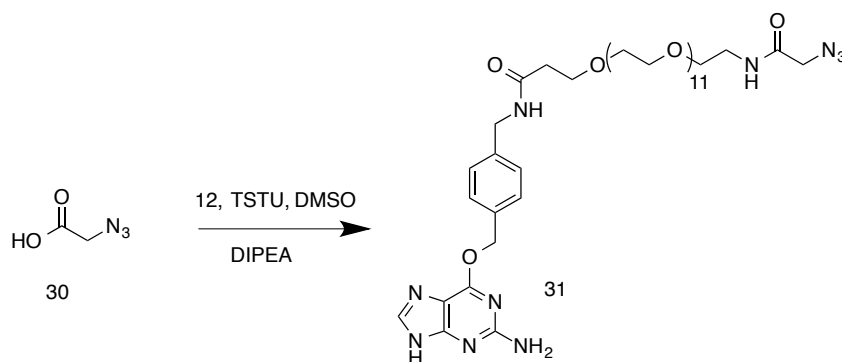
Compound 27: The NR derivative **26**^{*} (90 mg, 0.2 mmol, 1.0 eq.) was mixed with dodecylamine (162 mg, 0.9 mmol, 4.0 eq.) in butanone-2 in the presence of K_2CO_3 (75.8 mg, 0.5 mmol, 2.5 eq.) and KI (18.2 mg, 0.1 mmol, 0.5 eq.). The reaction mixture was refluxed for 48h. An extraction in EtoAc-Brine was performed and the product was collected in the organic phase. The product was then dissolved in DMF and was purified by HPLC (30 – 100% ACN). An alkaline extraction in NaOH 0.1 M/DCM was performed after lyophilisation and the free base was collected in the organic phase (32.0 mg, 26% yield). MS (ESI, positive mode) calculated for $C_{35}H_{50}N_3O_3$ [$M+H^+$] 559.79; found 560.25. 1H NMR (400 MHz, MeOD) δ 7.57 (d, 1 H, J = 8.8 Hz), 7.45 (d, 1 H, J = 2.5 Hz), 7.07 (d, 1 H, J = 9.1 Hz), 6.72 (dd, 1 H, J = 2.6 Hz, J = 8.7 Hz), 6.41 (dd, 1 H, J = 2.6 Hz, J = 9.2 Hz), 6.13 (d, 1 H, J = 2.6 Hz), 5.81 (s, 1 H), 3.96 (m, 2 H), 3.09-3.10 (m, 6 H), 2.89 (m, 4 H), 2.04 (m, 2 H), 1.54 (d, 2 H, J = 7.4 Hz), 1.02 (m, 22 H), 0.63-0.65 (m, 3 H).

* **26** was synthesized as reported before⁵⁷.

Figure S9: Synthesis of Compound **29**.

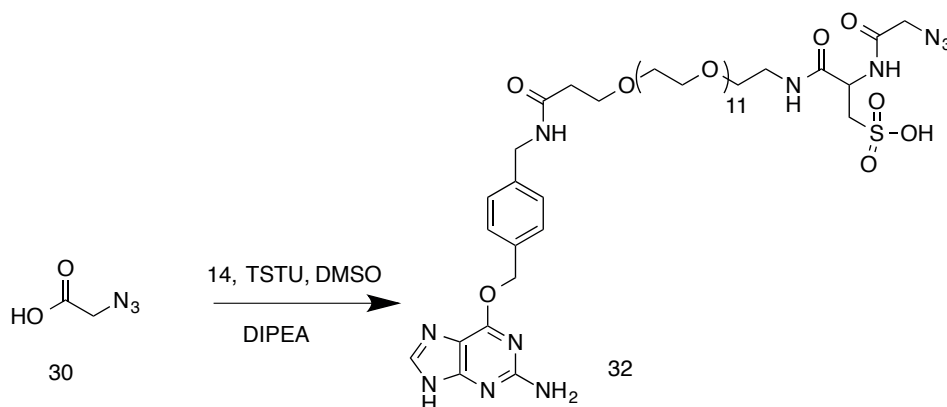
Compound 28: The amine derivative **27** (32.0 mg, 57.0 μmol , 1 eq.) was dissolved in 1 mL of dry DMF under inert atmosphere. Then 1,3-propanesultone (2.5 μL , $\rho=1.392\text{ g/mL}$, 28.0 μmol , 0.5 eq.) was added to the solution. The reaction mixture was stirred at 80°C for 48 h. After cooling, the product was purified by HPLC and was lyophilized (16.0 mg, 41.1% yield). MS (ESI, positive mode) calculated for $\text{C}_{38}\text{H}_{56}\text{N}_3\text{O}_6\text{S}$ $[\text{M}+\text{H}^+]$ 681.93; found 682.20. ^1H NMR (400 MHz, CD_2Cl_2) δ 10.64 (dd, 1 H), 7.92 (d, 1 H, $J = 8.5\text{ Hz}$), 7.73 (s, 1 H), 7.42 (d, 1 H, $J = 8.7\text{ Hz}$), 6.96-6.91 (m, 1 H), 6.67-6.61 (m, 1 H), 6.39 (m, 1 H), 6.31 (s, 1 H), 5.24 (s, 2 H), 4.13 (m, 2 H), 3.41 (m, 4 H), 3.08 (s, 2 H), 3.00 (s, 1 H), 2.26 (d, 3 H, $J = 3.2\text{ Hz}$), 1.69 (d, 2 H, $J = 6.3\text{ Hz}$), 1.62 (s, 1 H), 1.21-1.16 (m, 22 H), 0.78 (m, 3 H).

Compound 29: The NR derivative **28** (16.0 mg, 23.0 μmol , 1 eq.) was dissolved in dry DMF under inert atmosphere. Then propargyl bromide (2.2 μL , $\rho=1.38\text{ g/mL}$, 26.0 μmol , 1.1 eq.) and K_2CO_3 (6.5 mg, 47.0 μmol , 2 eq.) were added to the solution. The reaction mixture was stirred at 50°C for 24 h. After cooling, an extraction was performed in DCM/ H_2O and the organic phase was dried O/N under vacuum to remove all traces of DMF present. The product was purified by preparative TLC (10-90 MeOH-DCM) and was lyophilized (8.0 mg, 43.1% yield). MS (ESI, positive mode) calculated for $\text{C}_{41}\text{H}_{58}\text{N}_3\text{O}_6\text{S}$ $[\text{M}+\text{H}^+]$ 719.98; found 720.20. ^1H NMR (400 MHz, CD_2Cl_2) δ 7.98 (d, 1 H, $J = 8.6\text{ Hz}$), 7.77 (s, 1 H), 7.38 (d, 1 H, $J = 9.3\text{ Hz}$), 7.04 (d, 1 H, $J = 8.7\text{ Hz}$), 6.50 (d, 2 H, $J = 7.9\text{ Hz}$), 6.27 (s, 1 H), 5.99 (s, 1 H), 4.30 (s, 2 H), 4.18 (m, 2 H), 3.69-3.74 (m, 2 H), 3.60-3.67 (m, 1 H), 3.50-3.57 (m, 1 H), 3.25-3.37 (m, 6 H), 2.90 (s, 1 H), 2.83 (t, 2 H, $J = 5.9\text{ Hz}$), 2.35 (m, 2 H), 2.20 (m, 2 H), 1.71 (m, 6 H), 1.14-1.32 (m, 23 H), 0.78 (m, 3 H).

Figure 60: Synthesis of Compound **31**.

Compound 31: To a solution of compound **30** (0.6 μ l, ρ =1.35 g/ml, 8.7 μ mol, 1.2 eq.) in DMSO were successively added DIPEA (3.9 μ l, 21.7 μ mol, 3 eq.) and TSTU (2.8 mg, 9.4 μ mol, 1.3 eq.). After 5 min, a 100 mM DMSO solution of **12**^{*} (72.4 μ l, 7.2 μ mol, 1.0 eq.) was added and the reaction was let 45 min at r.t. Then, after addition of AcOH (3.9 μ l), the reaction was purified by HPLC. The product was lyophilized (3.1 mg, yield 44.9%). MS (ESI, positive mode) calculated for $C_{42}H_{69}N_{10}O_{15}$ $[M+H]^{2+}$ 476.53; found 477.25. ¹H NMR (400 MHz, MeOD) δ 8.30-8.27 (m, 0 H), 8.19 (s, 1 H), 7.41 (d, 2 H, J = 8.0 Hz), 7.25 (d, 2 H, J = 8.0 Hz), 5.54 (s, 2 H), 4.31 (m, 2 H), 3.79 (s, 2 H), 3.65 (t, 2 H, J = 5.9 Hz), 3.53-3.46 (m, 48 H), 2.39 (t, 2 H, J = 5.9 Hz).

* Compound **12** was synthesized as reported before.¹²⁷

Figure 61: Synthesis of Compound **32**.

Compound 32: To a solution of compound **30** (0.5 μ l, ρ =1.35 g/ml, 7.4 μ mol, 1.2 eq.) in DMSO were successively added DIPEA (3.3 μ l, 18.5 μ mol, 3 eq.) and TSTU (2.4 mg, 8.0 μ mol, 1.3 eq.). After 5 min, a 100 mM DMSO solution of **14** (61.8 μ l, 6.2 μ mol, 1 eq.) was added and the reaction was let 45 min at r.t. Then, after addition of AcOH (3.3 μ l), the reaction was purified by HPLC. The product was lyophilized (3.7 mg, yield 54.3%). MS (ESI, positive mode) calculated for $C_{45}H_{73}N_{11}O_{19}S$ $[M+H]^+$ 1103.18 ; found 1104.25. ¹H NMR (400 MHz, MeOD) δ 8.37 (s, 1 H), 7.43 (m, 2 H), 7.27 (d, 2 H, J = 8.1 Hz), 5.57 (s, 2 H), 4.32 (s, 2 H), 3.87 (d, 2 H, J = 5.0 Hz), 3.65 (t, 3 H, J = 5.9 Hz), 3.53-3.44 (m, 51 H), 3.28-3.25 (m, 2 H), 3.15-3.11 (m, 2 H), 2.40 (t, 2 H, J = 5.9 Hz), 1.83-1.52 (m, 2 H).

Compound 10: To a 100 mM solution of compound **29** (33.3 μ l, 3.3 μ mol, 1 eq.) in DMSO was added a solution of compound **31** (3.2 mg, 3.3 μ mol, 1.0 eq.) under argon. In another eppendorf, CuSO₄ (83.4 μ l from 20 mM stock in DMSO, 1.7 μ mol, 0.5 eq), TBTA (16.7 μ l from 20 mM stock in DMSO, 0.3 μ mol, 0.5 eq.) and sodium ascorbate (6.7 μ l from 500 mM stock in H₂O, 3.3 μ mol, 1.0 eq.) were mixed. The solutions of the two eppendorfs were mixed together under argon and the reaction was let shaking in room temperature for 3 h. The reaction was purified by HPLC and the product was lyophilized (5.2 mg, 93.2% yield). MS (ESI, positive mode) calculated for C₈₃H₁₂₆N₁₃O₂₁S [M+H]²⁺ 837.52; found 837.20. ¹H NMR (600 MHz, MeOD) δ 8.47 (s, 1 H), 8.38 (s, 1 H), 8.15 (dd, 1 H, J = 1.1, 8.7 Hz), 8.12 (d, 1 H, J = 2.1 Hz), 7.65 (m, 1 H), 7.51 (m, 2 H), 7.36 (d, 2 H, J = 8.1 Hz), 7.29-7.27 (m, 1 H), 6.92-6.91 (m, 1 H), 6.67 (s, 1 H), 6.30 (d, 1 H), 5.63 (s, 2 H), 5.31 (s, 2 H), 4.78 (s, 2 H), 4.42 (s, 2 H), 4.40-4.36 (m, 2 H), 3.76 (t, 2 H, J = 5.9 Hz), 3.65-3.54 (m, 56 H), 3.45-3.43 (m, 2 H), 3.37 (s, 6 H), 2.95 (t, 2 H, J = 6.6 Hz), 2.51 (m, 2 H), 2.42-2.36 (m, 2 H), 2.00-1.94 (m, 2 H), 1.39 (d, 3 H, J = 3.1 Hz), 0.89 (t, 3 H, J = 7.0 Hz).

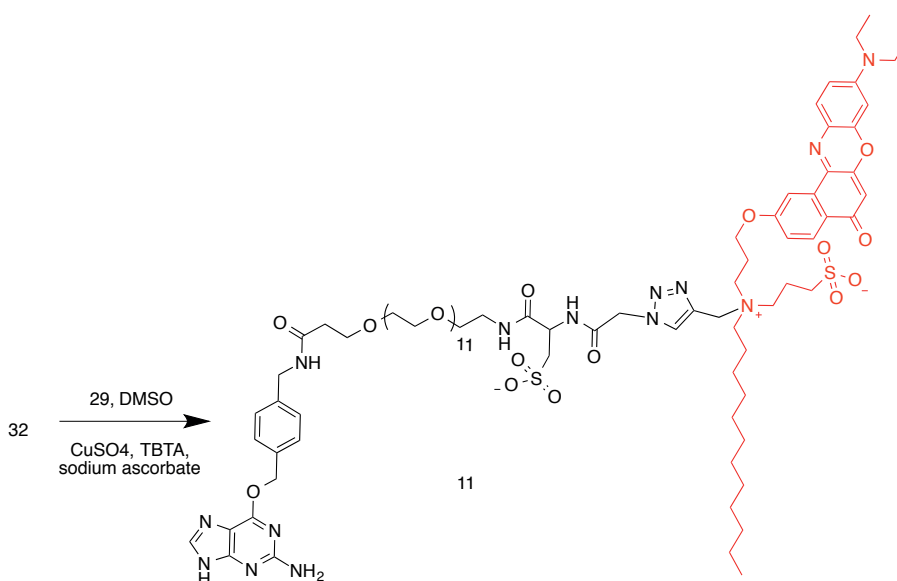


Figure 63: Synthesis of Compound **11** (BG-PEG11-Cya-NR12S).

Compound 11: To a 100 mM solution of compound **29** (34.7 μ L, 3.5 μ mol, 1.0 eq.) in DMSO was added a solution of compound **32** (3.8 mg, 3.5 μ mol, 1.0 eq.) under argon. In another eppendorf, CuSO₄ (86.9 μ L from 20 mM stock in DMSO, 1.7 μ mol, 0.5 eq), TBTA (17.3 μ L from 20 mM stock in DMSO, 0.3 μ mol, 0.5 eq.) and sodium ascorbate (6.9 μ L from 500 mM stock in H₂O, 3.5 μ mol, 1 eq.) were mixed. The solutions of the two eppendorfs were mixed together under argon and the reaction was let shaking in room temperature for 3 h. The reaction was purified by HPLC and the product was lyophilized (2.3 mg, 36.3% yield). MS (ESI, positive mode) calculated for C₈₆H₁₃₀N₁₄O₂₅S₂ [M+H]²⁺ 912.50; found 912.75. ¹H NMR (600 MHz, MeOD) δ 8.53 (d, 1 H, J = 4.4 Hz), 8.39 (s, 1 H), 8.11-8.08 (m, 1 H), 8.02-8.00 (m, 1 H), 7.64-7.61 (m, 1 H), 7.49 (d, 2 H, J = 8.0 Hz), 7.36 (d, 2 H, J = 8.1 Hz), 7.24-7.22 (m, 1 H), 6.95-6.93 (m, 1 H), 6.65-6.64 (m, 1 H), 6.30-6.29 (m, 1 H), 5.59 (s, 2 H), 5.51 (s, 1 H), 5.37 (s, 2 H), 4.42 (s, 2 H), 4.34 (s, 2 H), 3.76 (t, 2 H, J = 5.9 Hz), 3.61-3.55 (m, 50 H), 3.51 (m, 3 H), 3.28-3.25 (m, 2 H), 2.99 (t, 2 H, J = 6.5 Hz), 2.51 (t, 3 H, J = 5.9 Hz), 2.45-2.39 (m, 2 H), 2.05-1.93 (m, 2 H), 1.40 (d, 4 H, J = 4.1 Hz), 0.88 (t, 4 H, J = 7.0 Hz).

7.2 Biology

General Information

Plasmids pDisplay-SNAP and pDisplay-SNAP-CLIP-HCA were kindly provided by Dr. M. Brun (EPFL, Switzerland).

QIAquick Gel Extraction Kits, QIAprep Spin Miniprep Kits and Qiagen Plasmid Midi Kit were purchased from Qiagen. Restriction enzymes were purchased at New England Biolabs (NEB) and Thermo Fischer. Prestained protein molecular weight marker was purchased from Fermentas. The SNAP- and CLIP-tag labeling substrates were synthesized or purchased from NEB. Polyornithine, bovine serum albumin (BSA), NaCl, SDS were purchased from Sigma. Tris was purchased from AppliChem. DMEM Glutamax medium, fetal bovine serum and Hank's buffered salt solution (HBSS) were purchased from Lonza. Lipofectamine 2000 was purchased at

Invitrogen. Protease inhibitor cocktail tablets were obtained from Roche. Glass coverslips were obtained from Glaswarenfabrik Karl Hecht KG. Ibidi dishes were purchased from Westfield medical. 12-well and 6-well tissue culture plates were purchased from TPP. 96-well clear-bottom black- well plates were purchased from Corning.

***In Vitro* Characterization of Fluorescent Properties of NR Derivatives**

The samples of the appropriate substrates were prepared in 1.5 mL tubes (Eppendorf) (1 μ M) in dioxane, Dubelcco's modified eagle medium (DMEM) + 10% fetal bovine serum (FBS), phosphate buffered saline (PBS). Fluorescence was measured in a 96-well plate on an Infinite M1000 spectro-fluorometer (TECAN). Fluorescence emission was detected while exciting at 520 nm, and the excitation spectrum was recorded at 700 nm emission wavelength. Both the excitation and emission bandwidth for all measurements were set to 10 nm.

Determination of Relative Fluorescent QY

Fluorescence QY of compounds **1–9** were measured in PBS, DMEM + FBS 10%, and dioxane using a solution of NR in methanol (MeOH) as a reference. Absorbance spectra of NR solutions of different concentrations were recorded using a SHIMADZU UV spectrophotometer UV-1800 in the 400–800 nm interval with 1 nm step and 1 nm fixed bandwidth. Afterward fluorescence of the same samples was measured in 96-well plates on an Infinite M1000 spectrofluorometer (TECAN). Both the excitation and emission bandwidth for all measurements were set to 10 nm. The spectra were recorded with a step size of 1 nm. The excitation wavelength was set to 520 nm, and the emission spectra were recorded in the 540–800 nm interval. Absorbance at 520 nm versus integrated fluorescence intensity was plotted. The ratio of the obtained slope values of each compound to the slope value of NR in MeOH multiplied by measured QY of NR in MeOH (38%)¹²⁸ and corrected by the refractive indexes of the solvents gave relative QY reported in Table 2, Table 5 and Table 6.

***In Vitro* Kinetic Experiments**

SNAP was diluted in PBS buffer with 0.1 mg mL⁻¹ BSA to the desired concentration (400 nM). The reaction was started by the addition of a 3-fold molar excess of a substrate (as a 1.2 μ M solution in DMSO). At each time point, 10 μ L of reaction mixture was withdrawn and immediately mixed with 10 μ L of stop buffer (2x SDS loading buffer supplemented with 150 μ M O⁶- benzylguanine) preheated to 95 °C. The samples were analyzed on a 12% SDS-PAGE gel, and in-gel fluorescence was recorded on a Pharos-FX (Biorad) scanner. Fluorescent band intensity was quantified using Quantity one (Biorad) and plotted against time. Data were fitted to a single exponential equation, and labeling rate constant *k* was calculated using the Equation 3:

$$k = \frac{\ln 2}{t_{1/2}C} \text{ M}^{-1} \text{ s}^{-1}$$

Equation 3: Calculation of Labeling Rate Constant *k*, where *t*_½ is the half-life time of labeling and *c* is the substrate concentration.

Cell Culture and Transfection

HEK 293T cells were grown on polyornithine-coated glass bottom culture Petri dishes (35 mm) in DMEM Glutamax medium (Lonza) supplemented with 10% FBS (Lonza) and transiently transfected by using Lipofectamine 2000 (Invitrogen) according to the manufacturer's protocol.

CHO cells stably expressing extracellular SNAP-tagged HIR were maintained in HAM's F-12 medium (Invitrogen) supplemented with 10% FBS and 600 $\mu\text{g mL}^{-1}$ G418 at 37 °C. CHO cells stably expressing extracellular SNAP-tagged HIR were grown on 35 mm uncoated glass bottom dishes in medium for 2 days. Starvation of cells followed by washing with F-12 HAM medium (w/o FBS) and incubating for 2 h at 37 °C.

Stable CHO Cell Line Expressing SNAP-tagged HIR

Homo sapiens HIR (NCBI Reference Sequence: NM_001079817), with the HindIII site before the start codon and XbaI after the stop codon, was subcloned by replacing the EGFP sequence of pEGFP-N1 (Clontech Takara). The SphI site was created by a silent mutation at Ala⁸¹² (GCT to GCA). The SNAP-tag was inserted at the C-terminus of the α -subunit, between Ser⁷⁴⁶ and Arg⁷⁴⁷, by replacing the BamHI-SphI fragment in the coding sequence. The HIR and the SNAP sequences were synthesized by GeneArt (life technologies). CHO-K1 cells were transfected with the SNAP-HIR plasmid using Lipofectamine LTX (Invitrogen). Twenty-four hours after transfection, the cells were selected in 600 $\mu\text{g mL}^{-1}$ G418, and stably expressing clones were isolated by limiting dilution method. The clones were screened with SNAP-Surface Alexa Fluor 488 (NEB).

SNAP & CLIP-tag Labeling on the Surface of Cells

We used HEK 293T cells transiently expressing pDisplay-SNAP-CLIP-HCA and extracellular SNAP-tagged HIR stably expressing CHO cells.

At 24 h after transfection, HEK 293T cells were labeled by incubation with a solution of 10 μM *O*²-benzylcytosine (BC) derivative in DMEM (without Phenol Red) supplemented with 10% FBS, in NPM (w/o FBS) or in EB (with or w/o FBS) for 10 min at 37 °C and washed three times with the labeling (and culture) medium. Then, the cells were labeled with the corresponding *O*⁶-benzylguanine (BG) derivative (500 nM) in DMEM (without Phenol Red) + FBS 10%, in NPM (w/o FBS), or in EB (with or w/o FBS) for 30 min at RT. After labeling, cells were imaged directly or after three washes with the labeling (and culture) medium in RT.

CHO cells stably expressing extracellular SNAP-tagged HIR were stained with 2 μM BG-PEG11-Cya-NR (4) in F-12 HAM medium (w/o FBS) supplemented with 15 mM HEPES for 30 min at RT and imaged directly or after three washes.

Wide Field Microscopy and Live Cell Imaging

Imaging of the labeled HEK 293T cells was performed using a Leica LAS AF 6000 wide-field microscope equipped with a 40x plan Apochromat 1.25 NA or a 63x plan Apochromat 1.40 NA oil immersion objective lens and a xenon arc lamp. The filter sets used are the following: for NR excitation at 572 nm (bandwidth 35 nm) and emission at 632 nm (bandwidth 60 nm), and for

AlexaFluor 488 excitation at 470 nm (bandwidth 40 nm) and emission at 520 nm (bandwidth 40 nm).

Confocal Microscopy

Imaging of the labeled SNAP-tagged HIR was performed using a Leica SP8 confocal microscope equipped with an HCX PL Apochromat CS 63X (1.40 NA) oil immersion objective. All of the fluorescent images were obtained under the same acquisition conditions, excitation at 514 nm (Ar laser) and detection at 560–645 nm using HyD detector. The images were deconvolved using the Huygens Essentials package.

Fluorescent Spectral Measurement on Live Cells

Compounds 1-11 and NR12S:

HEK 293T cells transiently transfected to express extracellular SNAP-tag were cultured on glass bottom dishes for 1 day and labeled with 500 nM of each NR compound in NPM medium (w/o FBS), followed by washing to remove excess dye. NPM is a salt buffer which consists of 1.8 mM CaCl₂, 0.8 mM MgCl₂, 10 mM glucose, 10 mM HEPES (pH 7.3), 5 mM KCl and 145 mM NaCl. Imaging of the labeled SNAP-tag was performed using a Leica SP8 confocal microscope equipped with an HC PL Apochromat 63X (1.20 NA) water immersion objective. The emission spectra of the NR compounds were measured using lamda mode, excitation at 514 nm (Ar laser) and detection at 560–695 nm (step: 5 nm) using HyD detector.

Compounds NR12S, 10 and 11 described in Table 8:

HEK 293T cells transiently transfected to express extracellular SNAP-CLIP-HCA were cultured on glass bottom dishes for 1 day and labeled with 500 nM of each Nile compound in EB medium (with or w/o FBS), and 1 μ M CLIP-Surface 647 followed by washing to remove excess dye. EB buffer contained (in mM): 150 NaCl, 5 KCl, 1 MgCl₂, 2 CaCl₂, 5 glucose, 10 HEPES; pH 7.4 adjusted with NaOH, 300 mOsm. Imaging of the labeled SNAP-tag was performed using a Leica SP5 confocal microscope equipped with Resonant Scanner activated and a 40X (1.25 NA) PL ApoUV oil immersion objective. The emission spectra of the NR compounds were measured using lamda mode, excitation at 488 nm and detection at 495–730 nm (step: 5 nm) using HyD detector (5 nm bandwidth). The pinhole size was set to 3 AU.

Fluorescent Spectral Measurement bound to SNAP in PBS

For the determination of $\lambda_{\text{max,fl}}$ after conjugation to SNAP in PBS, a 3-fold excess of SNAP (1.5 μ M) was added to compounds **4**, **8-11** (500 nM) in PBS solution (w/o BSA) and the measurement started after 1 h of incubation at RT. The solutions were placed on glass bottom dishes. Imaging of the labeled SNAP-tag was performed using a Leica SP8 confocal microscope equipped with an HC PL Apochromat 63X (1.20 NA) water immersion objective. The emission spectra of the NR compounds were measured using lamda mode, excitation at 514 nm (Ar laser) and detection at 560–695 nm (step: 5 nm) using HyD detector.

Fluorescent Spectral Measurement on DPPC Liposomes

Lipids used were 1,2-dipalmitoyl-*sn*-glycero-3-phosphatidyl- choline (DPPC), 1,2-dimyristoyl-*sn*-glycero-3-phosphatidylglycerol (DMPG), and 1,2-dioleoyl-*sn*-glycero-3-[(N-(5-amino-1-carboxypentyl)iminodiacetic acid)succinyl)] (NTA-lipid) from Avanti, USA. Small unilamellar vesicles were made by tip-sonication after hydration of a lipid film in 15 mM NaCl, 0.5 mM imidazole, 5 mM K₂HPO₄ pH 8.0 to 5 mg lipid mL⁻¹. The following lipid compositions (expressed in mass %) were used for the NTA-containing vesicles: 80% PC, 10% PG, 10% NTA-lipid, and control vesicles without NTA: 90% PC, 10% PG. Compound **4** was diluted in PBS buffer with 0.1 mg mL⁻¹ BSA to the desired concentration (1 μM). The addition of a 10-fold molar excess of SNAP (10 μM) followed. The reaction mixture was incubated for 1 h at RT and then was applied to the lipid vesicles. An incubation of 15 min followed, and then the fluorescence emission spectra of the samples were measured using a Leica SP8 confocal microscope equipped with an HC PL Apochromat 63X (1.20 NA) water immersion objective. The emission spectra of the NR compounds were measured using lambda mode, excitation at 514 nm (Ar laser) and detection at 560–695 nm (step: 5 nm) using HyD detector. The spectra were treated using a Lorentzian fit as a guide for the eye and for calculating the $\lambda_{\max,fl}$.

FLIM Microscopy

Fluorescence lifetime imaging (FLIM) was performed using an inverted-type scanning confocal microscope (LEICA SP8 FLIM mode) with an HC PL Apochromat 63X (1.20 NA) water immersion objective. A white laser (514 nm, notch filter) was used as an excitation source with a pulse frequency 20 MHz. Emission was collected at 560–645 nm using HyD detector. FLIM measurement was performed multiple times for each sample. The settings for scanning were: × 2.5 zoom, scan speed 400 Hz, image format 128 × 128 pixels, pinhole 1 Airy unit (AU).

Time-resolved fluorescence decay curves were obtained from FLIM images and fluorescence lifetimes were evaluated according to non-linear least-squares iterative curve fitting using the SymPhoTime software. Two exponential decay model: $I(t) = A_1 e^{-t/\tau_1} + A_2 e^{-t/\tau_2}$, where $I(t)$ is the time-dependent fluorescence intensity, A is the amplitude, and τ is the lifetime, was used for the curve fitting. All lifetime values shown in this study mean amplitude-weighted average lifetime, $\langle \tau_{ave} \rangle$, hereafter, which is defined as

$$\tau_{ave} = \frac{\sum_i A_i \tau_i}{\sum_i A_i}$$

Equation 4: Calculation of Average Fluorescence Lifetime, $\tau_{ave, ampli}$.

The goodness of fit of a given set of observed data and the chosen function was evaluated by the χ^2 ratio. A fit was considered acceptable when plots of the weighted residuals and the autocorrelation function showed random deviation about zero with a minimum χ^2 value not more than 1.2.

Patch Clamp

HEK293T cells were plated on 14 mm diameter glass bottom dishes, transiently transfected with lipofectamine 2000 and 100 ng of DNA to express SNAP on the extracellular surface of the

membrane. 24 h to 48 h later, cells were labeled with NR compounds **2,4-11** and NR12S for 30 min at RT in extracellular buffer (EB). This buffer contained (in mM): 150 NaCl, 5 KCl, 1 MgCl₂, 2 CaCl₂, 5 glucose, 10 HEPES; pH 7.4 adjusted with NaOH, 300 mOsm. Cells were mounted on a stage of inverted microscope Zeiss Axiobserver A.1 and continuously superfused with extracellular solution. Whole cell patch clamp recordings were done using HEKA EPC 10 amplifier and borosilicate pipette electrodes with 3-7 MOhm resistance when filled with following intracellular buffer (in mM): 140 CsCl, 10 HEPES, 10 HEDTA, pH 7.35 adjusted with CsOH, 290 mOsm. After establishing whole cell configuration cell capacitance and access resistance were routinely compensated.

Simultaneous imaging and voltage clamping was performed for measuring of voltage sensitivity. Voltage steps to from -100 mV to 100 mV with 50 mV interval were applied from a holding potential of -50 mV. Oil-immersion 40x objective with NA 1.3 was used to focus light from 100 W mercury lamp (with 70% fluorescence attenuator). Band pass excitation (540-552 nm) and emission long-pass (LP590) filters were used for NR compounds. Images were taken with Axiocam MR camera with 10 to 30 ms exposure, performed with Uniblitz shutter and 2x2 binning. Membrane of the cells and background regions were selected manually in ImageJ, mean fluorescence intensities for each region of interest were measured. Background fluorescence was subtracted from cell membrane fluorescence. Each voltage step fluorescence was normalized to previous -50 mV step to generate % $\Delta F/F$ traces for each cell. Linear fit was used to calculate % $\Delta F/F$ for each cell, and mean % $\Delta F/F$ was calculated from n=5 to 13 cells. Statistical analysis was performed using GraphPad Prism. One-way anova test was used to identify statistical significance of voltage sensitivity of patched cell membrane versus control cell (not connected electrically to the patched cell). Final data were presented as mean \pm SEM.

Finally, our method was validated using another voltage sensitive probe – VoltageFluor – which showed a 20% increase in fluorescence intensity upon 100 mV change in membrane potential; a value which was according to the literature.¹⁰³

Appendix

Amino acid Sequences for the Used Fusion Proteins⁹

PDISPLAY_SNAP_CLIP_HCA

METDTLLLVLLLVPGSTGDYPYDVPDYAGAQPARSMDKDCEMKRTTLDSPLGKLESGCEQGLHEIFLG
KGTSAADAVEVPAPAAVLGGPEPLMQATAWLNAYFHQPEAIEFPVPALHHPVFQQESFTRQVLWLLKVV
KFGEVISYSHLAALAGNPAATAAVKTALSGNPVPILIPCHRNVVQGDLDVGGYEGGLAVKEWLLAHEGHRLGKP
GLGGRLEVLFGPKAFLEMDKDCEMKRTTLDSPLGKLESGCEQGLHKIIFLGKGTSAADAVEVPAPAAVLGG
PEPLIQATAWLNAYFHQPEAIEFPVPALHHPVFQQESFTRQVLWLLKVVKFGEVISESHLAALVGNPAATAA
VNTALDGNPVPILIPCHRNVVQGDSDVGPYLGGLAVKEWLLAHEGHRLGKPGLGALAGGMSHHWGYGKH
N GPEHWHKDFPIAKGERQSPVDIDTHTAKYDPSLKPLSVSYDQATSLRILNNGHAFNVEFDDSDQKAVLKGGPL
DGTYRLIQFHFHWGSLDGQGEHTVDKKKYAAELHLVHWNTKYGDFGKAVQQPDGLAVLGIFLKVGSAPKG
LQKVVDVLDSIKTKGSADFTNFDPLLPESLDYWTYPGSLTTPPLLECVTWIVLKEPISVSSEQVLKFRKLNFG
EGEPEELMVDNWRPAQPLKNRQIKASFVDEQKLISEEDLNAVGGDTQEIVVPHSLPFKVVVISAILALVVTI
ISLIILIMLWQKKPR

Red: Signal peptide

Blue: SNAP

Green: CLIP

Violet: HCA

Grey: Transmembrane domain

PDISPLAY_SNAP

METDTLLLVLLLVPGSTGDYPYDVPDYAGAQPARSMDKDCEMKRTTLDSPLGKLESGCEQGLHEIFLGK
G TSAADAVEVPAPAAVLGGPEPLMQATAWLNAYFHQPEAIEFPVPALHHPVFQQESFTRQVLWLLKVVKFG
E VISYSHLAALAGNPAATAAVKTALSGNPVPILIPCHRNVVQGDLDVGGYEGGLAVKEWLLAHEGHRLGKPG
LGGRLEVLFGVDQKLISEEDLNAVGGDTQEIVVPHSLPFKVVVISAILALVVTIISLIILIMLWQKKPR

Red: Signal peptide

Blue: SNAP

Violet: Transmembrane domain

⁹ All the plasmids for bacterial and mammalian expression of were provided from Dr. Matthias Brun, apart from the plasmid for mammalian expression of SNAP-HIR_A, which was provided from Dr Miwa Umebayashi.

SNAP_HIS TAG

MDKDCEMKRRTLDSPLGKLELSGCEQGLHEIIFLGKGTSAADAVEVPAPAAVLGGPELMQATAWLNAYFHQP
 EAIEEFVPALHHPVFQQESFTRQVLWKLLKVVKFGEVISYSHLAALAGNPAATAAVKTALSGNPVPILPCHRV
 VQGDLDVGGYEGGL AVKEWLLAHEGHR LG KPGLGHHHHHHHHH

Blue: SNAP

Red: His tag

SNAP_HIR_A

MATGGRRGAAAAPLLVAVAALLGAAGHLYPGEVCPGMDIRNNLTRLHELENC SVIEGHLQILLMFKTR
 EDFRDLSPFKLIMITDYLLLFVYGLSEKDLFPNLT VIRGSRLFFNYALVIFEMVHLKELGLYNLMNITRGSV
 RIEKNNELCYLATIDWSRILDSVEDNYIVLNKDDNEECGDICPGTAKGTNCPATVINGQFVERCWTHSHC
 QKVCPTICKSHGCTAEGLCCHSECLGNCSQPDDPTKCVACRN FYLDGRCVETCPPYYHFQDWRCVNFS
 FCQDLHHKCKNSRRQGCHQYVIHNNKCIPECPSGYTMNSSNLLCTPCLGPCPKVCHLLEGEKTIDSVTSA
 QELRGCTVINGSLIINIRGGNNLAAELEANGLIEISGYLKIRRSYALVLSFFRKLRLIRGETLEIGNYSFYAL
 DNQNLRLQLDWWSKHNLITQGKLFHYNPKLCLSEIHKMEEVSGTKGRQERN DIALKTNGDQASCENEL
 LKFSYIRTSFDKILLRWEPYWPPDFRDLLGFMLFYKEAPYQNVTEFDGQDACGSNSWTVVDIDPPLRSND
 PKSQNHPGWL MRGLKPWTQY AIFVKTLVTFSDERRTYGAKSDIYVQTDATNPSVPLDPISVSNSSSQIILK
 WKPPSPDPNGNITHYLVFWERQAEDSELFEDYCLKGLKLP SRTWSPPFESDSQKHNQSEYEDSAGECCS
 CPKTD SQILKELEESSFRKTFEDYLHN VVFVRPMSDKDCEMKRRTLDSPLGKLELSGCEQGLHEIIFLGK
 TSAADAVEVPAPAAVLGGPELMQATAWLNAYFHQPEAIEEFVPALHHPVFQQESFTRQVLWKLLK
 VKFGEVISYSHLAALAGNPAATAAVKTALSGNPVPILPCHRVVQGDLDVGGYEGGLAVKEWLLAHEGHR
 LGKPGLGRKRRSLGDVG NVTVA VPTVA AFPNTSSTS SVPTSPEEHRPF EKVVNKESLVISGLRHFTGYRIELQ
 ACNQDTPEERCSVAAYVSARTMPEAKADDIVGPVTHEIFENNVVHLMWQEPKEPNGLIVLYEVS YRRYG
 DEELHLCVSRKH FALERGCRLRGLSPGNYSVRIRATSLAGNGSWTEPTYFYVTDYLDVPSNIAKIIIGPLIFVF
 LFSVIGSIYLF LRKRQPDG PLGPLYASSNPEYLSASDV FPCSVYVPDEWEVSREKITLLREL GQGSFGMVVE
 GNARDIIKGEAETRVAVKTVNESASLRERIEFLNEASVMKGFTCHHVVRLLGVVSKGQPTLVVMELMAH
 GDLKSYLRSLRPEAENNPGRPPPTLQEMIQMAAEIADGMAYLNAKKFVHRDLAARNCMVAHDFTVKIG
 DFGMTRDIYETDYRKGGKGLLPVRWMAPESLKDGVFTTSSDMWSFGVVLWEITSLAEQPYQGLSNEQ
 VLKFVMDGGYLDQPDNCPERVTDLMRM CWQFNPKMRPTFLEIVNLLKDDLHPSFEVSFFHSEENKAP
 ESEEELEMEFEDMENVPLDRSSH CQREEAGGRDGGSSLGFKRSYEEHIPYTHMNGGKKNGRILTLP RSNPS

Black: Human insulin Receptor – A

Blue: SNAP

Fluorescence Spectra and FLIM Experiment Images

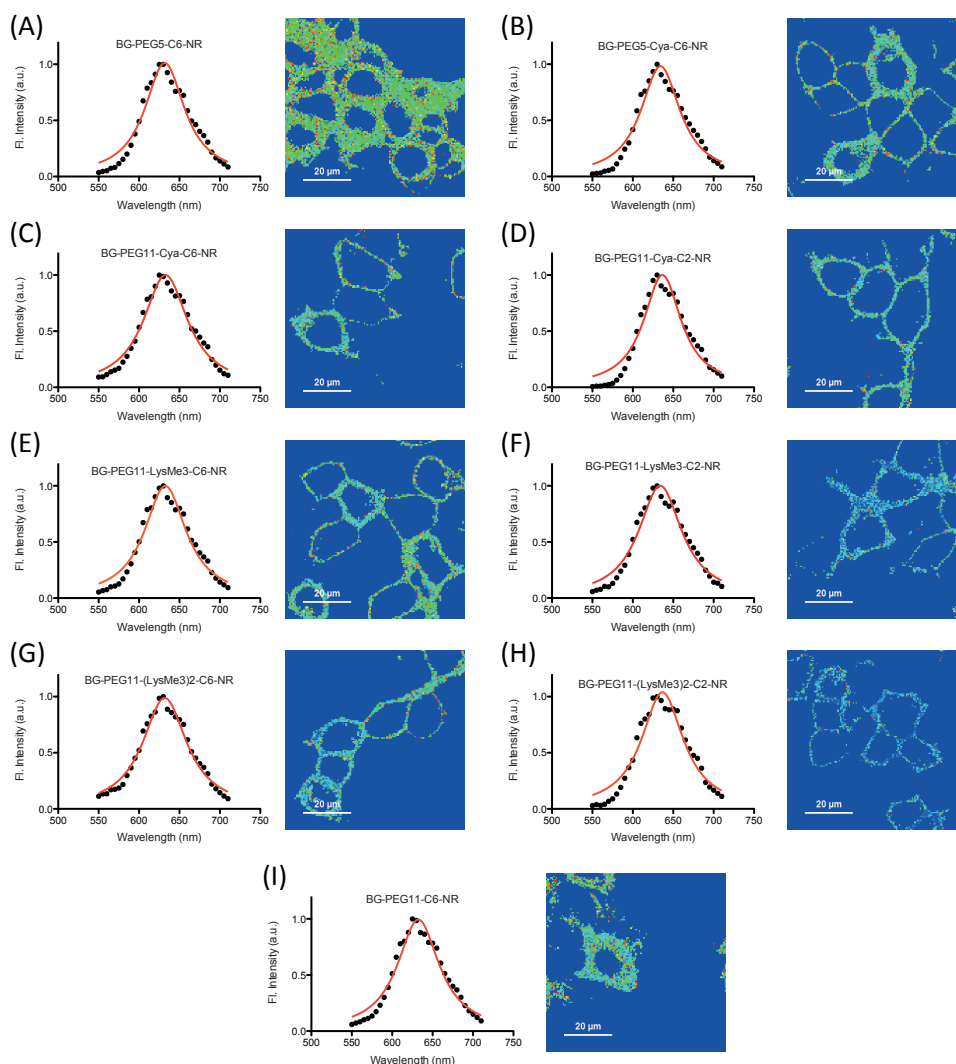


Figure 64: Emission spectra and $\tau_{ave, ampl}$ of compounds **1-9** bound to SNAP-tag expressed on the extracellular surface of the plasma membrane in HEK 293T cells under confocal microscope in NPM (w/o FBS). (A) BG-PEG5-C6-NR (**1**), (B) BG-PEG5-Cya-C6-NR (**3**), (C) BG-PEG11-Cya-C6-NR (**4**), (D) BG-PEG11-Cya-C2-NR (**7**), (E) BG-PEG11-LysMe₃-C6-NR (**5**), (F) BG-PEG11-LysMe₃-C2-NR (**8**), (G) BG-PEG11-(LysMe₃)₂-C6-NR (**6**), (H) BG-PEG11-(LysMe₃)₂-C2-NR (**9**) and (I) BG-PEG11-C6-NR (**2**).

References

- (1) Campbell, I. D. (2008) The Croonian lecture 2006. Structure of the living cell. *Philos. Trans. R. Soc. Lond. B. Biol. Sci.* 363, 2379–91.
- (2) Chiarini-Garcia, H.; Melo, R. (2011) Light microscopy: methods and protocols. *Springer*.
- (3) Lichtman, J. W., and Conchello, J.-A. (2005) Fluorescence microscopy. *Nat. Methods* 2, 910–9.
- (4) Vicidomini, G., Schönle, A., Ta, H., Han, K. Y., Moneron, G., Eggeling, C., and Hell, S. W. (2013) STED Nanoscopy with time-gated detection: Theoretical and experimental aspects. *PLoS One* 8, e54421.
- (5) Bornhop, D., and Licha, K. (2003) Fluorescent Probes in Biomedical Applications, in *Biomedical Photonics Handbook*. CRC Press.
- (6) Lakowicz, J. R. (2006) Principles of fluorescence spectroscopy.
- (7) Yang, F., Moss, L. G., Phillips, G. N., Phillips Jr., G. N., and Phillips, G. N. (1996) The molecular structure of green fluorescent protein. *Nat. Biotechnol.* 14, 1246–51.
- (8) Yano, Y., and Matsuzaki, K. (2009) Tag–probe labeling methods for live-cell imaging of membrane proteins. *Biochim. Biophys. Acta - Biomembr.* 1788, 2124–31.
- (9) Chudakov, D., Matz, M., Lukyanov, S., and Lukyanov, K. (2010) Fluorescent proteins and their applications in imaging living cells and tissues. *Physiol. Rev.* 90, 1103–1163.
- (10) Shimomura, O., Johnson, F. H., and Saiga, Y. (1962) Extraction, purification and properties of Aequorin, a bioluminescent protein from the luminous hydromedusan Aequorea. *J. Cell. Comp. Physiol.* 59, 223–39.
- (11) M Chalfie, Y Tu, G Euskirchen, WW Ward, D. P. (1994) Green fluorescent protein as a marker for gene expression. *Science* (80-.). 263, 802–5.
- (12) Roger Heim, Cubitt, A. B., and Tsien, R. Y. (1995) Improved Green Fluorescence. *Nature*.
- (13) Tsien, R. Y. (1998) The green fluorescent protein. *Annu. Rev. Biochem.* 67, 509–44.
- (14) Yan, Q., and Bruchez, M. P. (2015) Advances in chemical labeling of proteins in living cells. *Cell Tissue Res.* 360, 179–194.
- (15) Marks, K. M., and Nolan, G. P. (2006) Chemical labeling strategies for cell biology. *Nat. Methods* 3, 591–6.
- (16) Miller, L. W., Cai, Y., Sheetz, M. P., and Cornish, V. W. (2005) In vivo protein labeling with trimethoprim conjugates: a flexible chemical tag. *Nat. Methods* 2, 255–7.
- (17) Keppler, A., Gendreizig, S., Gronemeyer, T., Pick, H., Vogel, H., and Johnsson, K. (2003) A general method for the covalent labeling of fusion proteins with small molecules in vivo. *Nat. Biotechnol.* 21, 86–9.
- (18) Gautier, A., Juillerat, A., Heinis, C., Corrêa, I. R., Kindermann, M., Beaufils, F., and Johnsson, K. (2008) An engineered protein tag for multiprotein labeling in living cells. *Chem. Biol.* 15, 128–36.
- (19) Los, G. V, Encell, L. P., Mcdougall, M. G., Hartzell, D. D., Karassina, N., Zimprich, C., Wood, M. G., Learish, R., Ohana, R. F., Urh, M., Simpson, D., Mendez, J., Zimmerman, K., Otto, P., Vidugiris, G., Zhu, J., Darzins, A., Klaubert, D. H., Bulleit, R. F., and Wood, K. V. (2008) HaloTag: A Novel Protein Labeling Technology for Cell Imagin and Protein Analysis. *ACS Chem. Biol.* 3, 373–82.
- (20) Yano, Y., Yano, A., Oishi, S., Sugimoto, Y., Tsujimoto, G., Fujii, N., and Matsuzaki, K. (2008) Coiled-coil tag - Probe system for quick labeling of membrane receptors in living cells. *ACS Chem.*

Biol. 3, 341–5.

(21) Marks, K., Rosinov, M., and Nolan, G. (2004) In Vivo Targeting of Organic Calcium Sensors via Genetically Selected Peptides. *Chem. Biol.* 11, 347–56.

(22) Adams, S. R., and Tsien, R. Y. (2008) Preparation of the membrane-permeant biarsenicals FIAsh-EDT2 and ReAsH-EDT2 for fluorescent labeling of tetracysteine-tagged proteins. *Nat. Protoc.* 3, 1527–34.

(23) Madani, F., Lind, J., Damberg, P., Adams, S. R., Tsien, R. Y., and Gräslund, A. O. (2009) Hairpin structure of a biarsenical-tetracysteine motif determined by NMR spectroscopy. *J. Am. Chem. Soc.* 131, 4613–5.

(24) Goldsmith, C. R., Jaworski, J., Sheng, M., and Lippard, S. J. (2006) Selective labeling of extracellular proteins containing polyhistidine sequences by a fluorescein-nitrilotriacetic acid conjugate. *J. Am. Chem. Soc.* 128, 418–19.

(25) Guignet, E. G., Hovius, R., and Vogel, H. (2004) Reversible site-selective labeling of membrane proteins in live cells. *Nat. Biotechnol.* 22, 440–44.

(26) Chen, I., Howarth, M., Lin, W., and Ting, A. Y. (2005) Site-specific labeling of cell surface proteins with biophysical probes using biotin ligase. *Nat. Methods* 2, 99–104.

(27) Fernández-Suárez, M., Baruah, H., Martínez-Hernández, L., Xie, K. T., Baskin, J. M., Bertozzi, C. R., and Ting, A. Y. (2007) Redirecting lipoic acid ligase for cell surface protein labeling with small-molecule probes. *Nat. Biotechnol.* 25, 1483–87.

(28) George, N., Pick, H., Vogel, H., Johnsson, N., and Johnsson, K. (2004) Specific labeling of cell surface proteins with chemically diverse compounds. *J. Am. Chem. Soc.* 126, 8896–7.

(29) Dean, K. M., and Palmer, A. E. (2014) Advances in fluorescence labeling strategies for dynamic cellular imaging. *Nat. Chem. Biol.* 10, 512–23.

(30) Nadler, A., and Schultz, C. (2013) The Power of fluorogenic probes. *Angew. Chemie Int. Ed.* 52, 2408–10.

(31) Bruchez, M. P. (2015) Dark dyes-bright complexes: fluorogenic protein labeling. *Curr. Opin. Chem. Biol.* 27, 18–23.

(32) Chen, Y., Tsao, K., and Keillor, J. W. (2014) Fluorogenic protein labelling: a review of photophysical quench mechanisms and principles of fluorogen design. *Can. J. Chem.* 1–10.

(33) Demchenko, A. P., Mély, Y., Duportail, G., and Klymchenko, A. S. (2009) Monitoring biophysical properties of lipid membranes by environment-sensitive fluorescent probes. *Biophys. J.* 96, 3461–70.

(34) Klymchenko, A., Duportail, G., and Mely, Y. (2013) Fluorescent methods to study biological membranes. *Springer Ser. Fluoresc.* 13, 51–70.

(35) Kuimova, M. K., Yahioglu, G., Levitt, J. A., and Suhling, K. (2008) Molecular rotor measures viscosity of live cells via fluorescence lifetime imaging. *J. Am. Chem. Soc.* 130, 6672–73.

(36) Goh, W. L., Lee, M. Y., Joseph, T. L., Quah, S. T., Brown, C. J., Verma, C., Brenner, S., Ghadessy, F. J., and Teo, Y. N. (2014) Molecular rotors as conditionally fluorescent labels for rapid detection of biomolecular interactions. *J. Am. Chem. Soc.* 136, 6159–62.

(37) Reichardt, C. (1994) Solvatochromic dyes as solvent polarity indicators. *Chem. Rev.* 94, 2319–58.

(38) Sasaki, S., Niko, Y., Klymchenko, A. S., and Konishi, G. (2014) Design of donor–acceptor geometry for tuning excited-state polarization: fluorescence solvatochromism of push–pull biphenyls with various torsional restrictions on their aryl–aryl bonds. *Tetrahedron* 70, 7551–9.

(39) Karpenko, I. A., Niko, Y., Yakubovskiy, V. P., and Gerasov, A. O. (2015) Push-pull dioxaborine as fluorescent molecular rotor: far-red fluorogenic probe for ligand-receptor interactions. *J. Mater. Chem. C.*

(40) Parasassi, T., Krasnowska, E. K., Bagatolli, L., and Gratton, E. (1998) Laurdan and Prodan as polarity-sensitive fluorescent membrane probes. *J. Fluoresc.* 8, 365–73.

(41) Lukinavičius, G., Reymond, L., D’Este, E., Masharina, A., Göttfert, F., Ta, H., Güther, A., Fournier, M., Rizzo, S., Waldmann, H., Blaukopf, C., Sommer, C., Gerlich, D. W., Arndt, H.-D., Hell,

- S. W., and Johnsson, K. (2014) Fluorogenic probes for live-cell imaging of the cytoskeleton. *Nat. Methods* 11, 731–3.
- (42) Masharina, A., Reymond, L., Maurel, D., Umezawa, K., and Johnsson, K. (2012) A fluorescent sensor for GABA and synthetic GABA B receptor ligands. *J. Am. Chem. Soc.* 134, 19026–34.
- (43) Brun, M. A., Tan, K., Griss, R., Kielkowska, A., Reymond, L., and Johnsson, K. (2012) A semisynthetic fluorescent sensor protein for glutamate. *J. Am. Chem. Soc.* 134, 7676–78.
- (44) Sun, X., Zhang, A., Baker, B., Sun, L., Howard, A., Buswell, J., Maurel, D., Masharina, A., Johnsson, K., Noren, C. J., Xu, M.-Q., and Corrêa, I. R. (2011) Development of SNAP-tag fluorogenic probes for wash-free fluorescence imaging. *ChemBioChem* 12, 2217–26.
- (45) Komatsu, T., Johnsson, K., Okuno, H., Bito, H., Inoue, T., Nagano, T., and Urano, Y. (2011) Real-time measurements of protein dynamics using fluorescence activation-coupled protein labeling method. *J. Am. Chem. Soc.* 133, 6745–51.
- (46) Doose, S., Neuweiler, H., and Sauer, M. (2009) Fluorescence quenching by photoinduced electron transfer: A reporter for conformational dynamics of macromolecules. *ChemPhysChem* 10, 1389–98.
- (47) Ueno, T., Urano, Y., Setsukinai, K. I., Takakusa, H., Kojima, H., Kikuchi, K., Ohkubo, K., Fukuzumi, S., and Nagano, T. (2004) Rational principles for modulating fluorescence properties of fluorescein. *J. Am. Chem. Soc.* 126, 14079–85.
- (48) Le Droumaguet, C., Wang, C., and Wang, Q. (2010) Fluorogenic Click Reaction. *Chem. Soc. Rev.* 39, 1233–9.
- (49) Adams, S. R., Campbell, R. E., Gross, L. a., Martin, B. R., Walkup, G. K., Yao, Y., Llopis, J., and Tsien, R. Y. (2002) New biarsenical ligands and tetracysteine motifs for protein labeling in vitro and in vivo: Synthesis and biological applications. *J. Am. Chem. Soc.* 124, 6063–6076.
- (50) Greenspan, P., and Fowler, S. D. (1985) Spectrofluorometric studies of the lipid probe, Nile Red. *J. Lipid Res.* 26, 781–9.
- (51) Greenspan, P., Mayer, E. P., and Fowler, S. D. (1985) Nile red: a selective fluorescent stain for intracellular lipid droplets. *J. Cell Biol.* 100, 965–73.
- (52) Dutta, A. K., Kamada, K., and Ohta, K. (1996) Spectroscopic studies of Nile Red in organic solvents and polymers. *J. Photochem. Photobiol. A* 93, 57–64.
- (53) Brun, M. a, Griss, R., Reymond, L., Tan, K.-T., Piguet, J., Peters, R. J. R. W., Vogel, H., and Johnsson, K. (2011) Semisynthesis of fluorescent metabolite sensors on cell surfaces. *J. Am. Chem. Soc.* 133, 16235–42.
- (54) Brun, M. A., Tan, K.-T., Nakata, E., Hinner, M. J., and Johnsson, K. (2009) Semisynthetic fluorescent sensor proteins based on self-labeling protein tags. *J. Am. Chem. Soc.* 131, 5873–84.
- (55) Jose, J., and Burgess, K. (2006) Syntheses and properties of water-soluble Nile Red derivatives. *J. Org. Chem.* 71, 7835–39.
- (56) Tajalli, H., Gilani, a. G., Zakerhamidi, M. S., and Tajalli, P. (2008) The photophysical properties of Nile red and Nile blue in ordered anisotropic media. *Dye. Pigment.* 78, 15–24.
- (57) Jose, J., and Burgess, K. (2006) Benzophenoxazine-based fluorescent dyes for labeling biomolecules. *Tetrahedron* 62, 11021–37.
- (58) Sarkar, N., Das, K., Nath, D. N., and Bhattacharyya, K. (1994) Twisted charge transfer process of Nile Red in homogeneous solution and in faujasite zeolite. *Langmuir* 10, 326–9.
- (59) Demchenko, A. P. (2009) Introduction to fluorescence sensing.
- (60) Cser, A., Nagy, K., and Biczok, L. (2002) Fluorescence lifetime of Nile Red as a probe for the hydrogen bonding strength with its microenvironment. *Chem. Phys. Lett.* 360, 473–78.
- (61) Yatsuhashi, T., Nakajima, Y., Shimada, T., Tachibana, H., and Inoue, H. (1998) Molecular mechanism for the radiationless deactivation of the intramolecular charge-transfer excited singlet state of aminofluorenones through hydrogen bonds with alcohols. *J. Phys. Chem. A* 102, 8657–63.
- (62) Yatsuhashi, T., and Inoue, H. (1997) Molecular mechanism of radiationless deactivation of aminoanthraquinones through intermolecular hydrogen-bonding interaction with alcohols and

- hydroperoxides. *J. Phys. Chem. A* **101**, 8166–73.
- (63) Biczok, L., Tibor, B., and Inoue, H. (1999) Effects of molecular structure and hydrogen bonding on the radiationless deactivation of singlet excited fluorenone derivatives. *J. Phys. Chem. A* **103**, 3837–42.
- (64) Inoue, H., Hida, M., Nakashima, N., and Yoshihara, K. (1982) Picosecond fluorescence lifetimes of anthraquinone derivatives. Radiationless deactivation via intra- and intermolecular hydrogen bonds. *J. Phys. Chem.* **485**, 3184–88.
- (65) Hicks, J. M., Vandersall, M. T., Sitzmann, E. V, and Eisenthal, K. B. (1987) Polarity-dependent barriers and the photoisomerization dynamics of molecules in solution. *Chem. Phys. Lett.* **135**, 413–20.
- (66) Prendergast, F. G. (1991) Time-resolved fluorescence techniques: methods and applications in biology. *Curr. Opin. Struct. Biol.* **1**, 1054–9.
- (67) Golini, C. M., Williams, B. W., and Foresman, J. B. (1998) Further solvatochromic, thermochromic and theoretical studies on Nile Red. *J. Fluoresc.* **8**, 395–404.
- (68) Cser, A., and Nagy, K. (2002) Fluorescence lifetime of Nile Red as a probe for the hydrogen bonding strength with its microenvironment Biczok **360**, 473–478.
- (69) Hawe, A., Sutter, M., and Jiskoot, W. (2008) Extrinsic fluorescent dyes as tools for protein characterization. *Pharm. Res.* **25**, 1487–99.
- (70) Nagy, K., Gokturk, S., and Biczok, L. (2003) Effect of microenvironment on the fluorescence of 2-hydroxy-substituted Nile Red dye : A new fluorescent probe for the study of micelles. *J. Phys. Chem. A* **107**, 8784–90.
- (71) Pham, N., Gal, M. R., Bagshaw, R. D., Mohr, a J., Chue, B., Richardson, T., and Callahan, J. W. (2005) A comparative study of cytoplasmic granules imaged by the real-time microscope, Nile Red and Filipin in fibroblasts from patients with lipid storage diseases. *J. Inherit. Metab. Dis.* **28**, 991–1004.
- (72) Liscum, L., and Underwood, K. W. (1995) Intracellular cholesterol transport and compartmentation. *J. Biol. Chem.*
- (73) Mukherjee, S., Raghuraman, H., and Chattopadhyay, A. (2007) Membrane localization and dynamics of Nile Red: effect of cholesterol. *Biochim. Biophys. Acta* **1768**, 59–66.
- (74) Krishnamoorthy, G., and Ira. (2002) Fluorescence lifetime distribution in characterizing membrane microheterogeneity. *J. Fluoresc.* **11**, 247–53.
- (75) Krishnamoorthy, G., and Ira. (2001) Probing the link between proton transport and water content in lipid membranes. *J. Phys. Chem. B* **105**, 1484–88.
- (76) Yang, Z., He, Y., Lee, J. H., Chae, W.-S., Ren, W., Lee, J. H., Kang, C., and Kim, J. S. (2014) A Nile Red/BODIPY-based bimodal probe sensitive to changes in micropolarity and microviscosity of endoplasmic reticulum. *Chem. Commun.* **50**, 11672–5.
- (77) Brown, M. B., Miller, J. N., and Seare, N. J. (1995) An investigation of the use of Nile Red as a long-wavelength fluorescent probe for the study of α 1-acid glycoprotein-drug interactions. *J. Pharm. Biomed. Anal.* **13**, 1011–17.
- (78) Daban, J. (2001) Fluorescent labeling of proteins with Nile red and 2-methoxy-2,4-diphenyl-3(2H)-furanone: Physicochemical basis and application to the rapid staining of sodium dodecyl sulfate polyacrylamide gels and Western blots. *Electrophoresis* **3**, 874–80.
- (79) Taikana, K.; Fujiwara, Y.; Okamoto, A. (2005) Nile Red nucleoside: Novel nucleoside analog with a fluorophore replacing the DNA base. *Nucleic Acids Symp. Ser.* **155**–6.
- (80) Karpenko, I. a, Kreder, R., Valencia, C., Villa, P., Mendre, C., Mouillac, B., Mély, Y., Hibert, M., Bonnet, D., and Klymchenko, A. S. (2014) Red fluorescent turn-on ligands for imaging and quantifying G Protein-Coupled Receptors in living cells. *ChemBioChem* **5**, 359–63.
- (81) Kucherak, O. a, Oncul, S., Darwich, Z., Yushchenko, D. a, Arntz, Y., Didier, P., Mély, Y., and Klymchenko, A. S. (2010) Switchable nile red-based probe for cholesterol and lipid order at the outer leaflet of biomembranes. *J. Am. Chem. Soc.* **132**, 4907–16.
- (82) Shynkar, V. V., Klymchenko, A. S., Kunzelmann, C., Duportail, G., Muller, C. D., Demchenko,

- A. P., Freyssinet, J. M., and Mely, Y. (2007) Fluorescent biomembrane probe for ratiometric detection of apoptosis. *J. Am. Chem. Soc.* **129**, 2187–93.
- (83) Saxena, R., Shrivastava, S., Haldar, S., Klymchenko, A. S., and Chattopadhyay, A. (2014) Location, dynamics and solvent relaxation of a Nile red-based phase-sensitive fluorescent membrane probe. *Chem. Phys. Lipids* **183**, 1–8.
- (84) Chattopadhyay, a, and London, E. (1987) Parallax method for direct measurement of membrane penetration depth utilizing fluorescence quenching by spin-labeled phospholipids. *Biochemistry* **26**, 39–45.
- (85) Saxena, R., Shrivastava, S., and Chattopadhyay, A. (2015) Cholesterol-induced changes in hippocampal membranes utilizing a phase-sensitive fluorescence probe. *Biochim. Biophys. Acta - Biomembr.* **1848**, 1699–1705.
- (86) Chiantia, S., Klymchenko, A. S., and London, E. (2012) A novel leaflet-selective fluorescence labeling technique reveals differences between inner and outer leaflets at high bilayer curvature. *Biochim. Biophys. Acta* **1818**, 1284–90.
- (87) Chiantia, S., Schwille, P., Klymchenko, A. S., and London, E. (2011) Asymmetric GUVs Prepared by M β CD-Mediated Lipid Exchange: An FCS Study. *Biophys. J.* **100**, L1–L3.
- (88) Darwich, Z., Klymchenko, A. S., Kucherak, O. a., Richert, L., and Mély, Y. (2012) Detection of apoptosis through the lipid order of the outer plasma membrane leaflet. *Biochim. Biophys. Acta - Biomembr.* **1818**, 3048–54.
- (89) Kreder, R., Pyrshev, K. a., Darwich, Z., Kucherak, O. a., Mély, Y., and Klymchenko, A. S. (2015) Solvatochromic Nile Red Probes with FRET Quencher Reveal Lipid Order Heterogeneity in Living and Apoptotic Cells. *ACS Chem. Biol.* **150306062704000**.
- (90) Ghoneim, N. (2000) Photophysics of Nile red in solution: steady state spectroscopy. *Spectrochim. Acta. A. Mol. Biomol. Spectrosc.* **56**, 1003–10.
- (91) Prifti, E., Reymond, L., Umebayashi, M., Hovius, R., Riezman, H., and Johnsson, K. (2014) A fluorogenic probe for SNAP-tagged plasma membrane proteins based on the solvatochromic molecule Nile Red. *ACS Chem. Biol.* **3**, 606–12.
- (92) Schena, A., and Johnsson, K. (2014) Sensing Acetylcholine and Anticholinesterase Compounds. *Angew. Chem. Int. Ed. Engl.* **53**, 1302–1305.
- (93) Leriche, G., Budin, G., Darwich, Z., Weltin, D., Mély, Y., Klymchenko, A. S., and Wagner, A. (2012) A FRET-based probe with a chemically deactivatable quencher. *Chem. Commun.* **48**, 3224–26.
- (94) Liu, T.-K., Hsieh, P.-Y., Zhuang, Y.-D., Hsia, C.-Y., Huang, C.-L., Lai, H.-P., Lin, H.-S., Chen, I.-C., Hsu, H.-Y., and Tan, K.-T. (2014) A Rapid SNAP-Tag Fluorogenic Probe Based on an Environment-Sensitive Fluorophore for No-Wash Live Cell Imaging. *ACS Chem. Biol.* **9**, 2359–65.
- (95) Erickson, H. P. (2009) Size and shape of protein molecules at the nanometer level determined by sedimentation, gel filtration, and electron microscopy. *Biol. Proced. Online* **11**, 32–51.
- (96) Massague, J., Pilch, P. F., and Czech, M. P. (1980) Electrophoretic resolution of three major insulin receptor structures with unique subunit stoichiometries. *Proc. Natl. Acad. Sci. U. S. A.* **77**, 7137–41.
- (97) Hedo, J. A., and Simpson, I. A. (1984) Internalization of insulin receptors in the isolated rat adipose cell. Demonstration of the vectorial disposition of receptor subunits. *J. Biol. Chem.* **259**, 11083–89.
- (98) Ward, C. W., and Lawrence, M. C. (2009) Ligand-induced activation of the insulin receptor: a multi-step process involving structural changes in both the ligand and the receptor. *BioEssays* **31**, 422–34.
- (99) Ebina, Y., Ellis, L., Jarnagin, K., Edery, M., Graf, L., Clauser, E., Roth, R. A., and Futter, W. J. (1985) The human insulin receptor cDNA: The structural basis for transmembrane signalling. *Cell* **40**, 747–758.
- (100) Black, S. L., Stanley, W. a, Filipp, F. V, Bhairo, M., Verma, A., Wichmann, O., Sattler, M.,

- Wilmanns, M., and Schultz, C. (2008) Probing lipid- and drug-binding domains with fluorescent dyes. *Bioorg. Med. Chem.* 16, 1162–73.
- (101) Cooper, G. M. (2000) The Cell. Sinauer Associates.
- (102) Bezanilla, F. (2008) How membrane proteins sense voltage. *Nat. Rev. Mol. Cell Biol.* 9, 323–32.
- (103) Woodford, C. R., Frady, E. P., Smith, R. S., Morey, B., Canzi, G., Palida, S. F., Araneda, R. C., Kristan, W. B., Kubiak, C. P., Miller, E. W., and Tsien, R. Y. (2015) Improved PeT molecules for optically sensing voltage in neurons. *J. Am. Chem. Soc.*
- (104) Peterka, D. S., Takahashi, H., and Yuste, R. (2011) Imaging voltage in neurons. *Neuron* 69, 9–21.
- (105) Canepari, M., Zecevic, D., and Bernus, O. (2011) Membrane potential imaging in the nervous system.
- (106) Cohen, L. B., Salzberg, B. M., Davila, H. V., Ross, W. N., Landowne, D., Waggoner, A. S., and Wang, C. H. (1974) Changes in axon fluorescence during activity: Molecular probes of membrane potential. *J. Membr. Biol.* 19, 1–36.
- (107) Lodish, H., Berk, A., Zipursky, S. L., Matsudaira, P., Baltimore, D., and Darnell, J. (2000) Molecular cell biology. W. H. Freeman.
- (108) Molleman, A. (2003) Patch Clamping: An introductory guide to patch clamping electrophysiology. John Wiley & Sons, Ltd.
- (109) Sakmann, B., and Neher, E. (1984) Patch clamp techniques for studying ionic channels in excitable membranes. *Annu. Rev. Physiol. Physiol.* 46, 455–72.
- (110) Villalba-Galea, C. a, Sandtner, W., Dimitrov, D., Mutoh, H., Knöpfel, T., and Bezanilla, F. (2009) Charge movement of a voltage-sensitive fluorescent protein. *Biophys. J.* 96, L19–21.
- (111) Blunck, R., Chanda, B., and Bezanilla, F. (2005) Nano to micro - fluorescence measurements of electric fields in molecules and genetically specified neurons. *J. Membr. Biol.* 208, 91–102.
- (112) Dragsten, P. R., and Webb, W. W. (1978) Mechanism of the membrane potential sensitivity of the fluorescent membrane probe merocyanine 540. *Biochemistry* 17, 5228–40.
- (113) Pucihar, G., Kotnik, T., and Miklavčič, D. (2009) Measuring the induced membrane voltage with di-8-ANEPPS. *J. Vis. Exp.* 3–5.
- (114) Fluhler, E., Burnham, V. G., and Loew, L. M. (1985) Spectra, membrane binding, and potentiometric responses of new charge shift probes. *Biochemistry* 24, 5749–55.
- (115) Loew, L. M., Scully, S., Simpson, L., and Waggoner, A. S. (1979) Evidence for a charge-shift electrochromic mechanism in a probe of membrane potential. *Nature* 281, 497–9.
- (116) Loew, L. M., and Simpson, L. L. (1981) Charge-shift probes of membrane potential: a probable electrochromic mechanism for p-aminostyrylpyridinium probes on a hemispherical lipid bilayer. *Biophys. J.* 34, 353–65.
- (117) Fromherz, P., and Lambacher, A. (1991) Spectra of voltage-sensitive fluorescence of styryl-dye in neuron membrane. *Biochim. Biophys. Acta* 1068, 149–56.
- (118) Grinvald, A., Hildesheim, R., Farber, I. C., and Anglistter, L. (1982) Improved fluorescent probes for the measurement of rapid changes in membrane potential. *Biophys. J.* 39, 301–8.
- (119) Ehrenberg, B., Montana, V., Wei, M. D., Wuskell, J. P., and Loew, L. M. (1988) Membrane potential can be determined in individual cells from the nernstian distribution of cationic dyes. *Biophys. J.* 53, 785–94.
- (120) Waggoner, A. S., Wang, C. H., and Tolles, R. L. (1977) Mechanism of potential-dependent light absorption changes of lipid bilayer membranes in the presence of cyanine and oxonol dyes. *J. Membr. Biol.* 33, 109–40.
- (121) Lakos, Z., Somogyi, B., Balazs, M., M. J. and D. S. (1990) The effect of transmembrane potential on the dynamic behavior of cell membranes. *Biochim. Biophys. Acta* 1023, 41–6.
- (122) González, J. E., and Tsien, R. Y. (1995) Voltage sensing by fluorescence resonance energy transfer in single cells. *Biophys. J.* 69, 1272–80.
- (123) Chanda, B., Asamoah, O. K., Blunck, R., Roux, B., and Bezanilla, F. (2005) Gating charge

displacement in voltage-gated ion channels involves limited transmembrane movement. *Nature* 436, 852–6.

(124) Montefusco, D. J., Asinas, A. E., and Weis, R. M. (2007) Liposome-mediated assembly of receptor signaling complexes. *Methods Enzymol.* 423, 267–98.

(125) Krishna, M. M. G. (1999) Excited-state kinetics of the hydrophobic probe Nile Red in membranes and micelles. *J. Phys. Chem. A* 103, 3589–95.

(126) Levitt, J. A., Chung, P.-H., and Suhling, K. (2015) Spectrally resolved fluorescence lifetime imaging of Nile red for measurements of intracellular polarity. *J. Biomed. Opt.* 20.

(127) Brun, M. a, Tan, K.-T., Nakata, E., Hinner, M. J., and Johnsson, K. (2009) Semisynthetic fluorescent sensor proteins based on self-labeling protein tags. *J. Am. Chem. Soc.* 131, 5873–84.

(128) Deda, M. La, Ghedini, M., Aiello, I., Pugliese, T., Barigelletti, F., and Accorsi, G. (2005) Organometallic emitting dyes: Palladium(II) Nile red complexes. *J. Organomet. Chem.* 690, 857–61.

List of Figures

Figure 1: (A) Jablonski diagram. Adapted from Lakowicz <i>et al.</i> ⁶ (B) A schematic representation of excitation and emission spectra.....	2
Figure 2: Fluorescence labeling techniques. (I) Fluorescent proteins: Protein structure of GFP (PDB ID: 1GFL) ⁷ . (II) Chemical tag - probe labeling techniques based on (A) Protein tag - ligand interactions, (B) Peptide tag - peptide interactions, (C) Peptide tag - fluorophore interactions, (D) Metal chelation and (E) Enzymatic reactions. Adapted from Yano <i>et al.</i> ⁸	4
Figure 3: (A) Typical structure of molecular rotors with the electron donating group (yellow), the electron accepting group (blue) and the spacer between them (grey). (B) An example of a molecular rotor: viscosity sensing probe 4,4'-difluoro-4-bora-3a,4a-diaza-s-indacene. (C) Structures of the solvatochromic dyes NR, Prodan and 4-Aminophthalimide.	7
Figure 4: Examples of fluorogenic labeling based on (A) FRET from the fluorophore (donor) to the quencher (acceptor) and (B) PeT quenching. Adapted from Chen <i>et al.</i> ³²	8
Figure 5: Photoinduced electron transfer (PeT) mechanisms. Adapted from Ueno <i>et al.</i> ⁴⁷	9
Figure 6: A NR derivative targeting a specific plasma membrane receptor turns fluorescent only upon binding to the target. The remaining excess of the dye, experiencing an aqueous environment, stays in its dark state, allowing “no wash” experiments.	10
Figure 7: SNAP-tag and CLIP-tag are two protein tags that react specifically with BG- and BC-derivatives respectively, thereby covalently binding the label.....	11
Figure 8: (A) TICT model for NR depending on the polarity of the solvent. (B) NR present in PBS, methanol, DMSO and dioxane (from left to right). (C) Emission spectrum of NR in solvents of different polarity (PBS, MeOH, DMSO and dioxane). (D) Polarity dependent TICT model for NR, where S_1^{np} and S_q^{tict} correspond to “Non polar” and “TICT” excited states respectively adapted from Sarkar <i>et al.</i> ⁵⁸ and charge separation of NR that leads to the formation of a dipole and explains the solvatochromism of NR.	12
Figure 9: Structure of NR12S. NR is in red and the anchor group consisting of the zwitterionic group and the long alkyl chain is in blue.	15
Figure 10: A cartoon of our idea for creating a fluorogenic probe for SNAP-tagged cell surface proteins. A BG-derivative of NR targeting SNAP was synthesized. We hypothesized that the probe on its own would not insert into membranes and therefore would be quenched. Upon reaction with SNAP, NR would be in very close proximity to the plasma membrane resulting in its	

subsequent membrane insertion. In the apolar environment the probe would turn fluorescent.19

Figure 11: Approximate estimation of the length of PEG linkers in nm calculated for compounds **3** and **4** in Chemdraw.20

Figure 12: Schematic structure of SNAP-tagged Human Insulin Receptor (SNAP-HIR). It contains two α subunits for the binding of insulin and two β subunits that are involved in signal transduction. SNAP is positioned at the C-terminus of the α subunit of the receptor.21

Figure 13: Structures of NR derivatives with different PEG linkers (compounds **1-4**). They consist of a benzylguanine moiety (blue), a linker (black), one or none negatively charged Cya (purple) and NR (red).22

Figure 14: (A) Excitation and (B) emission spectra of the BG-derivative **4** in dioxane and PBS showing typical spectroscopic properties of NR. The intensities have been normalised to those of dioxane. Fluorescence emission was detected while exciting at 520 nm, and the excitation spectrum was recorded at 700 nm emission wavelength.22

Figure 15: **Imaging after three washes in DMEM + FBS 10%**. HEK 293T cells transiently expressing pDisplay SNAP-CLIP-HCA labeled with BC-AlexaFluor 488 (10 μ M, 10 min incubation at 37 $^{\circ}$ C, three washes with DMEM + FBS 10%) and compounds **1-4** (500 nM, 30 min incubation at RT, DMEM + FBS 10%) imaged after three washes. Scale bar, 50 μ m. (N.B. The pictures in this figure have all been treated with the same settings. However, note that the settings between Figure 15 - Figure 18 are not the same.)25

Figure 16: **“No wash” imaging in DMEM + FBS 10%**. HEK 293T cells transiently expressing pDisplay SNAP-CLIP-HCA labeled with BC-AlexaFluor 488 (10 μ M, 10 min incubation at 37 $^{\circ}$ C, three washes with DMEM + FBS 10%) and compounds **1-4** (500 nM, 30 min incubation at RT, DMEM + FBS 10%) imaged without wash. Scale bar, 50 μ m. (N.B. The pictures in this figure have all been treated with the same settings. However, note that the settings between Figure 15 - Figure 18 are not the same.)26

Figure 17: **Imaging after three washes in NPM**. HEK 293T cells transiently expressing pDisplay-SNAP-CLIP-HCA labeled with BC-AlexaFluor 488 (10 μ M, 10 min incubation at 37 $^{\circ}$ C, three washes with NPM) and compounds **1-4** (500 nM, 30 min incubation at RT, NPM) imaged after three washes. Scale bar, 20 μ m. (N.B. The pictures in this figure have all been treated with the same settings. However, note that the settings between Figure 15 - Figure 18 are not the same.)27

Figure 18: **“No wash” imaging in NPM**. HEK 293T cells transiently expressing pDisplay-SNAP-CLIP-HCA labeled with BC-AlexaFluor 488 (10 μ M, 10 min incubation at 37 $^{\circ}$ C, three washes with NPM) and compounds **1-4** (500 nM, 30 min incubation at RT, NPM) imaged without wash. Scale bar, 20 μ m. (N.B. The

pictures in this figure have all been treated with the same settings. However, note that the settings between Figure 15 - Figure 18 are not the same.)	28
Figure 19: Imaging of SNAP-HIR with compound 4. CHO cells stably expressing extracellular SNAP-tagged HIR labeled with compound 4 (2 μ M, 30 min incubation at 37 °C in F-12 HAM medium), imaged before (no wash) and after three washes. Scale bar, 10 μ m.	29
Figure 20: Methods to transport molecules through the plasma membrane: Passive transport (passive diffusion, facilitated diffusion by channel and carrier proteins) and Active transport.....	32
Figure 21: Ionic distribution in the extracellular and intracellular media. In resting conditions of the cell, there are 10 times more K^+ channels open than Na^+ or Cl^- , therefore the interior of the cell is negatively charged, leading to a resting membrane potential of -70 mV. These gradients of ions are maintained by the Na^+/K^+ pump. The figure is adapted from Cooper <i>et al.</i> ¹⁰¹	33
Figure 22: Changes in membrane potential during an action potential of excitable cells. The resting potential of the cell corresponds to the dashed line (-70 mV).....	34
Figure 23: Patch clamp technique steps. A glass microelectrode is used to patch a cell. After seal formation, applying a strong pulse of suction ruptures the membrane of the cell and the microelectrode gets in contact with the intracellular medium of the cell.	35
Figure 24: Four response mechanisms of membrane potential sensitive probes. (A) Electrochromic dyes change their electronic structure. (B) Dyes that reorient in the plasma membrane. (C) Dyes that redistribute upon change of the membrane potential. (D) Negatively charged fluorophores that act as FRET acceptors and move to the inner side of the lipid bilayer upon depolarization.	36
Figure 25: Chemical structures of examples of organic voltage sensitive probes. (A) Merocyanine 540 (fast-response probe, reorientation). (B) di-4-ANEPPS and di-8-ANEPPS (fast response probes, electrochromism). (C) DIBAC ₄ (3) (slow response probe, redistribution).	37
Figure 26: Structures of NR derivatives with multiple charges (compounds 2 and 4-9). They consist of a benzylguanine moiety (blue), a PEG11 linker (black), different charges (purple), a C-2 or C-6 linker between the charge and NR (green) and NR (red).	39
Figure 27: Imaging after three washes in DMEM + FBS 10%. HEK 293T cells transiently expressing pDisplay-SNAP-CLIP-HCA labeled with BC-AlexaFluor 488 (10 μ M, 10 min incubation at 37 °C, three washes with DMEM + FBS 10%) and compounds 2 and 4-9 (500 nM, 30 min incubation at RT, DMEM + FBS 10%) imaged after three washes. Scale bar, 20 μ m. (<i>N.B.</i> The pictures in this	

figure have all been treated with the same settings. However, note that the settings between Figure 27-Figure 30 are not the same.)41

Figure 28: **“No wash” imaging in DMEM + FBS 10%.** HEK 293T cells transiently expressing pDisplay-SNAP-CLIP-HCA labeled with BC-AlexaFluor 488 (10 μ M, 10 min incubation at 37 $^{\circ}$ C, three washes with DMEM + FBS 10%) and compounds **2** and **4-9** (500 nM, 30 min incubation at RT, DMEM + FBS 10%) imaged without wash. Scale bar, 20 μ m. (*N.B.* The pictures in this figure have all been treated with the same settings. However, note that the settings between Figure 27-Figure 30 are not the same.)43

Figure 29: **Imaging after three washes in NPM.** HEK 293T cells transiently expressing pDisplay-SNAP-CLIP-HCA labeled with BC-AlexaFluor 488 (10 μ M, 10 min incubation at 37 $^{\circ}$ C, three washes with NPM) and compounds **2**, **4-9** (500 nM, 30 min incubation at RT, NPM) imaged after three washes. Scale bar, 20 μ m. (*N.B.* The pictures in this figure have all been treated with the same settings. However, note that the settings between Figure 27-Figure 30 are not the same.)44

Figure 30: **“No wash” imaging in NPM.** HEK 293T cells transiently expressing pDisplay-SNAP-CLIP-HCA labeled with BC-AlexaFluor 488 (10 μ M, 10 min incubation at 37 $^{\circ}$ C, three washes with NPM) and compounds **2** and **4-9** (500 nM, 30 min incubation at RT, NPM) imaged without wash. Scale bar, 20 μ m. (*N.B.* The pictures in this figure have all been treated with the same settings. However, note that the settings between Figure 27-Figure 30 are not the same.)46

Figure 31: (A) Protocol of membrane potential change followed during the experiment. (B) HEK 293 T Cells expressing extracellular SNAP labeled with compound **4**. The white arrows indicate an example of patched and non-patched cells, which were analysed.47

Figure 32: (A) Measurement of fluorescence intensity relative to the membrane potential of HEK 293T cells expressing extracellular SNAP and labeled with compounds **4-9** in EB for patched and non-patched cells using the patch clamp method. (B) Change of Fl. intensity of compounds **4-9** upon 100 mV membrane potential change for patched cells (black) and non-patched cells (red).48

Figure 33: Structures of compound NR12S and NR.49

Figure 34: **Imaging of live cells with NR12S.** HEK 293T cells, non-transfected, labeled with NR12S (500 nM, 7min at RT) and imaged directly after labeling (No wash) or after three washes (A) in DMEM + FBS 10%, and (B) in NPM (w/o FBS). Scale bar, 20 μ m. (*N.B.* The images in this figure have been treated with the same settings.).....51

Figure 35: (A) Protocol of membrane potential change followed during the experiment. (B) Change of Fl. intensity of compound NR12S upon 100 mV

membrane potential change for patched cells (5% decrease), non-patched cells and background.....	52
Figure 36: Structures of compounds 10 and 11 . They consist of a benzylguanine moiety (blue), a hydrophilic linker (black), negative charge (purple) and NR12S (red).....	53
Figure 37: Imaging of transfected cells in DMEM + FBS 10% . HEK 293T cells transiently expressing pDisplay-SNAP-CLIP-HCA labeled with BC-AlexaFluor 488 (10 μ M, 10 min incubation at 37 $^{\circ}$ C, three washes with DMEM + FBS 10%) or BC-Cy5 (10 μ M, 20 min incubation at 37 $^{\circ}$ C, three washes with DMEM + FBS 10%) and compounds 4 , 10 and 11 (500 nM, 30 min incubation at RT, DMEM + FBS 10%) imaged (A) after three washes and (B) directly after labeling. Scale bar, 20 μ m. (<i>N.B.</i> The pictures in this figure have been treated with the same settings in each subsection “wash” and “no wash”. However, note that the settings between Figure 37–Figure 40 are not the same.)	55
Figure 38: Imaging of non-transfected cells in DMEM + FBS 10% . HEK 293T cells, non-transfected labeled with compounds 4 , 10 and 11 (500 nM, 30 min incubation at RT in DMEM + FBS 10%) imaged (A) after three washes and (B) directly after labeling. Scale bar, 20 μ m. (<i>N.B.</i> The pictures in this figure have been treated with the same settings in each subsection “wash” and “no wash”. However, note that the settings between Figure 37-Figure 40 are not the same.)	57
Figure 39: Imaging of transfected cells in NPM (w/o FBS) . HEK 293T cells transiently expressing pDisplay-SNAP-CLIP-HCA labeled with BC-AlexaFluor 488 (10 μ M, 10 min incubation at 37 $^{\circ}$ C, three washes with NPM) or BC-Cy5 (10 μ M, 20 min incubation at 37 $^{\circ}$ C, three washes with NPM) and compounds 4 , 10 and 11 (500 nM, 30 min incubation at RT, NPM) imaged (A) after three washes and (B) directly after labeling. Scale bar, 20 μ m. (<i>N.B.</i> The pictures in this figure have been treated with the same settings in each subsection “wash” and “no wash”. However, note that the settings between Figure 37-Figure 40 are not the same.)	59
Figure 40: Imaging of non-transfected cells in NPM (w/o FBS) . HEK 293T cells, non-transfected labeled with compounds 4 , 10 and 11 (500 nM, 30 min incubation at RT in NPM) imaged (A) after three washes and (B) directly after labeling. Scale bar, 20 μ m. (<i>N.B.</i> The pictures in this figure have been treated with the same settings in each subsection “wash” and “no wash”. However, note that the settings between Figure 37-Figure 40 are not the same.)	61
Figure 41: (A) Comparison of emission spectra of compounds 11 and 4 bound to SNAP-tag expressed on cells in EB w/o FBS. Compound 11 is blue shifted compared to 4 . (B) Comparison of emission spectra of compound 11 measured on cells in EB w/o FBS and in EB + FBS 10%.	63
Figure 42: Change in fluorescence intensity of compounds (A) NR12S, 10 and 11 on non-transfected cells (nt) in EB (w/o FBS) and (B) 10 and 11 on	

transfected cells (tr) expressing pDisplay-SNAP-CLIP-HCA measured in EB (with 10% FBS or w/o FBS) per 100 mV change in membrane potential.....64

Figure 43: Speculations about the position of NR. It is not clearly defined yet if (A) the NR molecules bound to SNAP tag insert in the plasma membrane after binding to SNAP-tag and experiencing the apolar environment fluoresce, or (B) NR is “trapped” in the hydrophobic environment of SNAP-tag and due to its apolar environment turns into its “fluorescent-on” state.65

Figure 44: (A) Comparison of emission maxima measured for **a.** compound **2** inserted in the membrane, **b.** BG-NR compounds (PEG11, C2) bound to SNAP on cells, **c.** BG-NR compounds (PEG11, C6) bound to SNAP on cells, **d.** BG-NR compounds (PEG5, C6) bound to SNAP on cells, **e.** BG-NR compounds (**2**, **4** and **8**) bound to SNAP in PBS solution, **f.** Compounds NR12S, **10** and **11** inserted in the membrane of non-transfected cells and **g.** Compounds NR12S, **10** and **11** bound to SNAP in PBS solution. Each spot corresponds to one molecule. This figure corresponds to the results presented in Table 9. (B) Emission spectrum of compound **4** applied on HEK 293T cells expressing SNAP-tag on the extracellular part of the plasma membrane. (C) Emission spectrum of compound NR12S applied on non-transfected HEK 293T cells. (B) and (C) emission spectra were measured under confocal microscope on lamda mode (step: 5 nm). The spectra were fitted using a Lorentzian fit as a guide for the eye. Scale bars, 10 μ m.....69

Figure 45: **Liposome experiment.** (A) A labeled SNAP-His with our NR derivatives is applied on DPPC liposomes containing Ni-NTA lipids leading to the anchoring of SNAP-tag on the surface of the liposomes. (B) Controls performed for the method.71

Figure 46: (A) Comparison of fluorescence lifetimes measured for **a.** Compound **2** inserted in the membrane, **b.** BG-NR compounds (PEG11, C2) bound to SNAP on cells, **c.** BG-NR compounds (PEG11, C6) bound to SNAP on cells, **d.** BG-NR compounds (PEG5, C6) bound to SNAP on cells, **e.** BG-NR compounds (**2**, **4** and **8**) bound to SNAP in PBS solution, **f.** Compounds NR12S, **10** and **11** inserted in the membrane of non-transfected cells and **g.** Compounds NR12S, **10** and **11** bound to SNAP in PBS solution. Each spot corresponds to one molecule. This figure refers to the results presented in Table 11. (B) Fluorescence decay of compound NR12S applied on non-transfected HEK 293T cells. (C) Fluorescence decay of compound **4** applied on HEK 293T cells expressing SNAP-tag on the extracellular part of the plasma membrane. Amplitude-averaged mean lifetimes for biexponential decays of fluorescence were calculated using Equation 4. For further details see Chapter 7.2.75

Figure 47: Synthesis of Compound **4** (BG-PEG11-Cya-C6-NR).84

Figure 48: Synthesis of Compound **2** (BG-PEG11-C6-NR).85

Figure 49: Synthesis of Compound **18**.86

Figure 50: Synthesis of Compound 3 (BG-PEG5-Cya-C6-NR).	87
Figure 51: Synthesis of Compound 1 (BG-PEG5-C6-NR).	88
Figure 52: Synthesis of Compound 5 (BG-PEG11-LysMe3-C6-NR).	89
Figure 53: Synthesis of Compound 7 (BG-PEG11-Cya-C2-NR).	90
Figure 54: Synthesis of Compound 8 (BG-PEG11-LysMe3-C2-NR).	90
Figure 55: Synthesis of Compound 25	91
Figure 56: Synthesis of Compound 6 (BG-PEG11-(LysMe3) ₂ -C6-NR).	92
Figure 57: Synthesis of Compound 9 (BG-PEG11-(LysMe3) ₂ -C2-NR).	92
Figure 58: Synthesis of Compound 27	93
Figure 59: Synthesis of Compound 29	94
Figure 60: Synthesis of Compound 31	95
Figure 61: Synthesis of Compound 32	95
Figure 62: Synthesis of Compound 10 (BG-PEG11-NR12S).	96
Figure 63: Synthesis of Compound 11 (BG-PEG11-Cya-NR12S).	97
Figure 64: Emission spectra and $\tau_{\text{ave, ampl}}$ of compounds 1-9 bound to SNAP-tag expressed on the extracellular surface of the plasma membrane in HEK 293T cells under confocal microscope in NPM (w/o FBS). (A) BG-PEG5-C6-NR (1), (B) BG-PEG5-Cya-C6-NR (3), (C) BG-PEG11-Cya-C6-NR (4), (D) BG-PEG11-Cya-C2-NR (7), (E) BG-PEG11-LysMe ₄ -C6-NR (5), (F) BG-PEG11-LysMe ₃ -C2-NR (8), (G) BG-PEG11-(LysMe ₃) ₂ -C6-NR (6), (H) BG-PEG11-(LysMe ₃) ₂ -C2-NR (9) and (I) BG-PEG11-C6-NR (2).	105

List of Tables

Table 1: Tag-probe labeling methods. Adapted from Yano <i>et al.</i> ⁸	5
Table 2: Spectroscopic properties Including absorption and emission maxima and QY for compounds 1-4 and NR.	23
Table 3: Rate constants k and $t_{1/2}$ of labeling reaction of SNAP with compounds 1-4 , measured by SDS-page gel.	23
Table 4: Rate constants k and $t_{1/2}$ of labeling reaction of SNAP as reported by Sun <i>et al.</i> ⁴⁴	24
Table 5: Spectroscopic properties including absorption and emission maxima and QY for compounds 2 and 4-9 , measured in PBS, DMEM + FBS 10% and dioxane.	40
Table 6: Spectroscopic properties including emission and absorption maxima and QY for compounds NR12S and NR measured in PBS, DMEM + FBS 10% and dioxane.	50
Table 7: Spectroscopic properties including absorption and emission maxima for compounds NR12S, 10 and 11 measured in PBS, DMEM + FBS 10% and dioxane.	54
Table 8: Measurement of $\lambda_{\text{max, emission}}$ of NR derivatives 10 and 11 (i) bound to SNAP-tag expressed on the surface of HEK 293T Cells in EB w/o FBS or EB + FBS 10% (Cells, Transfected), (ii) applied on non-transfected HEK 293T cells in EB w/o FBS (Cells, Non-Transfected) and (iii) bound to SNAP-tag in PBS solution (SNAP). The spectra were fitted using a Lorentzian fit to calculate the $\lambda_{\text{max, fl}}$	62
Table 9: Measurement of $\lambda_{\text{max, emission}}$ of NR derivatives (i) bound to SNAP-tag expressed on the surface of HEK 293T Cells in NPM w/o FBS (or EB w/o FBS when indicated with *) (ii) bound to SNAP-tag in PBS solution (w/o BSA) and (iii) bound to BSA in PBS solution. The spectra were fitted using a Lorentzian fit for calculation of the $\lambda_{\text{max, fl}}$	68
Table 10: Measurement of $\lambda_{\text{max, emission}}$ of NR derivatives (i) after conjugation to His-tagged SNAP applied on DPPC lipid vesicles containing NTA-lipids and on control vesicles lacking the NTA lipids and (ii) directly on DPPC lipid vesicles containing NTA-lipids and on control vesicles lacking the NTA-lipids.	71
Table 11: Measurement of fluorescence lifetime ($\tau_{\text{ave, ampli}}$) of NR derivatives bound to SNAP on the surface of HEK 293T Cells in NPM w/o FBS (Cells), bound to SNAP-tag in PBS solution (SNAP) and bound to BSA in PBS solution (BSA). Amplitude-averaged mean lifetimes for biexponential decays of	

fluorescence were calculated using Equation 4. For further details see Chapter 7.2.	73
Table 12: Measurement of fluorescence lifetimes for NR derivatives (i) after conjugation to His-tagged SNAP applied on DPPC lipid vesicles containing NTA lipids and on control vesicles lacking the NTA lipids and (ii) directly applied on DPPC lipid vesicles containing NTA-lipids and on control vesicles lacking the NTA-lipids. Amplitude-averaged mean lifetimes for biexponential decays of fluorescence were calculated using Equation 4. For further details see Chapter 7.2.	76

List of Equations

Equation 1: Relation between fluorescence QY and fluorescence lifetime, where Φ_f and τ_f are the fluorescence QY and fluorescence lifetime respectively.	13
Equation 2: Relation between kinetic radiative and non-radiative decay rate constants and fluorescence lifetime, where τ_f is the fluorescence lifetime and k_r and k_{nr} are the kinetic radiative and non-radiative decay rate constants respectively. ⁵⁸	13
Equation 3: Calculation of Labeling Rate Constant k , where $t_{1/2}$ is the half-life time of labeling and c is the substrate concentration.....	98
Equation 4: Calculation of Average Fluorescence Lifetime, $\tau_{ave, ampl}$	101

Curriculum Vitae

Ms Efthymia (Fay) PRIFTI

Avenue d'Echallens 61,
1004 Lausanne, Switzerland

Born 17.10.1988, in Athens, Greece

fay.prifti@gmail.com

+41 (0) 78 673 64 37

EDUCATION

- | | |
|-------------|---|
| 2012 – 2016 | Swiss Federal Institute of Technology (EPFL), Lausanne
PhD in Chemistry |
| 2006 – 2011 | Pharmacy School, University of Athens, Greece
Diploma in Pharmacy (5 year program equivalent to MSc)
<u>G.P.A.:</u> 8.13/10 (Graduated 3 rd /52 students) |

EXPERIENCE

- | | | |
|-----------------|--|------------------------------------|
| 2012 - 2016 | EPFL, Switzerland
Developed a new fluorogenic probe for visualizing membrane proteins based on the molecule Nile Red.
Supervisor: Prof. Kai Johnsson | PhD Marie Curie Fellow |
| 2015 (1 month) | EMBL, Italy
Got introduced in patch clamp and electrophysiology and performed experiments for my thesis.
Supervisor: Dr Paul Heppenstall | Visiting researcher |
| 2011 (3 months) | General Hospital of Athens, Greek Red Cross, Greece | Intern Pharmacist |
| 2010 (8 months) | Welsh School of Pharmacy, UK
Performed my Diploma thesis in the department of Pharmacology.
Investigated the role of different endocytic pathways in the development of Alzheimer's disease.
Supervisor: Dr Emma Kidd | Erasmus student |
| 2010 (2 months) | John Innes Centre&Sainsbury Laboratory, UK
Accomplished the synthesis of three carbohydrate molecules.
Supervisor: Prof. Rob Field | Undergraduate researcher |
| 2009 (2 months) | Cambridge University, UK
Worked in the Department of Pathology and familiarized myself with molecular&cell biology techniques.
Supervisor: Prof. Vassilis Koronakis | Undergraduate Amgen Scholar |

TEACHING EXPERIENCE

Master thesis supervision of Nicole Vassali “Voltage Sensors Based on Nile Red”, EPFL, Lausanne Switzerland, September 2013 – February 2014

Teaching assistant for the practical course “Experimental Biochemistry and Biophysics” (Spring, 2013-2015)

Teaching assistant of the course “Introduction to organic chemistry I” (Autumn, 2013)

ORAL PRESENTATIONS

“Fluorescent Probes for Plasma Membrane Proteins”, New Frontiers in Membrane Biology Conference, Amsterdam, 2016

“A Fluorogenic Probe for SNAP-tagged Plasma Membrane Proteins Based on Nile Red”, NCCR Chemical Biology Meeting, Villars-sur-Ollon, Switzerland, 2014

“Chemical Tools to Dissect Plant Cell Wall Biosynthesis”, Summer Program Symposium, John Innes Centre, Norwich, UK, 2010

POSTER PRESENTATIONS

“A fluorogenic Probe for Plasma Membrane Proteins”, NCCR Chemical Biology Meeting, Geneva, Switzerland, 2013

“*Salmonella* tyrosine phosphatase SptP downregulation of the host actin cytoskeleton”, Amgen Scholars Symposium, Cambridge, UK, 2009

PUBLICATIONS

Prifti, E., Reymond, L., Umebayashi, M., Hovius, R., Riezman, H. and Johnsson, K. (2014) A fluorogenic probe for SNAP-tagged plasma membrane proteins based on the solvatochromic molecule Nile Red, *ACS Chem. Biol.*, 9 (3), pp 606–612 (**ACS Editor’s Choice**)

Prifti, E., Goetz, S., Nepogodiev, S., and Field, R. (2011) Synthesis of fluorescently labelled rhamnosides: probes for the evaluation of rhamnogalacturonan II biosynthetic enzymes. *Carbohydr Res.* Sep 6; 346 (12): 1617-21

